



OSPAR
COMMISSION

Atmospheric deposition of selected heavy metals
and persistent organic pollutants to the
OSPAR Maritime Area (1990 - 2005)

The Convention for the Protection of the Marine Environment of the North-East Atlantic (the “OSPAR Convention”) was opened for signature at the Ministerial Meeting of the former Oslo and Paris Commissions in Paris on 22 September 1992. The Convention entered into force on 25 March 1998. It has been ratified by Belgium, Denmark, Finland, France, Germany, Iceland, Ireland, Luxembourg, Netherlands, Norway, Portugal, Sweden, Switzerland and the United Kingdom and approved by the European Community and Spain.

La Convention pour la protection du milieu marin de l'Atlantique du Nord-Est, dite Convention OSPAR, a été ouverte à la signature à la réunion ministérielle des anciennes Commissions d'Oslo et de Paris, à Paris le 22 septembre 1992. La Convention est entrée en vigueur le 25 mars 1998. La Convention a été ratifiée par l'Allemagne, la Belgique, le Danemark, la Finlande, la France, l'Irlande, l'Islande, le Luxembourg, la Norvège, les Pays-Bas, le Portugal, le Royaume-Uni de Grande Bretagne et d'Irlande du Nord, la Suède et la Suisse et approuvée par la Communauté européenne et l'Espagne.

contents

Executive Summary	4
Récapitulatif.....	7
1. Introduction.....	9
2. Definitions of the OSPAR regions and sub-regions	10
3. Short description of MSC-E heavy metal and POP models	11
3.1 Heavy metal chemical transport model MSCE-HM.....	11
3.2 Multi-compartment transport model MSCE-POP	12
4. Heavy metals.....	15
4.1 Atmospheric emissions of heavy metals	15
4.2 Atmospheric depositions of heavy metals to the OSPAR maritime area ...	18
4.3 Comparison of computed versus measured deposition at OSPAR coastal monitoring stations	22
5. Persistent organic pollutants	25
5.1 Atmospheric emission of POPs.....	25
5.2 Atmospheric depositions of POPs to the OSPAR maritime area.....	27
5.3 Comparison of computed versus measured deposition at monitoring stations	28
6. Uncertainty of model estimates	30
7. Comparison of estimated depositions with results of previous studies	31
8. Conclusions	33
References	35
Abbreviations.....	38
Annex A: Data products for heavy metals.....	39
Annex B: Data products for Persistent organic pollutants.....	83

Acknowledgement

This report was prepared at request of the OSPAR Commission by

- A. Gusev
- I. Ilyin
- O. Travnikov
- V. Shatalov
- O. Rozovskaya

of the Meteorological Synthesizing Centre (East) (MSC-E) of the Co-operative Programme for Monitoring and Evaluation of the Long Range Transmission of Air Pollutants in Europe (EMEP) (Krasina pereulok, 16/1, 123056 Moscow, Russia, Tel: +7 495 981 15 66, Fax: +7 495 981 15 67, e-mail: msce@msceast.org, website: <http://www.msceast.org>). EMEP retains all rights on the data, measured under the EMEP Programme and modelled for this report, and related data products (tables and figures). This work has been supported and financed by the Convention for the Protection of the Marine Environment of the North-East Atlantic (OSPAR Convention).

Executive Summary

Emissions of selected heavy metals and POPs significantly decreased in 1990 – 2005

The analysis of the emissions data has shown that **lead**, **cadmium**, and **mercury** emissions significantly decreased in most OSPAR countries during the period 1990 – 2005. The highest emission reduction was noted for lead (from 61% to 97%). Changes of cadmium emissions varied from a reduction of 84% to an increase of 6% in different OSPAR countries. For mercury, variation of emission changes in emissions was even higher ranging from a 85% reduction to a 55% increase. The total emissions of lead, cadmium, and mercury decreased for all OSPAR countries by 93%, 61%, and 68%, respectively. This is higher than the emission decrease in Europe as a whole because of less pronounced emission reductions in Central and Eastern European countries.

Annual emissions of **PCB-153** from OSPAR countries decreased essentially by 77% in the period 1990 – 2005. Among OSPAR countries, the most significant decline of PCB-153 emission can be noted for Norway (88%), the Netherlands (87%), and Denmark (86%). According to officially reported information and expert estimates γ -**HCH** emission to the atmosphere decreased in the period 1990 – 2005 by almost 90% in OSPAR countries.

Models suggest continuous but varied decline in atmospheric deposition for each pollutant and OSPAR region

According to the model estimates, total depositions of **lead** and **cadmium** in 2005 to the OSPAR maritime area demonstrate a pronounced decline from European coast to the open sea westward and northward (from 1.2 to 0.5 mg/m²/y for lead and from 0.03 to 0.005 mg/m²/y for cadmium). This can be explained by the significant influence of European emission sources. The net deposition flux is considerably lower and exhibits a more marked decline towards the centre of the Wider Atlantic (down to 0.01 and 0.003 mg/m²/y, respectively).

Both total depositions and net atmospheric inputs of **lead** and **cadmium** to the OSPAR Regions decreased during the period 1990 – 2005, following emission reductions in Europe. The highest decrease of total depositions took place in Region IV (Bay of Biscay) and reached up to 60% for lead and cadmium. The lowest decrease was obtained for Region V (Wider Atlantic) and amounted to 30% for lead and 25% for cadmium. In general, the decrease in deposition was somewhat lower than that in emissions because of the effect of wind re-suspension of previous atmospheric depositions accumulated in soil and seawater.

The spatial distribution of total **mercury** depositions in 2005 does not exhibit a distinct gradient from European coast towards the open sea, mainly because of the significant impact of global mercury transport from other continents on the depositions to the OSPAR maritime area. Somewhat elevated depositions to the Northern Atlantic (more than 0.008 mg/m²/y) are caused by relatively high concentrations of the oxidants and elevated precipitation amount in this Region. The net deposition flux of mercury has a similar spatial pattern but with lower deposition values (mostly below 0.005 mg/m²/y). A distinctive feature of the estimated mercury net flux pattern is the negative values over the coastal waters and regional seas of Europe.

A gradual long-term decrease of **mercury** deposition during the period 1990 – 2005 took place in Region II (Greater North Sea) and Region III (Celtic Seas) amounting to 35% and 25%, respectively. At the same time, the decrease of total deposition in other OSPAR Regions did not exceed 15% because of the large contribution from global sources. In all OSPAR Regions, net atmospheric inputs of mercury are significantly lower than total deposition which indicates the significant role of re-emission. In the coastal areas, the estimated net atmospheric input of mercury dropped to a negligible value in the middle of the assessment period and alters around zero during the following years, demonstrating a balance between depositions and re-emission.

Combustion processes remain key emission sources and contributors to deposition

The key emission source category “Combustion in power plants and in industry and industrial processes” was the largest (70 – 90%) contributor to depositions of **lead**, **cadmium** and **mercury** to the OSPAR Regions and sub-regions of the Greater North Sea. The second most important contributor varies for different metals: “Transport” for lead, “Commercial, residential and other combustion” for cadmium, and “Waste” for mercury.

Modelled wet deposition fluxes of **lead**, **cadmium** and **mercury** are in satisfactory agreement with most annual mean measured values. The most reasonable agreement between modelled and observed fluxes was obtained for stations in Denmark, Germany, Norway, France and Iceland. Model estimates of lead and mercury depositions reproduced well both general values and long-term changes of observations. Calculated cadmium depositions underestimated the measured depositions at a number of stations, which is likely to be connected with uncertainties of available emission data, uncertainties of model parameterisation of wind re-suspension, and inaccuracy of measurements at the very beginning of the period.

Highest levels of computed **PCB-153** depositions in 2005 to the OSPAR maritime area were calculated for Region II (Greater North Sea) ($5 \cdot 10^{-5}$ mg/m²/y and higher). The lowest values of PCB-153 deposition are characteristic for Region I (Arctic Waters) (about $1 \cdot 10^{-5}$ mg/m²/y and lower). The spatial pattern of γ -HCH depositions in 2005 follows in general that of PCB-153. It is characterised by high values of deposition flux in Region II (Greater North Sea) ($1 \cdot 10^{-3}$ – $3 \cdot 10^{-3}$ mg/m²/y). Deposition levels are decreasing to the north up to $1 \cdot 10^{-4}$ – $2 \cdot 10^{-4}$ mg/m²/y in Region I (Arctic Waters) and to the west up to $2 \cdot 10^{-4}$ – $5 \cdot 10^{-4}$ mg/m²/y in Region V (Wider Atlantic).

For the considered period 1990 – 2005, the decline of **PCB-153** total annual deposition, following achieved emission reductions, varies within the OSPAR maritime area from 3.3 to 3.7 times. Highest reductions of PCB-153 total depositions took place in Region V (Wider Atlantic). The reduction of the net deposition flux is more significant and to a factor of four in the most of the Regions.

Total annual depositions of γ -**HCH** to the OSPAR maritime area declined in the period 1990 – 2005 by a factor ranging from 5.5 to 9.3, depending on the Region concerned. The highest decrease of deposition took place in Region II (Greater North Sea) and Region IV (Bay of Biscay). Following the essential reduction or elimination of γ -HCH emission, a substantial influence of re-emission can be noted for a number of sub-regions of the Region II (Greater North Sea).

Model results reasonably agree with observation data but uncertainties remain

A comparison of computed deposition fluxes of **PCB-153** with available measurements of the EMEP monitoring network revealed that model predictions reasonably match the variations of observed deposition fluxes for most of the observation sites with the exception for the period 1998 – 2001 where significant differences (more than a factor of 3) were obtained. This might be caused by uncertainties in the description of temporal variations of PCB-153 emissions during this period.

The computed deposition fluxes of γ -**HCH** reasonably agree with available measurements of the OSPAR monitoring network. For most of the observation sites, the model reproduces reasonably well the temporal variations of measured wet deposition fluxes of γ -HCH. Significant differences were noted between model results and the measurements at the monitoring station in Iceland both for γ -HCH and PCB-153. This is likely to be due to an overestimation of boundary conditions, uncertainties in model parameterisation of removal processes or the representativeness of measurements of this site.

Récapitulatif

Emissions de métaux lourds et de POP sélectionnés: diminution significative entre 1990 et 2005

L'analyse des données sur les émissions révèle que les émissions de **plomb**, de **cadmium** et de **mercure** ont diminué de manière significative dans la plupart des pays OSPAR entre 1990 et 2005. La réduction la plus importante relevée concerne le plomb (elle est passée de 61% à 97%). Les changements concernant les émissions de cadmium varient. Ils vont d'une réduction de 84% à une augmentation de 6% dans les divers pays OSPAR. Dans le cas du mercure, ces changements sont encore plus importants allant d'une réduction de 85% à une augmentation de 55%. Les émissions totales de plomb, de cadmium et de mercure ont diminué dans tous les pays OSPAR, respectivement de 93%, 61% et 68%. Ce qui correspond à une diminution supérieure à la moyenne européenne car les émissions accusent une réduction moindre dans les pays d'Europe centrale et de l'Est.

Les émissions annuelles de **PCB-153** provenant des pays OSPAR ont diminué essentiellement de 77% entre 1990 et 2005. On note que les pays OSPAR qui ont obtenu les diminutions les plus importantes des émissions de PCB-153 sont la Norvège (88%), les Pays-Bas (87%) et le Danemark (86%). Selon les informations notifiées officiellement et les estimations des experts, les émissions atmosphériques de **γ -HCH** ont diminué de presque 90% dans les pays OSPAR entre 1990 et 2005.

Les modèles suggèrent un déclin continu mais varié des retombées atmosphériques pour chaque polluant et chaque région OSPAR

Selon les estimations de la modélisation, les retombées totales de **plomb** et de **cadmium** dans la zone maritime OSPAR en 2005 accusent un déclin prononcé, des côtes européennes à la haute mer vers l'Ouest et vers le Nord (de 1,2 à 0,5 mg/m²/an pour le plomb et de 0,03 à 0,005 mg/m²/an pour le cadmium). Ceci s'explique par l'influence significative des sources d'émission européennes. Le flux net des retombées est beaucoup plus bas et accuse un déclin plus marqué vers le centre de l'Atlantique au large (ramené à 0,01 et 0,003 mg/m²/an, respectivement).

Les retombées totales ainsi que les apports atmosphériques nets de **plomb** et de **cadmium** dans les régions OSPAR ont diminué entre 1990 et 2005, à la suite des réductions d'émission en Europe. On a relevé la diminution la plus importante des retombées totales dans la Région IV (Golfe de Gascogne). Elle a atteint 60% pour le plomb et le cadmium. La diminution la plus faible est dans la Région V (Atlantique au large) et correspond à 30% pour le plomb et 25% pour le cadmium. Dans l'ensemble, la diminution des retombées est quelque peu inférieure à celle des émissions, ceci est dû à l'effet de la resuspension avec le vent des retombées atmosphériques précédentes qui s'accumulent dans la terre et l'eau de mer.

La distribution spatiale des retombées totales de **mercure** en 2005 ne révèle pas de gradient distinct, des côtes européennes à la haute mer. Ceci est essentiellement dû à l'impact significatif du transport global du mercure, provenant d'autres continents, sur les retombées dans la zone maritime OSPAR. Les retombées quelque peu élevées dans l'Atlantique septentrional (plus de 0,008 mg/m²/an) sont dues à des concentrations relativement élevées des oxydants et aux précipitations importantes dans cette région. Le flux net de retombées de mercure présente une distribution spatiale similaire mais les retombées sont plus faibles (essentiellement en dessous de 0,005 mg/m²/an). Le flux net estimé de mercure présente une caractéristique distinctive, à savoir des valeurs négatives dans les eaux côtières et des mers régionales d'Europe.

Une diminution graduelle à long terme des retombées de **mercure** s'est produite, entre 1990 et 2005, dans les Régions II (Mer du Nord au sens large) et III (Mers celtiques), respectivement de 35% et 25%. En même temps, la diminution des retombées totales dans les autres régions OSPAR n'a pas dépassé 15% du fait de la contribution importante des sources globales. Dans toutes les régions OSPAR, les apports atmosphériques nets de mercure sont significativement plus faibles que les retombées totales ce qui indique le rôle significatif des réémissions. Dans les zones côtières, les apports atmosphériques nets estimés ont baissé pour atteindre une valeur négligeable vers le milieu de la période d'évaluation et se situent aux environs de zéro lors des années suivantes ce qui révèle un équilibre entre les retombées et les réémissions.

Les processus de combustion restent les principales sources d'émission et contribuent le plus aux retombées

La "combustion dans les centrales électriques et dans l'industrie et les processus industriels" représente la principale catégorie de sources d'émission et contribue le plus (70 à 90%) aux retombées de **plomb**, de **cadmium** et de **mercure** dans les régions et les sous-régions OSPAR de la mer du Nord au sens large. Le deuxième contributeur important varie d'un métal à l'autre. Il s'agit du « transport » pour le plomb, de la « combustion commerciale, domestique et autre » pour le cadmium, et des « déchets » pour le mercure.

Les flux de retombées humides modélisés de **plomb**, de **cadmium** et de **mercure** correspondent de manière satisfaisante à la plupart des valeurs moyennes annuelles relevées. Les flux modélisés qui correspondent le mieux aux flux relevés sont ceux des stations du Danemark, de l'Allemagne, de la Norvège, de la France et de l'Islande. Les estimations de la modélisation pour les retombées de plomb et de mercure représentent bien les valeurs générales, de même que les changements à long terme relevés. Les retombées de cadmium calculées sous-estiment les retombées relevées dans un certain nombre de stations. Il est fort probable que ceci soit lié aux incertitudes que présentent les données disponibles sur les émissions, la paramétrisation de la resuspension avec le vent modélisée et les inexactitudes des mesures tout au début de la période.

Le calcul des retombées de **PCB-153** dans la zone maritime OSPAR en 2005 donne les niveaux les plus élevés pour la Région II (Mer du Nord au sens large) ($5 \cdot 10^{-5}$ mg/m²/an et plus). Les valeurs les plus faibles des retombées de PCB-153 sont typiques de la Région I (Eaux arctiques) (environ $1 \cdot 10^{-5}$ mg/m²/an et moins). La tendance spatiale des retombées de γ -HCH en 2005 suit en général celle du PCB-153. Elle se caractérise par des valeurs élevées du flux des retombées dans la Région II (Mer du Nord au sens large) ($1 \cdot 10^{-3}$ à $3 \cdot 10^{-3}$ mg/m²/an). Les niveaux des retombées diminuent vers le Nord pour atteindre $1 \cdot 10^{-4}$ à $2 \cdot 10^{-4}$ mg/m²/an dans la Région I (Eaux arctiques) et à l'Ouest où ils se situent entre $2 \cdot 10^{-4}$ et $5 \cdot 10^{-4}$ mg/m²/an dans la Région V (Atlantique au large).

Le déclin des retombées annuelles totales de **PCB-153** pour la période considérée, de 1990 à 2005, à la suite des réductions des émissions obtenues, se situe, dans la zone maritime OSPAR, entre 3,3 et 3,7 fois. Les réductions les plus élevées des retombées totales de PCB-153 se trouvent dans la Région V (Atlantique au large). La réduction du flux net des retombées est quatre fois plus significative dans la plupart des régions.

Les retombées annuelles totales de γ -HCH dans la zone maritime OSPAR ont décliné, entre 1990 et 2005, de 5,5 à 9,3 fois, selon la région concernée. La diminution la plus importante des retombées se trouve dans les Régions II (Mer du Nord au sens large) et IV (Golfe de Gascogne). On note une influence importante des réémissions pour un certain nombre de sous-régions de la Région II (Mer du Nord au sens large) à la suite de la réduction essentielle ou de l'élimination des émissions de γ -HCH.

Les résultats de la modélisation correspondent assez bien aux données découlant des observations mais des incertitudes subsistent

Une comparaison des flux de retombées de **PCB-153** calculés et des données disponibles du réseau de surveillance EMEP révèle que les prédictions de la modélisation correspondent assez bien aux variations des flux de retombées observés pour la plupart des sites à l'exception de la période entre 1998 et 2001 pour laquelle on obtient des différences significatives (plus de 3 fois). Ceci pourrait être dû aux incertitudes que présente la description des variations temporelles des émissions de PCB-153 durant cette période.

Les flux de retombées de γ -HCH calculés correspondent assez bien aux données disponibles du réseau de surveillance OSPAR. La modélisation reproduit assez bien, pour la plupart des sites d'observation, les variations temporelles des flux des retombées humides de γ -HCH mesurés. On note des différences significatives entre les résultats de la modélisation et les données de la station de surveillance en Islande aussi bien pour le γ -HCH que le PCB-153. Il est fort probable que ceci soit dû à une surestimation des conditions de limites, des incertitudes de la paramétrisation de la modélisation des processus de retrait ou de la représentativité des données de ce site.

1. Introduction

The protection of the marine environment from contamination by heavy metals and persistent organic pollutants (POPs) is a subject of concern for many international organisations and programs. These toxic pollutants can have significant adverse effects on marine biota (OSPAR 2000). Input of heavy metals and POPs to the marine environment occurs via various routes, such as direct discharges, riverine inputs and atmospheric depositions. Contribution of the atmospheric depositions to the total input can be significant. For example, it can range from 17 to 25% for cadmium and from 55 to 57% for lead over the entire OSPAR maritime area (OSPAR 2000). However, importance of the atmospheric route can significantly vary in different regions of the OSPAR area as well as in time. This report was prepared by the Meteorological Synthesizing Centre (East) (MSC-E) of the Co-operative Programme for Monitoring and Evaluation of the Long Range Transmission of Air Pollutants in Europe (EMEP) at the request of the OSPAR Commission and is focused on the evaluation of atmospheric inputs of lead (Pb), cadmium (Cd), mercury (Hg), polychlorinated biphenyls (PCBs) and γ -hexachlorocyclohexane (γ -HCH) to the OSPAR maritime area. It is based on emission data of the OSPAR Contracting Parties Belgium, Denmark, Finland, France, Germany, Iceland, Ireland, Luxembourg, the Netherlands, Norway, Portugal, Spain, Sweden, Switzerland, and the UK (hereinafter the "OSPAR countries"), and the two European countries outside the OSPAR Convention area Poland and the Russian Federation. This report supplements the data collection by OSPAR under the OSPAR Comprehensive Atmospheric Monitoring Programme (CAMP) (OSPAR, 2001) and supports the upcoming 2009 OSPAR assessment of atmospheric concentrations and deposition and the Quality Status Report 2010.

The presented results are based on the application of heavy metal and POP models developed by EMEP/MSC-E (MSCE-HM and MSCE-POP, respectively). These models are actively used for operational calculations of heavy metals and POPs transboundary pollution within the European region and in the Northern Hemisphere within the EMEP programme and in other activities relating to the UNECE Convention on Long-Range Transboundary Air Pollution (LRTAP Convention). The MSCE-HM and MSCE-POP are well documented in the EMEP/MSC-E reports. Their formulation and performance was thoroughly evaluated within the EMEP/TFMM Workshop on the MSC-E models review (ECE/EB.AIR/GE.1/2006/4). For the purpose of the OSPAR calculation the standard EMEP model grid was extended to cover the entire OSPAR maritime area. Besides, the hemispheric versions of the models were applied for evaluation of boundary conditions. It is particularly important for such global pollutants as mercury, PCBs and γ -HCH. Emissions used in modelling of heavy metal and γ -HCH depositions were based on officially reported data, and supplemented by expert estimates when official information was not available. For computations of PCBs depositions emission expert estimates were applied.

The following topics are included and discussed in the report:

- Annual emissions of three heavy metals (Pb, Cd, Hg) and two POPs (PCB-153, γ -HCH) from the OSPAR Contracting Parties and selected countries outside the OSPAR area in the period 1990-2005.
- Spatial distribution of modelled atmospheric depositions of the selected heavy metals and POPs over the OSPAR maritime area in 2005 with particular emphasis on the OSPAR Region II (Greater North Sea).
- Modelled time-series of the selected heavy metals and POPs depositions to 5 regions of the OSPAR maritime area (Arctic Waters, Greater North Sea, Celtic Seas, Bay of Biscay and Wider Atlantic) and to 13 sub-regions of the Region II (Greater North Sea) for each year of the period from 1990 to 2005.
- Evaluation of modelling results versus available monitoring data from the OSPAR monitoring network (CAMP) for the whole period 1990-2005. For evaluation of the PCB modelling results measurement data from the EMEP monitoring network were used.
- Contribution of key emission source categories to lead, cadmium and mercury deposition to the main regions of the OSPAR maritime area and to 13 sub-regions of the Region II (Greater North Sea).

The main results are presented in the form of maps and tables and are briefly discussed in the text below. Besides, all data products are also available on the MSC-E website (<http://www.msceast.org/ospar/>).

2. Definitions of the OSPAR regions and sub-regions

Annual deposition of selected heavy metals and POPs were calculated for the five main regions of the OSPAR maritime area and for 13 sub-regions of OSPAR Region II - Greater North Sea.

The OSPAR maritime area is divided into five main regions (see Figure 1a):

- Region I: Arctic Waters – 5.5×10^6 km²
- Region II: Greater North Sea – 7.6×10^5 km²
- Region III: Celtic Seas – 3.6×10^5 km²
- Region IV: Bay of Biscay and Iberian Coast – 5.3×10^5 km²
- Region V: Wider Atlantic – 6.3×10^6 km²

The sub-regions of OSPAR Region II - Greater North Sea are related to the Boxes of the International Council for the Exploration of the Sea (ICES) in the following way (see Figure 1b):

- Sub-region 1: ICES Box 1 – 8.1×10^4 km²
- Sub-region 2: ICES Box 2a – 6.0×10^4 km²
- Sub-region 3: ICES Box 2b – 5.2×10^4 km²
- Sub-region 4: ICES Box 3a – 4.7×10^4 km²
- Sub-region 5: ICES Box 3b – 4.0×10^4 km²
- Sub-region 6: ICES Box 4 – 4.9×10^4 km²
- Sub-region 7: ICES Box 5a – 1.8×10^4 km²
- Sub-region 8: ICES Box 5b – 3.4×10^4 km²
- Sub-region 9: ICES Box 6 – 8.5×10^4 km²
- Sub-region 10: ICES Box 7a – 9.5×10^4 km²
- Sub-region 11: ICES Box 7b – 6.8×10^4 km²
- Sub-region 12: ICES Box 8 – 6.0×10^4 km²
- Sub-region 13: ICES Box 9 – 8.0×10^4 km²

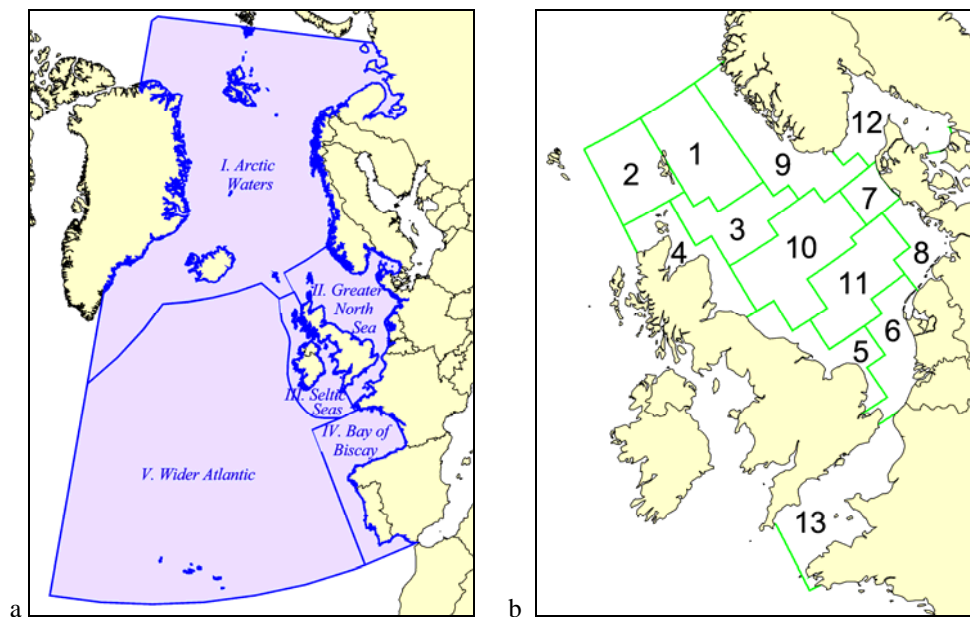


Figure 1. Five main regions of the OSPAR maritime area (a) and 13 sub-regions of the OSPAR Region II – Greater North Sea (b)

3. Short description of MSC-E heavy metal and POP models

3.1 Heavy metal chemical transport model MSCE-HM

The European-scale atmospheric transport model MSCE-HM is actively used for operational calculations of heavy metal transboundary pollution within the European region in connection with the EMEP programme and other activities relating to the LTRAP Convention. Detailed description of the model is available in Travnikov and Ilyin, (2005). The model formulation and performance was thoroughly evaluated within the EMEP/TFMM Workshop on the model review (ECE/EB.AIR/GE.1/2006/4). A brief model overview is presented below.

The EMEP/MSCE-E regional model of heavy metals airborne pollution (MSCE-HM) is a three-dimensional Eulerian type chemical transport model driven by off-line meteorological data. The model considers heavy metal emissions from anthropogenic and natural sources, transport in the atmosphere, chemical transformations (of mercury only) both in gaseous and aqueous phases, and deposition to the surface. The model computation domain is defined on the polar stereographic projection and covers the standard EMEP region by a regular grid with 50×50 km spatial resolution at 60°N. For the purpose of the model application for OSPAR calculations, the model grid was modified to cover the entire OSPAR maritime area (Figure 2). The vertical structure of the model is formulated in the sigma-pressure coordinate system. The model domain consists of 15 irregular sigma-layers and has a top at 100 hPa.

Heavy metals such as lead and cadmium and their compounds are characterised by very low volatility. It is assumed in the model that these metals (as well as some others – nickel, chromium, zinc etc.) are transported in the atmosphere only in the composition of aerosol particles. It is believed that their possible chemical transformations do not change properties of their carrying particles with regard to removal processes. On the contrary, mercury transformations in the atmosphere include transitions between the gaseous, aqueous and solid phases, chemical reactions in the gaseous and aqueous environment. The chemical scheme of mercury transformation in the atmosphere is based on the kinetic mechanism developed by Petersen *et al.*, (1998). The physical and chemical transformations of mercury include dissolution in cloud droplets, gas-phase and aqueous-phase oxidation by ozone, chlorine and hydroxyl radical, aqueous-phase reduction via decomposition of sulphite complexes, formation of chloride complexes, and adsorption by soot particles in cloud water.

Model description of removal processes includes dry deposition and wet scavenging. The dry deposition scheme is based on the resistance analogy approach (Wesely and Hicks, 2000) and allows taking into account deposition to different land cover types (forests, grassland, water surface etc.). Dry deposition of particles to vegetation is described using the theoretical formulation by Slinn (1982) and fitted to experimental data (Ruijgrok *et al.*, 1997; Wesely *et al.*, 1985). The parameterization of dry deposition to water surfaces is based on the approach suggested by Williams (1982) taking into account the effects of wave breaking and aerosol washout by seawater spray. The model distinguishes in-cloud and sub-cloud wet scavenging of particulate species and highly soluble reactive gaseous mercury based on empirical data.

MSCE-HM model is driven by off-line meteorological data pre-processed by MM5 - Fifth Generation Penn State/NCAR Mesoscale Model (Grell *et al.*, 1995). The pre-processor utilises the re-analysis of the US National Centre for Atmospheric Research (NCAR) and the US National Centres for Environmental Prediction (NCEP) or data of the European Centre for Medium-Range Weather Forecasts (ECMWF) as the input information and provides 6-hour weather prediction data along with estimates of the atmospheric boundary layer parameters with the same spatial resolution as that of the transport model.

Boundary conditions for the regional modelling, particularly, of such global pollutant as mercury were evaluated via application of the hemispheric version of the model MSCE-HM-Hem. Model domain of the hemispheric model covers the whole Northern Hemisphere with resolution 2.5° ×2.5° (Figure 3). Detailed description of the model formulation is available in Travnikov and Ryaboshapko (2002).

3.2 Multi-compartment transport model MSCE-POP

The MSCE-POP model is developed to meet the requirements of the UNECE Convention on Long-Range Transboundary Air Pollution on the evaluation of POP long-range transport and accumulation within the European region taking into account the influence of POP intercontinental transport from distant sources of the Northern Hemisphere. The model formulation and performance was evaluated during the model review carried out in the framework of EMEP Task Force on Measurements and Modelling (TFMM). One of the main conclusions of the TFMM Workshop on the Review of the EMEP Models on Heavy Metals and Persistent Organic Pollutants held in Moscow in 2005 was that MSCE-POP model represented the state of the science and was fit for the purpose of evaluating the contribution of long-range transport to the environmental impacts caused by POPs (ECE/EB.AIR/GE.1/2006/4). It was recognised that it reasonably reproduced spatial and temporal variations of observed atmospheric levels of the selected POPs in Europe and provided reasonable agreement with long-term temporal trends of air pollution at most EMEP monitoring sites. This section of the summary report presents brief description of the MSCE-POP model. Detailed description of the model can be found in MSC-E reports (Gusev *et al.*, 2005a; Gusev *et al.*, 2005b).

Two versions of MSCE-POP model (hemispheric and regional) have been developed to provide modelling results at hemispheric scale and for the European region with finer spatial resolution. The regional version of MSCE-POP model is a three-dimensional Eulerian multi-compartment model operating within the geographical scope of the EMEP region. The model computation domain is defined on the polar stereographic projection and covers the standard EMEP region by a regular grid with 50×50 km spatial resolution at 60°N. The vertical structure of the model is formulated in the sigma-pressure coordinate system and includes 15 irregular sigma-layers with the model top at approximately 15km. The MSCE-POP model domain covers practically the whole troposphere, upper layer of soil of 20 cm, and seawater compartment within the model grid. The model is driven by off-line meteorological data pre-processed by MM5 - Fifth Generation Penn State/NCAR Mesoscale Model (Grell *et al.*, 1995). The pre-processor utilises the NCAR/NCEP re-analysis or ECMWF data as the input information and provides 6-hour weather prediction data along with estimates of the atmospheric boundary layer parameters with the same spatial resolution as that of the transport model.

Hemispheric MSCE-POP model has been developed for the domain covering the entire Northern Hemisphere with a spatial resolution of 2.5°×2.5°. In the vertical direction the model domain consists of nine irregular levels up to the height of approximately 15 km. The terrain-following sigma-pressure (σ -p) coordinates are defined as a ratio of local atmospheric pressure to the ground surface pressure (Jacobson, 1999). The hemispheric model is used for the evaluation of pollution of the European region by remote sources, the estimation of the significance of POP intercontinental transport, and for assessing levels of pollution of remote regions like, for example, the Arctic region. It is also applied for the evaluation of initial and boundary concentrations for regional MSCE-POP model calculations.

The MSCE-POP model considers main environmental compartments (atmosphere, soil, seawater, and vegetation) and includes a description of basic processes of POP behaviour: emission, long-range transport, partitioning between the gaseous and particulate phase, deposition, degradation, gaseous exchange between the atmosphere and the underlying surface, as well as the processes of POP behaviour within the environmental compartments. The selection of compartments and processes is based on the current understanding of their importance with regard to the description of POP dispersion and accumulation in the environment.

For the description of removal of POPs from the atmosphere, the following processes are included into the model: dry deposition, wet scavenging, and degradation. The dry deposition scheme for particle-bound POPs is based on the resistance analogy approach and allows taking into account deposition to different land cover types (forests, seawater, and soil). The description of dry deposition of particle-bound POPs to forest is based on Ruijgrok *et al.* (1997). Two types of forest are distinguished in the model: deciduous forest and coniferous forest. For the description of POP removal with precipitation, wet deposition of POPs in gaseous and particulate phase is considered. The degradation process of POPs in the atmosphere is considered as the gas-phase reaction of pollutants with hydroxyl radicals.

To take into account the influence of POP distribution and accumulation in underlying surface and re-emission, the MSCE-POP model contains three modules, which describe processes taking place for POPs within the soil, seawater, and vegetation compartments. The gaseous exchange of POPs between the atmosphere and underlying surface (soil, vegetation, and seawater) is described on the basis of the resistance analogy. The soil module is based on a modification of the soil model

developed by C.M.J. Jacobs and W.A.J. van Pul (1996). The soil compartment is represented by the upper 20 cm soil layer, separated into seven horizontal sub-layers of different thickness. The vegetation compartment within the model is represented by the following types of vegetation: coniferous forest, deciduous forest, and grass. The information on vegetation types is based on the land cover data. The model considers the forest litter as an intermediate medium between vegetation and soil. An important feature of the MSCE-POP model is the description of POP transport within the seawater with allowance for redistribution of POPs between dissolved and particle-bound phases and sedimentation. The distinct feature of the hemispheric MSCE-POP model is a further elaborated seawater compartment module, which takes into account POP exchange between the atmosphere and seawater, ice compartment and sea ice dynamics.

In order to obtain atmospheric depositions of selected POPs in the framework of this study, both regional and hemispheric versions of the MSCE-POP model were used.

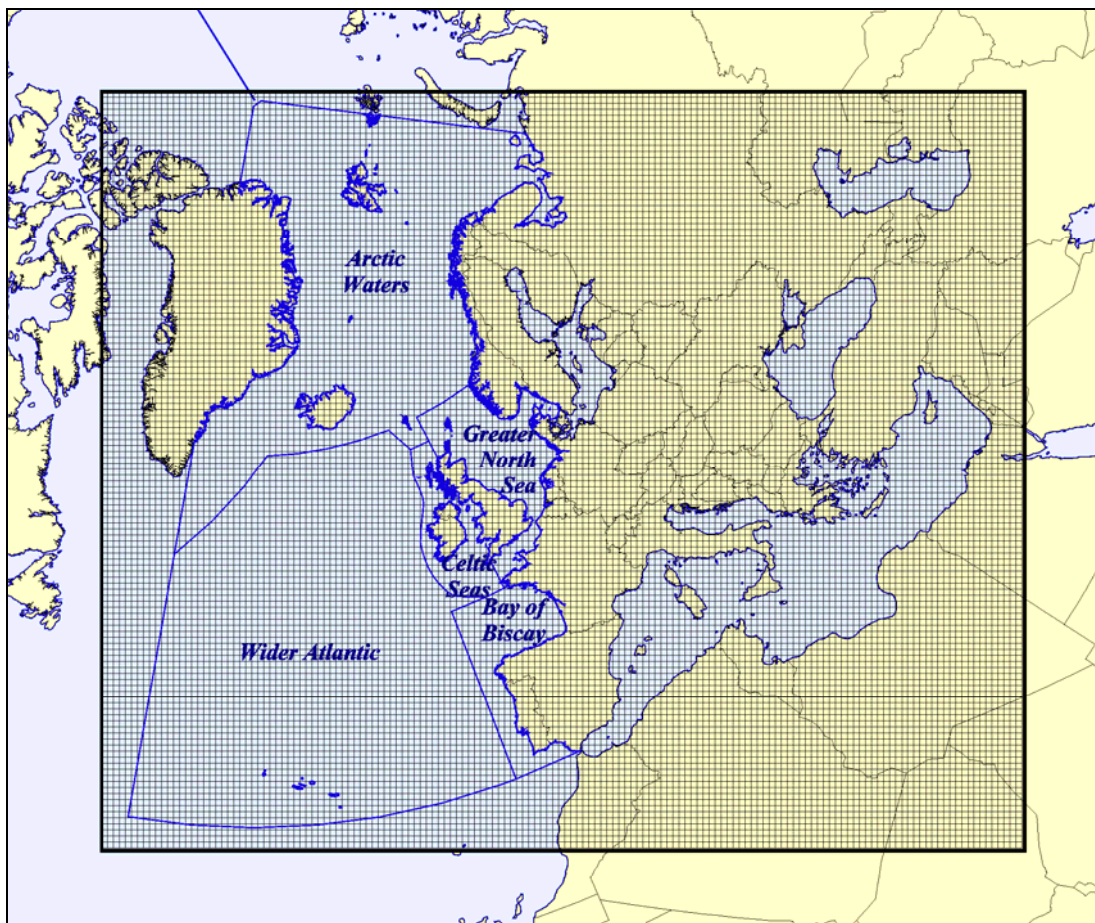


Figure 2. Modified EMEP 50x50 km grid covering Europe and the OSPAR maritime area

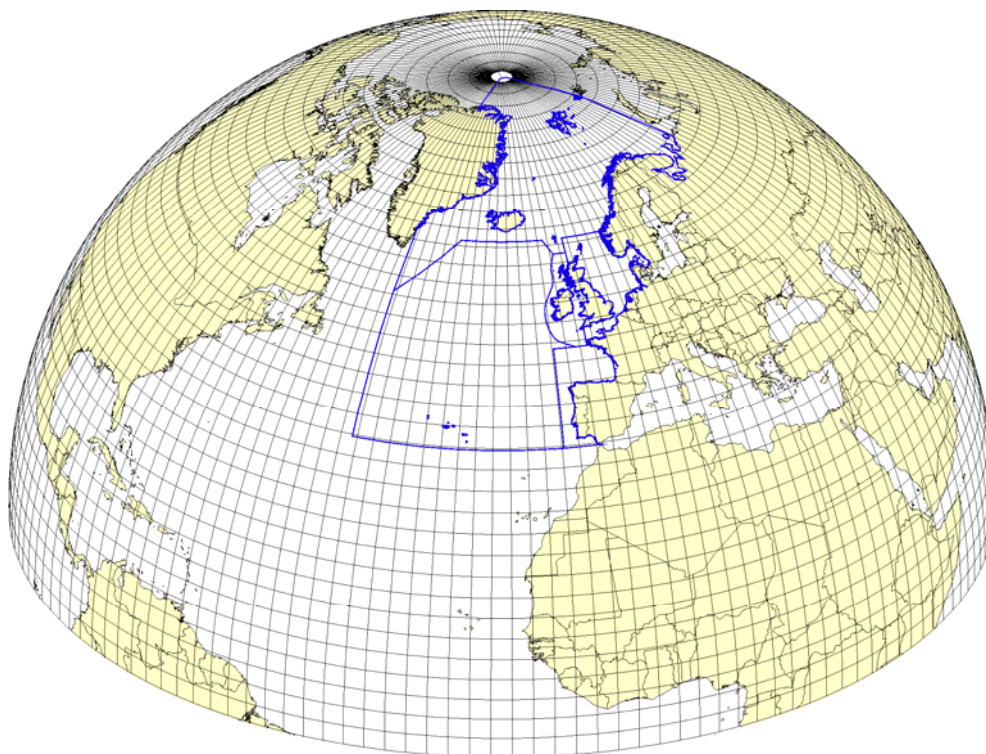


Figure 3. Hemispheric 2.5° x 2.5° model grid covering the whole Northern Hemisphere

4. Heavy metals

4.1 Atmospheric emissions of heavy metals

Calculations of atmospheric depositions of heavy metals to the OSPAR maritime area presented in this report were mostly based on emissions data officially reported by the Parties to the LRTAP Convention and available in the WEBDAB database (<http://webdab.emep.int>). All OSPAR countries are Parties to the LRTAP Convention. The gaps in officially reported data were filled with different expert estimates. Besides, a model parameterization of natural emission and re-emission of previous atmospheric depositions was applied. A short description of the utilised emissions data is presented below.

Officially reported emissions data for the period 1990 – 2005 were available for the majority of European countries (about 70% of annual totals). Gaps in time series of the reported data were filled by linear interpolation. For countries who had not submitted any national data, expert estimates were applied (Berdowski *et al.*, 1997; Denier van der Gon *et al.*, 2005). Expert estimates were also used for the spatial distribution of emission sources where no gridded national data were available.

Changes of anthropogenic emissions of lead, cadmium and mercury in the OSPAR Contracting Parties and in two other selected countries (Poland and the Russian Federation) in the period 1990 – 2005 are shown in Figures A.1, A.2 and A.3, respectively. Poland and the Russian Federation were included into the consideration because of their large contribution to heavy metal deposition over the OSPAR maritime area (Ilyin *et al.*, 2007). Numerical data on heavy metal emissions in the above-mentioned countries along with total emissions from the EMEP area are presented in Tables A.1-A.3.

Lead emissions significantly decreased during the period 1990 – 2005 in all OSPAR countries as well as in the two selected countries outside the OSPAR Convention area (Figure A.1 and Table A.1). The emission reductions varied from 61% (Poland and Portugal) to 97% (France, Iceland, Luxembourg and Norway). France was the largest emitter of lead (4283 t/y) among the OSPAR countries in 1990, whereas the most significant emission in 2005 was in Spain (266 t/y) and Portugal (244 t/y). Total emission of lead in the OSPAR countries decreased by 93% for the indicated period and amounted to 1072 t/y in 2005. The reduction of total lead emission in all EMEP countries was somewhat smaller (87%) because of less pronounced emission reduction in Central and Eastern European countries. Lead emission in Poland decreased by 61% since 1990 and amounted to 536 t/y in 2005. Emission reduction in the Russian Federation amounted to 39% for the period 1990 – 2003, however, lead emissions drastically decreased in this country almost 7 times (according to the officially reported data) between 2003 and 2004.

Changes of cadmium emissions in 1990 – 2005 are presented in Figure A.2 and in Table A.2. The highest reduction of cadmium emissions took place in the United Kingdom (84%), the lowest, in the Netherlands (18%); emissions in Portugal even increased by 6%. The largest emitters of cadmium among the OSPAR countries in 1990 were the United Kingdom, Spain and France. In spite of the fact that Spanish emissions decreased by 30% for the considered period, they remained the most significant contribution in 2005 and amounted to 16.7 t/y. Comparatively, cadmium emissions in Poland and the Russian Federation in 2005 were 46 t/y and 59.4 t/y, respectively. These national emissions are each comparable with the total emissions of all OSPAR countries in 2005 (43 t/y). Similar to lead, the cadmium emission reduction in all OSPAR countries (61%) was higher than the decrease of total EMEP emissions (50%).

Mercury emission data for the considered period are presented in Figure A.3 and in Table A.3. The reduction of mercury emissions varied from 85% (Germany and Switzerland) to 4% (Luxembourg). In contrast, emissions in Iceland and Portugal increased by 55% and 8%, respectively. The most significant mercury emissions in the OSPAR area in 1990 were in the United Kingdom (37.7 t/y), France (27 t/y) and Germany (19.2 t/y), whereas Spain became the largest emitter in 2005 (10 t/y). Total mercury emission of the OSPAR countries decreased by 68% since 1990 and amounted to 41 t/y in 2005. This is a significantly larger reduction than the total emission reduction in the EMEP countries (49%).

It should be noted that completeness and uncertainties of officially reported heavy metal emission data is an issue of significant concern within the LRTAP Convention (ECE/EB.AIR/89). The recent EMEP Workshop on uncertainties of emission inventories, monitoring and modelling for example has concluded that an improvement in the detailed activity data and emission factors is essential in order

to make significant progress in the scientific quality of heavy metal emission inventories (EMEP/TFMM/TFEIP Workshop, Dublin, October 2007). Estimates of the uncertainty associated with reported heavy metal emission data are very scarce. Available uncertainty estimates performed by national experts vary from 25% (Finland) to 260% (Denmark).

In order to assess the contribution of different emission source categories to heavy metal depositions over the OSPAR regions a complete set of gridded sector emissions data was prepared for 2005. As mentioned above, the officially reported emission data are incomplete. This is particularly related to emission data split into source sectors and information on spatial distribution of emission sources. Therefore, the reported data were supplemented with non-official expert estimates made by the Netherlands Organisation for Applied Scientific Research (TNO) (Denier van der Gon *et al.*, 2005). However, the nomenclature of emission sectors adopted within the LRTAP Convention for reporting (NFR) considerably differs from that used in the TNO inventory (which is mostly based on the EMEP/CORINAIR Selected Nomenclature for Air Pollutants (SNAP)). Therefore, the emission sectors from both datasets were aggregated in four key source categories:

- 1) Combustion in power plants and industry & Industrial processes;
- 2) Transport;
- 3) Commercial, residential and other combustion;
- 4) Waste.

The procedure for preparing the gridded sector emission data was the following. For EMEP countries, who officially reported gridded sector data, those data were taken as they are. For countries, who did not reported any national data, the gridded sector data were taken from the TNO inventory. And finally, for countries who reported national totals but did not report gridded sector data (e.g. Belgium, Ireland, Luxembourg, Norway, Poland, Portugal, and Switzerland), those data were taken from the TNO inventory but scaled to obtain the sum of the officially reported national total. This approach allows the construction of a complete gridded emission dataset which includes officially reported data as far as possible but can lead to some inconsistencies in the calculation of the contribution of emission sectors for a number of countries. In particular, the so-calculated contributions of the emission sectors to the national total can differ from those reported by a country.

The contributions of key source categories to the total emission of lead, cadmium, and mercury in the OSPAR countries and the two selected countries outside OSPAR Convention area in 2005 are presented in Tables A.4, A.5 and A.6, respectively. The category "Combustion in power plants and industry & Industrial processes" makes up the largest contribution to lead (76%), cadmium (85%) and mercury (81%) emissions in the OSPAR Convention area. The second most important source category is "Transport" (17%) for lead emissions; "Commercial, residential and other combustion" (8%) for cadmium emissions and "Waste" (13%) for mercury emissions.

In order to set up boundary conditions for the regional modelling of mercury atmospheric transport, the hemispheric version of the model was applied. For this purpose, global mercury emission datasets were used, which are available for the years 1990, 1995, and 2000 (CGEIC website; Pacyna *et al.*, 2003; Pacyna *et al.*, 2006). For the years 2001 – 2005, the emission values for the year 2000 were used. For all other years of the assessment period, emission values were derived by linear interpolation. The spatial distribution of mercury anthropogenic emissions in the Northern Hemisphere in 2000 is presented in Figure 4 together with the relative contribution of the different continents. As can be seen, the hemispheric emission of mercury is dominated by contributions from emission sources located in Asia.

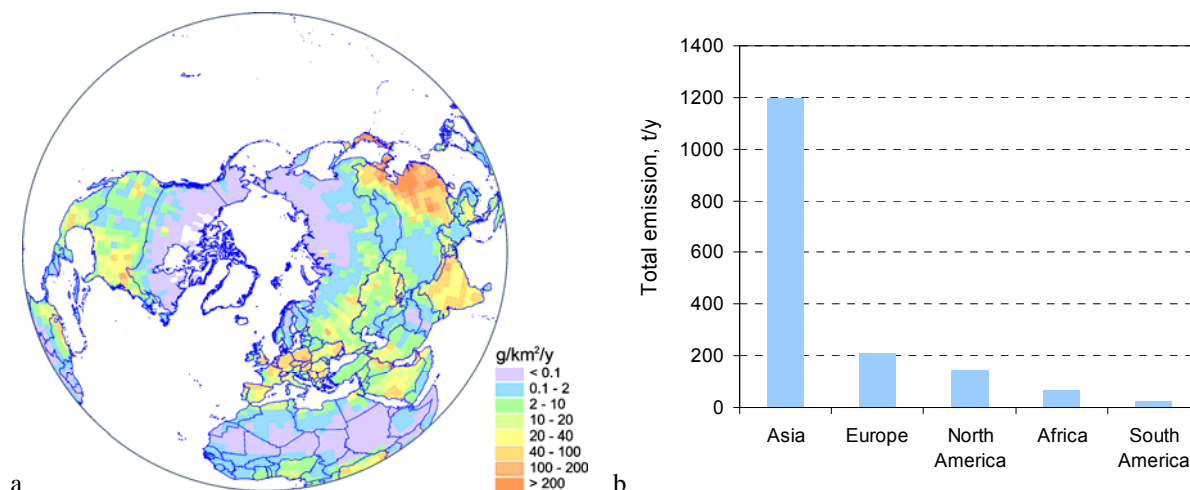


Figure 4. Spatial distribution (a) and contribution of different continents (b) to mercury anthropogenic emissions in the Northern Hemisphere in 2000

Natural emission and re-emission of mercury from soil and seawater was taken into account using global estimates by Lamborg *et al.* (2002). The spatially resolved emission flux was obtained by distributing the global emission values over the Earth's surface, depending on the soil temperature for emissions from land, and proportional to the primary production of organic carbon for emissions from the oceans (Travnikov and Ryaboshapko, 2002). It was assumed that mercury is emitted from natural surfaces in gaseous form. The temperature dependence of soil emission was described by an Arrhenius type equation with empirically derived activation energy about 20 kcal/mol (Kim *et al.*, 1995; Carpi and Lindberg, 1998; Poissant and Casimir, 1998; Zhang *et al.*, 2001). Evasion of mercury from geochemical mercuriferous belts (Gustin *et al.*, 1999) was assumed to be 10 times higher than that from background soils. Monthly mean satellite-based data on the ocean's primary production of carbon (Behrenfeld and Falkowski, 1997) were utilised to distribute the natural mercury emission flux over the ocean.

Wind re-suspension of particle-bound heavy metals (like lead and cadmium) from soil and seawater appears to be an important process affecting the ambient concentration and deposition of these pollutants, particularly in areas with low direct anthropogenic emissions. Pilot parameterization of heavy metal wind re-suspension was included in the MSCE-HM model (Gusev *et al.*, 2006; Ilyin *et al.*, 2007). The parameterization is based on the approaches widely applied in contemporary mineral dust production models (e.g. Gomes *et al.*, 2003; Zender *et al.*, 2003; Gong *et al.*, 2003). Particularly, suspension of dust aerosol from soil is considered as combination of two major processes – saltation and sandblasting – presenting horizontal movement of large soil aggregates driven by wind stress and ejection of fine dust particles, respectively. The dust suspension is estimated for non-vegetated surfaces (deserts and bare soils, agricultural soils during the cultivation period, and urban areas). The generation of sea-salt and wind suspension of heavy metals from the sea surface was also considered based on the empirical Gong-Monahan parameterization (Gong, 2003). The spatial distribution of wind re-suspension of lead for 1990 in comparison to lead emission from anthropogenic sources is illustrated in Figure 5.

Total values of natural emission and re-emission of lead, cadmium and mercury from the OSPAR maritime area are included to Tables A.1, A.2, and A.3, respectively.

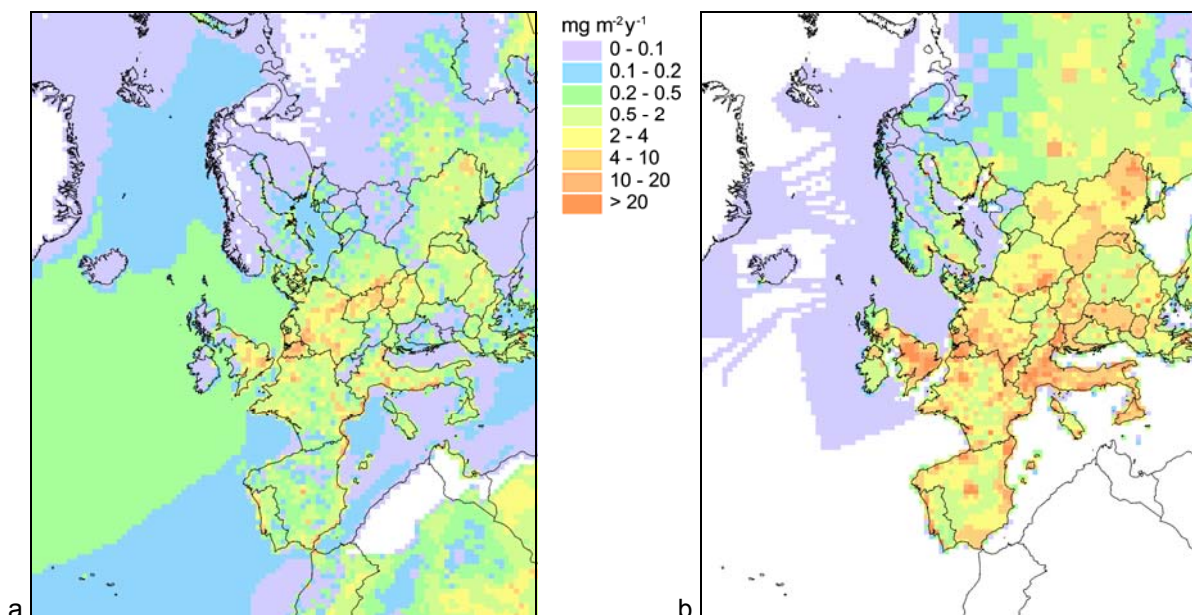


Figure 5. Spatial distribution of lead emission due to re-suspension (a) and anthropogenic emission of lead (b) for 1990, $\text{mg m}^{-2} \text{y}^{-1}$

4.2 Atmospheric depositions of heavy metals to the OSPAR maritime area

Atmospheric deposition of lead, cadmium and mercury to the OSPAR maritime area was calculated for the period 1990 – 2005. The spatial distribution of the modelled total annual deposition of each of the considered heavy metals in the five main OSPAR Regions in 2005 is presented in Figures A.4, A.6, and A.8. More detailed information on the deposition fluxes of each heavy metal over the OSPAR Region II (Greater North Sea) is presented in Figures A.5, A.7, and A.9.

Atmospheric deposition of heavy metals to the sea surface is accompanied by re-emission of the pollutants to the atmosphere. This is particularly relevant for mercury which can be easily reduced in seawater to the dissolved elemental form and evade back to the atmosphere. But the other two particle-bound heavy metals (lead and cadmium) can also be re-suspended from the ocean surface with sea salt. The re-emitted heavy metals are partly deposited to the ocean surface again, thus increasing the total deposition flux. This process leads to partial cycling of heavy metals between the atmosphere and the ocean. In order to evaluate net atmospheric input of heavy metals to the ocean, the net deposition flux was calculated as the difference between total deposition and estimated re-emission. Maps of the spatial distribution of the net deposition flux of the heavy metals are also included in Figures A.4 – A.9. However, it should be noted that this supplementary information should be taken with some caution because of the preliminary and rough character of the re-emission estimates as described in Section 4.2.

Lead depositions in 2005 have a pronounced declining gradient from Europe to the open sea westward and northward, thus demonstrating the significant influence of European emission sources (Figure A.4a). The highest depositions (more than $1.2 \text{ mg/m}^2/\text{y}$) take place over the Greater North Sea, the lowest over the high Arctic (below $0.05 \text{ mg/m}^2/\text{y}$). The relatively even distribution of lead depositions ($0.3\text{-}0.4 \text{ mg/m}^2/\text{y}$) over the Wider Atlantic can be explained by a significant contribution of wind re-suspension to lead depositions in this region which is located far from major anthropogenic sources. This fact is clearly seen from the comparison of the pattern of total deposition with the distribution of net deposition flux shown in Figure A.4b. The net deposition flux is considerably lower (below $0.2 \text{ mg/m}^2/\text{y}$) and exhibits a more marked decline towards the centre of the Wider Atlantic. In contrast, the difference between the total deposition and the net flux is less pronounced in the Greater North Sea, indicating a dominant role of anthropogenic emissions in depositions to waters in the vicinity of major emission sources (Figure A.5). Both the total deposition and the net flux have similar spatial distribution patterns in this Region, with levels decreasing from the German and Dutch coasts to the open sea. Elevated depositions are also predicted near the southern and south-western coast of Norway which is connected with the large precipitation amount in this area.

The spatial distribution of cadmium depositions in 2005 (Figure A.6a) follows that of lead depositions in general, with the highest fluxes in the Greater North Sea (more than 0.03 mg/m²/y) which decline towards the Wider Atlantic (below 0.01 mg/m²/y) and to the Arctic Waters (below 0.005 mg/m²/y). Similar to lead, a significant contribution of cadmium re-suspension with sea salt to the depositions over the Wider Atlantic results in a relatively even distribution of cadmium depositions in this region (0.008-0.01 mg/m²/y). Somewhat elevated depositions over the Central Atlantic and near the southern coast of Greenland (over 0.01 mg/m²/y) are caused by high annual precipitation amount in these areas (more than 2000 mm/y). The net deposition flux in the Arctic Waters and the Wider Atlantic does not exceed 0.003 and 0.005 mg/m²/y, respectively (Figure A.6b). In contrast, the difference between total deposition and net deposition flux is less significant for the Greater North Sea, demonstrating an insignificant role of re-suspension from seawater in this region (Figure A.7). Total deposition decreases from 0.032 mg/m²/y near the Belgian, Dutch, German and Danish coasts to 0.012 mg/m²/y in the open sea. The decline of the net flux is somewhat higher (from 0.032 to 0.008 mg/m²/y).

The deposition pattern of mercury fundamentally differs from that of lead and cadmium because of different mechanism of the dispersion of mercury in the atmosphere. In contrast to particle-bound metals, mercury is emitted and dispersed in the atmosphere in different forms: long-lived gaseous elemental form and short-lived oxidized gaseous and particulate forms. Mercury deposition in the immediate vicinity of emission sources are defined by the oxidized forms, whose atmospheric residence time varies from hours to days. In contrast, gaseous elemental mercury has a residence time ranging from months to one year and can be transported all over the globe; it forms a well mixed atmospheric pool of mercury with a very even distribution of air concentrations in remote regions (1.3-1.7 ng/m³). Besides, in the free troposphere or in marine boundary layer, elemental mercury can be oxidized by some reactive compounds (e.g. ozone, hydroxyl radical, and halogens) with following removal by precipitation or surface uptake. Thus, mercury transport and deposition to remote regions is mostly determined by elemental gaseous form.

Contrary to lead and cadmium, there is no noticeable gradient of mercury depositions from the coast to the open sea in 2005 (Figure A.8a). This can be explained by the fact that short-lived mercury forms from European sources are most deposited over the continent, whereas mercury depositions over the ocean are defined by *in situ* oxidation of elemental mercury not only of European origin but also from other continents (e.g. from Asia). Somewhat elevated depositions over the Northern Atlantic (more than 0.008 mg/m²/y) are caused by a combination of two factors: relatively high concentrations of the oxidants (first of all tropospheric ozone) and elevated precipitation amounts in this region. This becomes particularly apparent near the southern coast of Greenland, south-western coast of Norway and to the north of the British Isles where depositions exceed 0.01 mg/m²/y. The lowest depositions are in the high Arctic (below 0.003 mg/m²/y).

The net deposition flux of mercury has a similar spatial pattern as total mercury depositions, but with lower deposition values (mostly below 0.005 mg/m²/y). High net fluxes are also characteristics of the area next to the southern coast of Greenland because of low re-emission and large precipitation in this area (Figure A.8b). A distinctive feature of the mercury net flux pattern is the negative values over the coastal waters and regional seas of Europe. These negative values mean that re-emission of mercury exceeds total deposition in these areas. As mentioned in Section 4.1, it has been accepted in the model that mercury re-emission from the ocean is proportional to carbon primary production in seawater. Therefore, estimated high re-emission fluxes near the coast are determined by intensive primary production of carbon in the coastal waters (Behrenfeld and Falkowski, 1997). In general, this agrees with conclusions of the previous OSPAR assessment made for the Greater North Sea that mercury re-emission flux is at least comparable with dry and wet depositions to this region (OSPAR, Region II, 2000). In contrast, model estimates performed by Hedgecock et al. (2006) suggest that total re-emission of mercury from the Mediterranean Sea is four times higher than total deposition to its waters. However, it should be noted that the above-presented estimates of the net deposition flux contain significant uncertainties because of the very rough and preliminary character of the re-emission estimates. Some restrictions of these results are also discussed below when considering the long-term variation of the net flux.

Total atmospheric depositions and net atmospheric inputs of lead, cadmium and mercury to the OSPAR maritime area in 1990 – 2005 are presented in Figures A.10 and A.15 and Tables A.7-A.12. For the considered period, total depositions of lead decreased over all main OSPAR Regions, following the reduction of anthropogenic emissions (Figure A.10, Table A.7). The highest reduction of depositions (~2.5 times) between 1990 and 2005 occurred in Region IV (Bay of Biscay/Iberian Coast),

followed by Region II (Greater North Sea) and Region III (Celtic Seas); the lowest reduction (about 1.4 times) was calculated for Region V (Wider Atlantic). The rate of reduction of net atmospheric input ranges from about 3 times (Region IV) to about 2 times (Region V). In Regions II, III and IV, the value of net atmospheric input does not differ significantly from that of total depositions. This can be explained by close location of these regions to land-based anthropogenic emission sources. Thus, depositions from anthropogenic sources are much higher compared to wind re-suspension flux. Over Regions I and V, the net atmospheric input is about 2 – 3 times smaller than total depositions of lead. This is caused by the remoteness of those regions from main European emission sources and more significant wind re-suspension in the open sea.

The long-term variation of the total deposition and net atmospheric input of lead to the sub-regions of OSPAR Region II (Greater North Sea) are shown in Figure A.11 and Tables A.13 and A.14. Similar to the Region as a whole, the difference between total deposition and net flux in the different sub-regions is insignificant and is particularly small over the coastal waters. A comparison of long-term tendencies of total depositions to the sub-regions and the atmospheric input resulting from emissions of riparian countries washed by the North Sea (Figure A.1) indicates that these tendencies are very alike: both demonstrate distinct reduction from 1990 to late nineties and then almost stable annual values till 2005. Some years, e.g. 1996 and 2003, are exceptions. Depositions in those years demonstrate an evident increase which is not in line with long-term emission trends. It is likely that the reasons for these outliers are connected with specific meteorological conditions in those years (atmospheric circulation, precipitation amount etc.). For example, 1996 is known to exhibit a strong negative index of North Atlantic Oscillation (NAO) compared to other years of the considered period (Hurrell *et al.*, 2003). This implies that atmospheric circulation patterns changed over Europe and North-Western Atlantic, which, in turn, affected atmospheric transport of pollutants.

The total deposition of cadmium to the main OSPAR Regions exhibits a lower decline compared to that of lead (Figure A.12, Table A.9). This is caused by a less significant reduction of cadmium emissions in Europe (Figure A.2). The largest decrease, expressed as ratio between values for 1990 and 2005, took place over Region IV (around 2.5 times), and the lowest over Region V (1.3 times). The decrease of net atmospheric input varies from 2.5 times (Region IV) to 1.5 times (Region V) in the considered period. Similar to lead, annual values of cadmium net atmospheric input are slightly lower than those of total deposition in Regions II, III and IV during the entire period, whereas in Regions I and V net inputs are 2 – 2.5 times lower than the total depositions.

Total depositions and net inputs of cadmium to the sub-regions of OSPAR Region II (Greater North Sea) are demonstrated in Figure A.13, Tables A.15, A.16. The reduction of total deposition varies from 20 – 30% in the sub-regions located in the northern part of the North Sea (sub-regions 1 – 3 and 9) to almost two-fold reduction in the sub-regions next to the continental coast (sub-regions 6 – 8 and 11 – 13). Total deposition and net atmospheric input are almost the same in most of the sub-regions, except sub-regions 1 – 3 and 10, where the difference is more distinct.

The relatively stable levels of lead and cadmium total deposition during last years of the assessment period can be explained first of all by a stagnation of reductions in anthropogenic emissions in Europe since late nineties (see Figures A1 and A2). Because of the significant decrease of direct anthropogenic emissions in comparison with the early nineties (up to an order of magnitude), the role of re-suspension has considerably increased. For example, the contribution of re-suspension from land to total depositions over the OSPAR Regions in 2005 varied from 15% in the Arctic Waters and Wider Atlantic to 65% in the Greater North Sea for lead and from 10% to 55% for cadmium. The contribution of lead and cadmium re-suspension from seawater to total depositions can reach 55% in the Arctic Waters and Wider Atlantic, however, as mentioned above, it does not necessarily lead to an increase of the pollutants in the marine environment.

Long-term changes of total mercury deposition during the period 1990 – 2005 differ for various OSPAR Regions (Figure A.14, Table A.11). A gradual long-term decrease of mercury deposition took place in Regions II and III (1.5 and 1.3 times, respectively). These regions are located relatively close to European emission sources and reflect the significant reduction of anthropogenic emissions achieved in Europe (Figure A.3). The decrease of total deposition in Regions I, VI, and V, however, did not exceed 15% because of the large contribution of global emission sources. According to recent estimates of global mercury emissions (Pacyna *et al.*, 2006), in spite of significant emission reductions in Europe and North America, the global amount of mercury emissions did not change significantly during last 15 years because of emission growth in other parts of the world (e.g. in Asia). In all OSPAR Regions, net atmospheric input of mercury is significantly lower than total deposition, indicating a

significant role of re-emission. In general, long-term changes of net flux follow those of total deposition. In Region IV, the net mercury flux dropped down to negligible values in the mid-nineties and altered around zero during the following years, demonstrating a balance between deposition and re-emission in this region.

Similar indication for net mercury fluxes was obtained for some sub-regions of OSPAR Region II located in coastal areas (Figure A.15, Tables A.17 and A.18). A significant positive net flux in the beginning of the assessment period decreased gradually up to the mid-nineties because of a decrease in atmospheric deposition associated with anthropogenic emission sources, and then altered around zero for the rest of the period (sub-regions 5 – 8, 11, and 13). As mentioned above, estimates of the net atmospheric input still contains significant uncertainties because of the preliminary character of the model evaluation for mercury re-emissions from seawater. Particularly, it does not take into account possible changes of mercury concentration in seawater during the considered period due to decrease of atmospheric loads and sequential changes of re-emission fluxes. A more accurate estimate of mercury re-emission requires the application of a multi-compartment model which is planned for the near future.

Depositions of lead, cadmium and mercury in 2005 to the main OSPAR Regions and the sub-regions of Region II (Greater North Sea) from key emission source categories are presented in Figures A.16 – A.21 and Tables A.19 – A.24. As can be seen, the major contribution to depositions of all three metals to the OSPAR Regions was made by Sector 1 “Combustion in power plants and in industry and industrial processes”.

In case of lead, the contribution of Sector 1 to anthropogenic depositions in 2005 ranges from 67% in Region I (Arctic Waters) to 88% in Region IV (Bay of Biscay and Iberian Coast). The second most important sector for lead depositions is Sector 2 “Transport”. Its contribution is highest in Region I (Arctic Waters) and Region II (Greater North Sea). As for the sub-regions of the Region II (Figure A.17, Table A.20), the highest contribution of the Sector 1 took place in sub-region 5 (82%), and the lowest in sub-region 12 (57%).

The contribution of Sector 1 to anthropogenic depositions of cadmium to the OSPAR Regions in 2005 varies from 69% in Region II (Greater North Sea) to 91% in Region IV (Bay of Biscay and Iberian Coast) (Figure A.18, Table A.21). In contrast to lead, the second most important sector for cadmium depositions is Sector 3 “Commercial, residential and other combustion”. Its contribution to anthropogenic depositions is the highest in Region I (23%) and the lowest in Region IV (4.2%). In Region II, the contribution of Sector 3 can exceed 40% in sub-region 12 (Figure A.19, Table A.22).

Sector 1 also dominates mercury depositions to the OSPAR Regions from anthropogenic sources in 2005 (Figure A.20, Table A.23). Its contribution varies from 71% in Region III (Celtic Seas) to 84% in Region IV (Bay of Biscay and Iberian Coast). Sector 4 “Waste” is the second important contributor to mercury depositions. Its contribution ranges from 12% in Region I to 18% in Region III. Among the sub-regions of Region II (Greater North Sea) (Figure A.21, Table A.24), the contribution of Sector 4 is the lowest in the sub-region 12 (9%) (where it yields levels of relative contribution similar to Sector 3) and the highest in the sub-region 4 (23%).

The contributions of OSPAR Contracting Parties to the deposition of lead, cadmium and mercury in 2005 to sub-regions of Region II (Greater North Sea) are shown in Figures A.22 – A.24 and Tables A.25 – A.27. In addition, data on the contribution of Polish emission sources to the deposition of these metals are also presented because of their significance for this Region.

The total contribution of all OSPAR Contracting Parties to net inputs of lead to the Greater North Sea from anthropogenic sources is around 82%. The main anthropogenic contributor to lead depositions to most sub-regions (except sub-region 12) is the United Kingdom (Figure A.22, Table A.25). The prevalence of British sources is explained by a combination of two main reasons. Firstly, the United Kingdom is characterised by high emissions compared to emissions of other countries surrounding the North Sea. Secondly, predominating western winds provide a significant atmospheric transport from the United Kingdom towards the North Sea. Poland is the second largest contributor to lead depositions in sub-regions 1 – 4, 7, and 9, and the main contributor in sub-region 12. Although this country is located eastward from the sea, its emissions are the highest in Europe and thus its contribution to depositions to Region II is essential. France, Belgium, Germany and the Netherlands are significant contributors to depositions in sub-regions 6 – 12. The contribution of Spain and Portugal is considerable for sub-region 13.

The contribution of the OSPAR Contracting Parties to anthropogenic depositions of cadmium to the Greater North Sea makes up 72%, where as the contribution of Poland is about 20%. The emissions of cadmium in the United Kingdom are relatively high compared to other OSPAR countries (Figure A.23, Table A.26). Therefore, the United Kingdom is the main contributor to cadmium deposition in sub-regions of Region II. However, cadmium anthropogenic emissions in Poland are greater than the total cadmium emissions of all OSPAR Contracting Parties. Therefore, the contribution of Polish emission sources to cadmium deposition is significant in almost all sub-regions with highest levels in sub-regions 7, 8, 9, and 12. Cadmium deposition in sub-regions 6 and 8 are characterised by considerable influence of French, Dutch and Belgian emission sources, and those in sub-region 13 by French and Spanish emission sources.

OSPAR Contracting Parties contributed as much as 90% to total anthropogenic depositions of mercury to the Greater North Sea. Similar to lead and cadmium, the major contributor to mercury depositions to Region II is the United Kingdom (Figure A.24, Table A.27). Its contribution is the highest in all sub-regions except for sub-region 12. Denmark is the main contributor to mercury depositions in sub-region 12 and the second important contributor to depositions in the sub-region 7. Although mercury emissions in this country are relatively low, Denmark is the nearest country to these sub-regions. In sub-regions 6, 7 and 8 considerable contributions to mercury depositions are made by emission sources of Belgium, France and the Netherlands. France is the second largest contributor in sub-region 13. Unlike lead and cadmium, the influence of Polish mercury sources is not so large.

4.3 Comparison of computed versus measured deposition at OSPAR coastal monitoring stations

The verification of computed annual wet deposition fluxes and air concentrations was carried out through comparison with observation data for the parameters from the OSPAR monitoring network. Information on measured concentrations in precipitation and precipitation amounts at these stations was obtained from the CAMP database of the OSPAR Comprehensive Atmospheric Monitoring Programme (CAMP) (<http://www.nilu.no/camp>).

According to the CAMP database, there were around 30 stations involved in monitoring of wet deposition of heavy metals under the OSPAR CAMP programme during 1990 – 2005. In order to obtain reliable data for the model verification, a comprehensive quality analysis of available measurements has been performed.

Firstly, monitoring stations were evaluated based on analytical laboratory inter-comparisons performed by the Chemical Co-ordinating Centre of EMEP (e.g., Uggerud and Hjelmbrekke, 2007). According to recommendations by EMEP/CCC, lead and cadmium wet deposition data from Irish (IE1, IE2), Portuguese (PT3, PT4, PT10) and Icelandic (IS2) stations were not used, because most concentration values measured at those stations were below detection limit. Mercury measurements at stations IE1 and IE2 were also excluded for the same reason. A number of weekly measurements of lead and cadmium in precipitation at the Spanish monitoring site ES8 in 2004 were also below detection limit so that statistically reliable monthly and annual data could not be obtained. Therefore, 2004 measurements at that site were not used in the analysis. Wet deposition data from the Belgian station BE4 showed a large variation in the results of co-located measurements obtained with bulk and wet-only samplers and were characterised by high detection limit. Therefore, those data were also omitted.

Secondly, at a number of stations, monthly mean concentrations in precipitation demonstrated unexpectedly high peak values. The reasons for such outliers are likely to be connected with measurement errors (e.g. sample contamination). To exclude the monthly outliers from the calculation of annual mean values, a statistical filtration procedure has been applied (Ilyin and Travnikov, 2005). According to the procedure, the linear trend of monthly mean values was evaluated for the whole period at each monitoring station, and the standard deviation of the monthly means from the trend was assessed. Monthly mean data differing from the trend more than by three standard deviations were classified as outliers and were omitted. It should be noted that only extremely high peaks (about 1% of all data) were removed by this procedure. And finally, annual mean values were assumed to be reliable if more than seven monthly values of the whole year were available. Otherwise, an annual value was omitted.

Comparisons of measured and modelled annual wet deposition fluxes of lead, cadmium and mercury for the period 1990 – 2005 are shown in Figures A.22 – A.26. Modelled depositions of lead well agree with the observed fluxes for the majority of stations (Figure A.22, A.23), particularly for the Danish,

German, Dutch and Icelandic stations. The difference between modelled and observed values is commonly within the $\pm 50\%$ range for most of the annual fluxes. Favourable agreement between modelled and measured fluxes was also obtained for the British stations GB90, GB91, GB17, and GB13. For stations providing long-term measurements, the model managed to capture a long-term decline of wet depositions (e.g., DE1, NL9, GB90, DK31 etc.). The modelled fluxes matched the fluxes observed at Norwegian site NO39 except for one year (1997). The observed deposition value for this year is probably an outlier. The model also captures well the levels at the French station FR90 for almost all the years with the exception of 1999, 2000, and 2001. The station is located at the westernmost point of the Brittany Peninsula and influenced mainly by transport from the Atlantic. This is why either the model or the measurements do not reflect any significant long-term trend. Satisfactory results were also obtained for the Swedish stations SE97 and SE98.

At some stations, the difference between the modelled and observed fluxes is, however, significant. For example, at some British stations modelled annual fluxes were underestimated (GB93, GB94, GB14). This underestimation often takes place for the early nineties and may be connected with uncertainties of measurements. For example, at station GB93 the fluxes for succeeding years can differ 3 times, and at GB94 even 5 times. It is very unlikely that these sharp changes in pollution levels at the background stations can be explained by changes in industrial activities or by meteorological peculiarities. Underestimation of fluxes at GB14 may be connected with the uncertainties of emission data, involved in modelling. Underestimation at station NO1 can be partly connected with some underestimation of precipitation amounts at this station. Nevertheless, the model reproduces the long-term decrease of lead wet deposition fluxes at this station.

The results of the comparison of modelled and measured lead concentrations in air are shown in Figures A.27 and A.28. A relatively small difference between measured and calculated air concentrations is noted for German, Danish, Dutch and most of the British stations. Good agreement was also achieved for the Swedish site SE14, Belgian site BE14 and the Icelandic site IS91. Most of the annual mean values for the period 1990 – 2005 agree within $\pm 50\%$ limits. For the British stations GB14 and GB90, the model exhibits a much better performance for the end of considered period than for the early and mid-nineties. In addition to this, at a number of stations (e.g., DE1, DK31, GB91, and NL9), the model successfully reproduced long-term trends of lead concentrations in air.

There are some stations where the difference between modelled and measured concentrations of lead in air is relatively large. Some annual values at the Belgian site BE90 and the Spanish sites ES8 and ES9 are significantly underestimated by the model (1.5 – 3 times). At the same time, the model overestimated some annual mean values measured at the British sites in the early nineties. This can most probably be explained by uncertainties associated with anthropogenic emission and/or wind re-suspension. The model also demonstrates a systematic underestimation of measured lead concentration at the high Arctic site NO42 in the order of 1.5 – 2. This is likely to be connected with long-term transport of the pollutant to the Arctic from emission sources located in the Asian part of Russia and not taken into account in the model.

At a number of stations, favourable agreement between modelled and observed fluxes of cadmium was achieved (Figures A.24 and A.25). Both absolute values and long-term tendencies of the observed fluxes were reproduced for stations in Denmark, Germany, the Netherlands, Norway, and Iceland (DK31, DK8, DE1, NL91, NO99, and IS90). Annual variability of wet depositions at the French station FR90 was captured for almost all years, except for 1999, 2000 and 2001. In the case of lead, the observed fluxes were underestimated for the same years. This implies some common reason for both metals and requires additional investigations. Underestimation of the observed fluxes was obtained for British stations, especially at the beginning of the considered period, as well as for Swedish and Norwegian sites.

A number of possible reasons can be proposed to explain the underestimation of cadmium fluxes at a number of stations. Severe underestimation in the beginning of the nineties at some stations (e.g., at GB93 and GB94) can be connected with the uncertainties of measurements. Similar for lead, this proposed explanation is indirectly confirmed by the fact that fluxes observed in two succeeding years can differ by a factor of 2 – 7. In addition to this, observed deposition fluxes at some stations in the early nineties look suspiciously high compared to measurements at other stations. Another reason can be connected with the incompleteness and uncertainties of the officially reported emission data (see, e.g., ECE/EB.AIR/WG.5/2007/15). In order to demonstrate the effect of the emission data on the modelling results, the calculations of cadmium fluxes for 2000 were performed on the alternative expert emission data prepared within the EU ESPREME project (<http://espreme.ier.uni-stuttgart.de>).

The ESPREME emission data are higher than the official values by a factor of 2.5 for Europe as a whole and a factor of 4.3 for OSPAR countries. The comparison of modelled wet depositions based both on the official emission data and the ESPREME estimates with measurements is shown in Figure 6. As can be seen from the figure, the modelled results based on two different emission datasets differ almost by a factor of 2. The application of the ESPREME estimates provides a much better agreement with the observations of British, Swedish and Norwegian stations. For stations in Germany, Denmark and the Netherlands, it leads to an overestimation compared with the measurements.

Concentrations of cadmium in air at Belgian, German, Dutch, Spanish, Swedish and some British stations were reproduced with satisfactory accuracy by the model (Figures A.31 and A.32). Most of the calculated annual mean values match the observed values within the $\pm 50\%$ range, and long-term variability of the observed concentrations was satisfactorily reproduced. However, at a number of stations the model tends to overpredict or underpredict the measured cadmium concentrations. For example, at Danish stations the model significantly underestimated concentrations measured in the late nineties, but showed a much better performance for 2002 – 2004. At station GB14 the modelled concentrations underpredict measurements in the mid-nineties, but agree favourably after 1999. Extremely large concentrations ($2 - 3 \text{ ng/m}^3$) measured at British station GB93 in the early nineties are likely to be linked with inaccuracies of the measurements. Besides, similar to lead, the model considerably underestimates observed concentrations at the Arctic site NO42. This is probably linked with unaccounted emission sources outside the model domain.

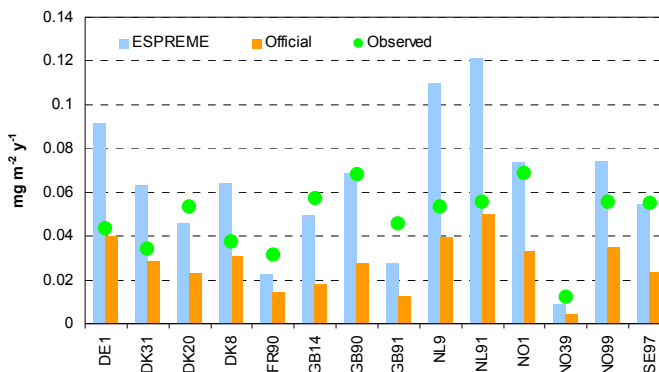


Figure 6. Comparison of modelled wet deposition fluxes of cadmium based on ESPREME and official emission data with the observations for 2000

All stations providing reliable measurements of mercury wet deposition fluxes are situated in Region II. Modelled wet deposition fluxes of mercury agree reasonably well with the observed fluxes (Figure A.26). The difference between measured and modelled annual wet deposition fluxes does not exceed 50% for the majority of stations. For some stations (SE2, DE1, NO99, and NL91) measurement time series are long enough to identify long-term trends. As can be seen, both modelled and observed wet depositions exhibit a decline for the period 1990 – 2005.

Most of the modelled annual mean concentrations of total gaseous mercury in air agree with measured concentrations within $\pm 20\%$ limits (Figure A.34). The model tends to somewhat underestimate observations at the Irish station IE31 and the Norwegian station NO99. Low spatial and temporal variability of both measured and modelled concentrations (mainly within $1.4 - 1.8 \text{ ng/m}^3$) can be explained by the long residence time of the dominant atmospheric mercury form in the free troposphere (from months to one year) that leads to a levelling out of its concentration all over the globe. Besides, according to the available estimates, global mercury emissions did not change significantly during the last fifteen years (Pacyna *et al.*, 2006).

5. Persistent organic pollutants

5.1 Atmospheric emission of POPs

The evaluation of atmospheric depositions of PCB-153 as indicator congener for the group of polychlorinated biphenyls, and γ -HCH to the OSPAR maritime area was carried out on the basis of available officially reported emission data to the EMEP emission database (<http://webdab.emep.int>) and expert estimates. To take into account the influence of intercontinental transport and re-emission of selected POPs from environmental compartments, available information from other sources on emissions within the European region and other regions of the Northern Hemisphere was used.

For the evaluation of PCB long-range transport, the global inventory of PCB usage and emission (Breivik *et al.*, 2007) was selected. The inventory provides historical emissions of PCBs to the atmosphere, obtained on the basis of available data on production and consumption of PCB mixtures and the projection of future levels of emissions up to 2100. The temporal variations of PCB emissions of individual countries have been described together with the spatial distribution of annual emissions of 22 individual PCB congeners on global scale with resolution $1^\circ \times 1^\circ$ has been prepared. To cover uncertainties in PCB emissions, the inventory includes three different scenarios of global PCB emissions, namely, minimum scenario, default scenario, and maximum scenario. The range of uncertainties of obtained PCB emission values is about one order of magnitude (Breivik *et al.*, 2002a,b). The spatial distribution of maximum PCB-153 annual emission for 2005 with resolution $1^\circ \times 1^\circ$ degree is presented in Figure 7. It can be seen that the most significant levels of PCB-153 emission fluxes are the characteristic of the European region.

Preliminary computations with the MSCE-POP model on the basis of these three emission scenarios allowed to evaluate what emission data could be used as input information for modelling, in order to achieve a reasonable description of pollution levels within the OSPAR Convention area. Taking this into account, the emission values between the maximum and default emission scenario were selected as a starting point for investigating the pollution of the Northern Atlantic by PCB-153. On the basis of this information the spatial distribution of PCB-153 emissions within the Northern Hemisphere with resolution $2.5^\circ \times 2.5^\circ$ and for the European region with resolution 50×50 km was prepared for the MSCE-POP model simulations. Since there was no information on seasonal variation of PCB emissions to the atmosphere it was assumed that it was uniformly distributed over a year.

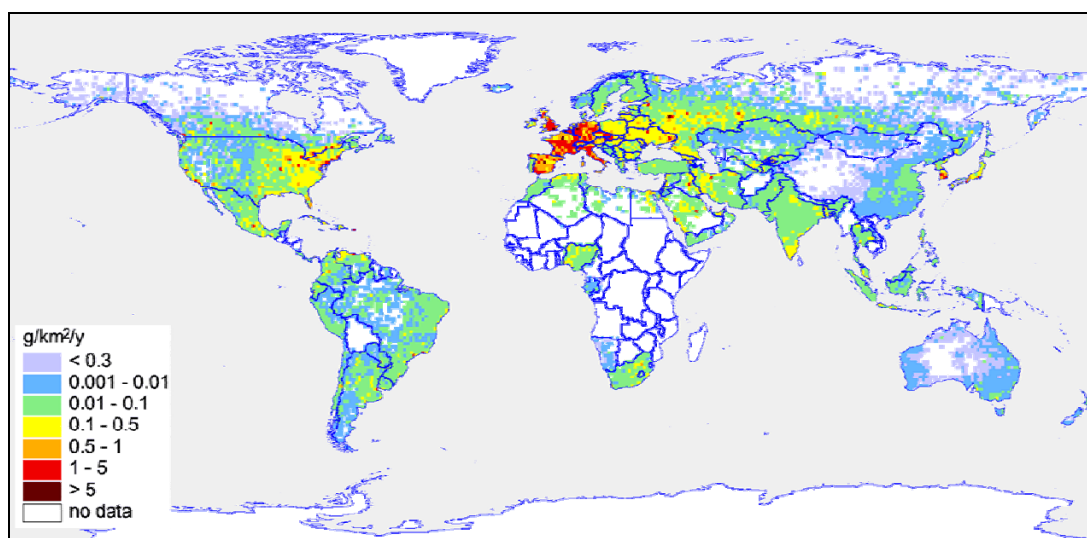


Figure 7. Spatial distribution of PCB-153 annual emission for 2005, g/km²/y

Time-series of total annual PCB-153 emissions of the OSPAR countries and the European region in the period 1990 – 2005 are presented in Figure B.1. PCB-153 annual emissions from OSPAR countries decreased in this period by 77%. Among the OSPAR countries the most significant decline of emission can be pointed out for Norway (88%), the Netherlands (87%), and Denmark (86%), while the smallest reduction took place in Belgium (47%). Emissions during this period were highest in France, Spain, Germany, and the United Kingdom. Those countries contributed about 90% to the total annual PCB-153 emission of the OSPAR countries in 2005. According to the officially reported data on PCB emission by sectors the most significant contribution to PCB emission of Germany is made up by the sub-sector “Iron and Steel production”. In case of the United Kingdom, a substantial contribution comes from the sub-sector “Capacitors, fragmentisers, transformers”. For France, the sub-sector “Commercial, residential, and other combustion” is the most important. The contribution of OSPAR countries to the total annual emission within the European region has changes from 70% in 1990 to 60% in 2005. It should be mentioned that the most significant emission fluxes within the Northern Hemisphere are characteristic of European region. Other regions are characterised by comparatively lower annual emissions.

γ -HCH is an isomer of hexachlorocyclohexane (HCH) which is an organochlorine insecticide widely used throughout the world in two main compositions – technical HCH (with a range of γ -HCH content from 8 to 15%) and lindane (containing not less than 99% of γ -isomer). The majority of the developed countries prohibited the application of technical HCH in the 1970s. Lindane applications became the basic source of γ -HCH emissions to the atmosphere. In the EU, all remaining uses of HCH and lindane (as biocide, pharmaceutical, technical intermediate etc.) have ceased by end of 2007.

The evaluation of γ -HCH atmospheric depositions to the OSPAR maritime area was carried out on the basis of emission data officially reported by OSPAR countries as Parties to the LRTAP Convention. This is supplemented by expert estimates of usage and emissions of γ -HCH within the Northern Hemisphere. It should be noted that the complete global emission inventory for γ -HCH is not currently available. Data on emissions or usage of γ -HCH for this study were compiled from several sources and cover only part of the Northern Hemisphere, so that the emission data are subject to significant uncertainties. Nevertheless, it is believed that this information permits to carry out preliminary estimates of γ -HCH pollution levels within the Northern Atlantic and the European region.

To evaluate atmospheric transport and deposition of γ -HCH, three groups of emission sources were considered: European, North American, and Chinese emission sources. The γ -HCH atmospheric emissions for the European region for 1990 – 2005 used in the model calculations are presented in Figure B.2. Available official data on γ -HCH emissions reported by Parties to the LRTAP Convention and available in the WEBDAB database (<http://webdab.emep.int>) along with expert estimates of emission and usage of γ -HCH were included in computations. Official information on HCH emission, at least for one year during 1990 – 2005, was reported by 11 EMEP countries, including 6 OSPAR countries (Belgium, Germany, the Netherlands, Norway, Spain, and the United Kingdom). In the officially reported information on emissions by Denmark, Finland, Iceland, Sweden, and Switzerland it was specified that there was no application of lindane in these countries during this period.

For countries, which did not submit official emission data or information on the application of γ -HCH, the information compiled by Pacyna *et al.* (1999) on γ -HCH usage in the period 1990 – 1996 and expert estimates of γ -HCH emission for 2000 (Denier van der Gon *et al.*, 2005) were used. According to van den Hout (1994), the emission factor for main category applications of lindane, in particular soil application, can range from 0.1 to 0.5. To obtain estimates of γ -HCH emission to the atmosphere on the basis of usage data of Pacyna *et al.* (1999), the lowest emission factor value was used which allowed a reasonable description of γ -HCH pollution levels in the atmosphere. Values of annual emissions in the period 1997 – 1999 were obtained by interpolation of emissions between 1996 and 2000. It should be stressed that estimates of γ -HCH emissions to the atmosphere and their spatial distribution are subject to significant uncertainties by a factor which can range from 2 to 5 (van den Hout, 1994).

According to this information, γ -HCH emissions to the atmosphere in OSPAR countries decreased in the period 1990 – 2005 by almost 90%. The most significant use of lindane can be noticed for France and Germany in 1990 – 1996, as well as in the United Kingdom and Spain during the whole period 1990 – 2005. The decline of γ -HCH emissions in the United Kingdom from 1990 to 2005 amounted to 85%. γ -HCH emissions in Spain increased during this period from 9 t/y to 11.5 t/y.

The γ -HCH emission values in Canada, the USA, and Mexico for 1990, and China for 1990 and 1995 were estimated on the basis of information on γ -HCH applications (Shatalov *et al.*, 2003; Li *et al.*, 1996; Li *et al.*, 2001; Macdonald *et al.*, 2000; and Gusev *et al.*, 2005b). For Canada, the USA and Mexico for 2000 and 2002, expert estimates of γ -HCH emission prepared by Li (2004) were used. According to Li (2004), the emissions of γ -HCH in North America amounted to 81 t in 2000.

The spatial distribution of γ -HCH emissions within the European region was obtained from the officially submitted data of Belgium, Germany, and Spain, and from expert estimates (Pacyna *et al.*, 1999; Denier van der Gon *et al.*, 2005). The gridded γ -HCH emissions for North America was prepared by Li (2004). For the evaluation of the spatial distribution of γ -HCH emissions in China over the $2.5^{\circ} \times 2.5^{\circ}$ calculation grid, data on cropland area was used from the Canadian Global Emissions Interpretation Centre (<http://www.ortech.ca/cgeic>). The spatial distribution of γ -HCH annual emissions for 2005 within the Northern Hemisphere is presented in Figure 8.

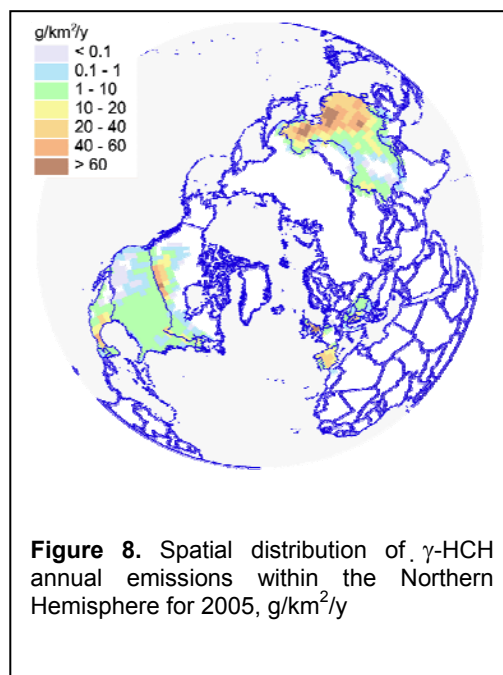


Figure 8. Spatial distribution of γ -HCH annual emissions within the Northern Hemisphere for 2005, $\text{g}/\text{km}^2/\text{y}$

5.2 Atmospheric depositions of POPs to the OSPAR maritime area

Bearing in mind the global character of the dispersion of PCB-153 and γ -HCH, emission sources located within the entire Northern Hemisphere were taken into account for a proper evaluation of PCB-153 and γ -HCH deposition levels to the OSPAR Regions. Due to the persistence of those pollutants in the environmental media, their accumulation in seawater and soil within a sufficiently long preceding period was considered. Such accumulation can lead to considerable re-emission fluxes from the media, and influence air concentration levels and, consequently, deposition fluxes. Therefore the evaluation of long-range transport and accumulation was carried out for PCB-153 for the period 1970 – 2005 and for γ -HCH for the period 1985 – 2005, with the help of a combined hemispheric/regional modelling approach. The results of the hemispheric MSCE-POP model simulations were used to obtain initial and boundary conditions for the regional MSCE-POP model runs.

Atmospheric depositions of the indicator congener PCB-153 and γ -HCH to the OSPAR maritime area were evaluated for the period 1990 – 2005 on the basis of available official emission data supplemented by expert estimates. Time-series of annual total depositions to the OSPAR Regions and to the 13 sub-regions of the Greater North Sea (Region II) are shown in Figures B.5 – B.8.

The spatial distribution of total annual depositions of PCB-153 and γ -HCH in 2005 is shown in Figures B.3 and B.4. Atmospheric deposition of PCB-153 and γ -HCH is accompanied by re-emission flux to the atmosphere. To evaluate net atmospheric input of these POPs to the oceanic surface, the net deposition flux from the atmosphere to seawater was calculated as the difference between direct deposition and re-emission fluxes. The spatial distribution of net annual deposition of PCB-153 and γ -HCH in 2005 to the OSPAR Regions is presented in Figures B.3 and B.4, respectively.

The levels of PCB-153 total depositions in 2005 are highest in Region II (Greater North Sea) with $5 \cdot 10^{-5} \text{ mg}/\text{m}^2/\text{y}$ and higher close to main European emission sources. They have a pronounced declining gradient from the coast to the open sea in northern and western directions. The lowest values of net deposition are characteristic for Region I (Arctic Waters) with about $1 \cdot 10^{-5} \text{ mg}/\text{m}^2/\text{y}$ and lower. Typical values of the total deposition flux in the Arctic Waters (Region I) and the Wider Atlantic (Region V) is between $1 \cdot 10^{-5} \text{ mg}/\text{m}^2/\text{y}$ and $3 \cdot 10^{-5} \text{ mg}/\text{m}^2/\text{y}$. The net deposition flux for PCB-153 has a similar spatial pattern but with lower values than total deposition. Some sub-regions of the Greater North Sea (sub-region 12) and a considerable part of the Celtic Sea (Region III) are even characterised by negative levels of net deposition flux in 2005. Spatial pattern of γ -HCH total deposition in 2005 is, in general, similar to the spatial distribution of PCB-153 total deposition. It is

characterised by high values of deposition flux in Region II (Greater North Sea) with values of $1 \cdot 10^{-3}$ – $3 \cdot 10^{-3}$ mg/m²/y. Deposition levels are decreasing to the north up to a range of $1 \cdot 10^{-4}$ – $2 \cdot 10^{-4}$ mg/m²/y in the Arctic Waters (Region I) and to the west up to a range of $2 \cdot 10^{-4}$ – $5 \cdot 10^{-4}$ mg/m²/y in the Wider Atlantic (Region V). Slightly negative values of net deposition flux are obtained for a part of sub-region 12 of the Greater North Sea.

Long-term trends of total depositions and net deposition fluxes for PCB-153 and γ -HCH in the period 1990 – 2005 are presented in Figures B.5 – B.8. For the considered period, the factor of decline of PCB-153 total deposition following emission reduction varies from 3.3 to 3.7 (Figure B.5). Maximum reduction of PCB-153 total deposition took place in the Wider Atlantic (3.7 times). The reductions of net deposition flux are more pronounced than those of total depositions and reach a factor of 4 in most of the Regions. The comparison of trends of total deposition with that of net deposition fluxes shows that, even in the Regions with positive values of net deposition, the process of re-emission can essentially contribute to the exchange between the atmosphere and seawater. In such Regions, as the Bay of Biscay and the Greater North Sea, the value of re-emission flux reaches about a half of the total deposition. It might be noted that these regions are quite close to Germany, France and the United Kingdom where PCB-153 emissions significantly declined in the assessment period. Thus, in the case of significant emission reductions, the re-emission from the environmental media can become a natural emission source comparable in magnitude to anthropogenic emissions. Long-term trends of total deposition and net annual input of PCB-153 to the sub-regions of OSPAR Region II (Greater North Sea) in the period 1990 – 2005 are shown in Figure B.6. Similar to Region II as a whole, a decrease of total deposition and net deposition flux took place in all the sub-regions (3.2 – 3.9 times). Maximum reduction (3.9 times) took place in sub-region 7. A significant decrease of total deposition (3.6 – 3.7 times) is characteristic for sub-regions 4, 5, 8, and 9. For a number of sub-regions, re-emission gained substantial influence, in particular towards the end of the assessment period.

Considering the temporal variations of γ -HCH total deposition to the OSPAR maritime area in the period 1990 – 2005, a significant decline in the deposition by a factor ranging from 5.5 to 9.3 depending on the OSPAR Region can be pointed out. The most pronounced decrease in total deposition took place in the Greater North Sea (9.3 times) and the Bay of Biscay. Both regions are located close to European emission sources. A slightly smaller decrease was obtained for the Celtic Sea (about 7 times). It might be noted that the Regions with maximum deposition decrease are also characterised by significant re-emission fluxes (about 30 – 50% of total deposition). Total deposition and net deposition flux to the sub-regions of the OSPAR Region II (Greater North Sea) within the period 1990 – 2005 are shown in Figure B.8. Similar to the depositions over the Region as a whole, a substantial decline of depositions took place in the sub-regions of Region II (7 – 17 times). Maximum reduction is obtained for sub-region 8 (about 17 times). Strong reductions of total deposition took place in sub-regions 4, 12, and 7. All these sub-regions are located near Germany, Norway and the United Kingdom, the countries with strong emission reductions. At the same time the reduction of total deposition in sub-regions 6 and 13 is less pronounced. This might be explained by the influence of emissions from France. The comparison of the plots of net deposition flux and total deposition shows also that for a number of sub-regions, the re-emission flux can reach 50% and more of the total deposition. In particular in sub-region 12, the re-emission flux compensates total deposition at the end of the assessment period.

5.3 Comparison of computed versus measured deposition at monitoring stations

For the verification of the obtained modelling results for γ -HCH, a comparison of computed annual wet deposition fluxes with measurements of the OSPAR CAMP monitoring network was carried out. Information from 11 CAMP monitoring stations on measured concentrations of γ -HCH in precipitation, deposition fluxes, and precipitation amounts was obtained from the CAMP database (<http://www.nilu.no/camp>) and used for the comparison. In spite of the fact that for a number of stations a significant number of measured concentrations in precipitation was below detection limit, measurements of all these sites were used for the comparison.

The results of the comparison of measured and computed annual wet deposition fluxes of γ -HCH for the period 1990 – 2005 are shown in Figure B.9. In general, measured and computed γ -HCH annual wet deposition fluxes agree. For most of the sites, the model reproduces reasonably well temporal

variations of measured wet deposition fluxes. In particular, computed values are in good agreement (on average about a factor of 2 or better) with long-term measurements at stations DE1, NO99, SE12, and IE2. Reasonable agreement is also obtained with the observed deposition fluxes at the stations NO1 for 2004 and 2005 and at station DK31 for 1990 – 1992. The model predictions of deposition fluxes for the site SE14 for 2003 – 2005 overestimate measured values slightly more than a factor of 2 with the exception of 2002, which is probably an outlier.

More substantial differences between computed and observed deposition fluxes of γ -HCH were obtained for the sites BE4, BE14, NL91, and IS91. On average, the model underestimates measured deposition fluxes at the sites BE4, BE14, and NL91 by a factor of 2 – 5. It is likely that γ -HCH emissions of France and Belgium, which can significantly influence observed levels at those sites, have essential uncertainties and are possibly underestimated. There is a need to note that a significant part of measured concentrations in precipitation at BE4, BE14, and NL91 in the assessment period were below detection limit. So the actual concentrations and fluxes could be somewhat lower than the reported estimates. In case of station IS91, the model significantly overestimates observed levels of wet deposition fluxes. This overestimation might be caused by the overestimation of boundary concentrations, as well as by other reasons related to model parameterisation of γ -HCH removal processes or representativeness of measurements of this site. However, the clarification of this disagreement requires further analysis.

A comparison of γ -HCH concentrations in air was carried out with measurements of 7 CAMP monitoring sites (IS91, NO42, NO1, NO99, SE2, SE12, and SE14) from CAMP database. Reasonable agreement between measured and computed γ -HCH annual mean air concentrations, mostly within a factor of 2, is obtained with long-term measurements at sites NO42, NO99, and SE12 (Figure B.11). Computed air concentrations agree with measurements at the stations NO1, SE2, and SE14 within a factor of 2 – 3. Similarly to wet deposition fluxes, the model overestimates measured γ -HCH in air at the site IS91 in the period 1995 – 2000 which can be due to overestimation of boundary concentrations. At the same time, the agreement between measured and computed concentrations for the period 2001 – 2005 is better, remaining within a factor of 2 on average.

Since under the OSPAR CAMP programme measurements of PCB concentrations have not been performed, the data from EMEP monitoring sites on PCBs were used for the verification of obtained modelling results. Information on measured concentrations of PCB-153 in precipitation, deposition fluxes, and precipitation amounts of 8 monitoring stations were obtained from the database of the Chemical Co-ordination Centre (CCC) of EMEP (<http://www.nilu.no/projects/ccc/emepdata.html>) and used for the comparison. Similar to γ -HCH all available measurement data were used for the comparison and no filtering of measurements was performed.

Results of the comparison of measured and computed annual wet deposition fluxes of PCB-153 obtained in this study for the period 1990 – 2005 are shown in Figure B.10. In general, reasonable agreement can be noted between measured and computed PCB-153 annual wet deposition fluxes. Most of these measurements were performed in the period 1995 – 2005. The model predictions of temporal variations of deposition fluxes closely reflect the variations of observed fluxes for most of the sites (DE1, DE9, NO1, SE2, SE14, and SE12). The differences are within a factor of 3 with the exception for the years 1998 – 2001 where more significant disagreement can be noted. Uncertainties in the description of temporal variations of PCB-153 emission during this period might be one of the reasons for such disagreement. Good agreement (within a factor of 3) between computed and observed deposition fluxes is obtained for the site FI96 with the exception for the year 1996.

The discrepancies between computed and observed deposition fluxes for DE1 and DE9 are most likely connected with the uncertainties in temporal variations of emissions in this period and their spatial distribution. In case of station SE12, the model significantly overestimates wet depositions for 2004 and 2005 by a factor of 3 – 6. This is most likely connected with the uncertainties in temporal variations of emissions in this period and their spatial distribution. Similar to γ -HCH significant differences in PCB-153 deposition fluxes are obtained for the site IS91. The overestimation might be caused by overestimated boundary concentrations provided by the hemispheric model version, uncertainties in model parameterisation of PCB-153 removal processes or representativeness of measurements of this site.

PCB-153 air concentrations were compared with measurements of 7 monitoring sites (IS91, NO42, NO1, SE2, FI96, SE12, and SE14) from the EMEP database (Figure B.12). Computed air concentrations of PCB-153 reasonably agree with measurements obtained at sites NO1, FI96, SE14,

and NO₄₂ for the period 2000 – 2005. More significant deviations about a factor of 2 – 3 were obtained for the sites SE2 and SE12. Similar to wet deposition fluxes, the model overestimates measured PCB-153 in air at the site IS91 which can be due to overestimation of boundary concentrations.

6. Uncertainty of model estimates

The uncertainty of model estimates is determined by different factors including restrictions of the model formulation and inaccuracies of input parameters (emissions, meteorological data etc.). Discrepancies between modelled values and observations are also caused by uncertainty of measurement data. An analysis of the sensitivity and uncertainty of the MSC-E heavy metal and POP models has been performed in the framework of the models review activity (ECE/EB.AIR/GE.1/2006/4).

A detailed analysis of the heavy metal model (MSCE-HM) performance was published in Travnikov and Ilyin (2005) and included in an extensive sensitivity study and uncertainty analysis. Sensitivity of the main model outputs was evaluated with regard to variation of emission data, meteorological parameters, boundary conditions, removal processes and characteristics of chemical transformations. The overall model uncertainty was assessed based on the uncertainties contributed by individual parameters and using the simple “square root approach”. Only the stochastic component of the uncertainty of the model input parameters was considered. A possible influence of the systematic error (e.g. possible underestimation of anthropogenic emissions) was not taken into account.

Table 1 presents estimates of the overall uncertainty of heavy metal deposition fluxes over the five main OSPAR Regions based on the analysis data described in Travnikov and Ilyin (2005). As can be seen, the uncertainty of modelled lead and cadmium depositions varied from 46% in Region II (Greater North Sea) to 52% in Region V (Wider Atlantic). The largest contributions to the overall model uncertainty is made by anthropogenic emissions, natural emission and re-suspension, and by meteorological parameters. The contribution of the uncertainty associated with re-suspension prevails in the remote Regions (Arctic Waters and Wider Atlantic), whereas inaccuracy of anthropogenic emissions is the most important factor of uncertainty for the North Sea which is located close to major emission sources.

Table 1. Overall uncertainty of estimated deposition fluxes of heavy metals over the five main OSPAR Regions. Values in parenthesis present 90% confidence interval of the uncertainty variation over the region. Units: percents

OSPAR Region	Lead and cadmium	Mercury
I. Arctic Waters	49 (34-64)	47 (35-59)
II. Greater North Sea	46 (26-63)	42 (24-57)
III. Celtic Seas	49 (31-63)	41 (28-53)
IV. Bay of Biscay	49 (28-67)	42 (23-58)
V. Wider Atlantic	52 (32-70)	48 (30-64)

The model uncertainty of mercury depositions varies from 41% in Region III (Celtic Seas) to 48% in Region V (Wider Atlantic). In contrast to lead and cadmium, the overall model uncertainty of mercury depositions is to a significant extent defined by uncertainties of boundary conditions and parameters of chemical reactions (oxidation of elemental mercury by ozone and OH radical). However, inaccuracies of anthropogenic emissions and their chemical speciation are still very important in the Regions located close to the coast (North Sea, Celtic Seas, and Bay of Biscay).

The description of long-range transport and depositions of POPs in the MSCE-POP model includes additional processes like gas-particle partitioning, degradation, and gaseous exchange with underlying surface and vegetation. Accuracy of the description of these processes within the model and of information on pollutant-related parameters significantly influences the quality of model output.

The analysis of the sensitivity of the MSCE-POP model output to a variation of pollutant-specific and environmental parameters was performed on the example of PCB-153 and is presented in Gusev *et al.* (2005a). It was found that the computed air concentrations and depositions were significantly sensitive to variations of ambient temperature and the parameters important for the description of deposition and re-emission processes, in particular the Henry’s law constant, washout ratio for aerosol

phase, and octanol/water partition coefficient. The uncertainty of computed depositions due to the variation of these parameters can reach 50% – 70% in remote regions.

In addition to this, the results of the verification of the MSCE-POP model computations on PCB-153 and γ -HCH, using available measurements presented in this report, can be considered. In particular, the comparison of model estimates with measurements revealed that the MSCE-POP model reasonably reproduced spatial and temporal variations of PCB-153 and γ -HCH air concentrations and depositions. On average, the agreement between computed and measured air concentrations and depositions is within a factor of 2 – 4.

7. Comparison of estimated depositions with results of previous studies

The computed depositions to the OSPAR Regions were compared with the results of previous studies. Particularly Nijenhuis *et al.* (2001) computed depositions of various heavy metals, including lead and cadmium, to the OSPAR Regions for 1990, using the EUTREND model. Depositions of lead and cadmium estimated for 1990 with the MSCE-HM model are significantly higher than those calculated by the EUTREND (Table 2). The highest difference is noted for Region I (Arctic Waters) and Region V (Wider Atlantic); the smallest difference is in Region II (Greater North Sea) and Region IV (Bay of Biscay). There are several reasons to explain the differences.

First of all, the EUTREND model domain did not cover Regions I and V entirely (Nijenhuis *et al.*, 2001). Hence, for these two regions the EUTREND should underestimate total depositions. Most probably Nijenhuis *et al.* (2001) did not take into account the contribution of natural emissions and re-suspension to lead and cadmium depositions either. According to the current estimates, the contribution of these processes can even exceed the contribution of direct anthropogenic emissions over remote regions (such as the Arctic and the wider Atlantic). This proposed explanation is confirmed by the fact that the discrepancy between the two estimates is less significant in the Regions located closer to the emission sources (Regions II, III, and IV).

Table 2. Depositions of lead (a) and cadmium (b) to the OSPAR Regions in 1990 calculated with the MSCE-HM model (this study) and with EUTREND models (Nijenhuis *et al.*, 2001)

OSPAR Region	Lead		Cadmium	
	MSCE-HM	EUTREND	MSCE-HM	EUTREND
I. Arctic Waters	1491	235	34.6	2.6
II. Greater North Sea	1689	915	27.2	8.7
III. Celtic Seas	442	152	8.6	1.5
IV. Bay of Biscay	633	507	12.8	4.5
V. Wider Atlantic	3111	346	73.7	3.5

Modelled time series of depositions to Region II (Greater North Sea) were also compared with the measurement-based estimates of total depositions of lead, cadmium and mercury published in OSPAR, Region II (2000). It is worth mentioning that the estimation of depositions to the sea surface on the basis of measurements is somewhat uncertain. Firstly, measured deposition fluxes commonly do not include a dry deposition component. Secondly, measurements are carried out at only few monitoring stations. And finally, the monitoring stations are located on the coast, whereas almost no measured data are available for the open sea. Nevertheless, the depositions of lead and cadmium to Region II (Greater North Sea) calculated by the MSCE-HM model and those estimated from monitoring data for the period 1990 – 1995 are in satisfactory agreement (Figure 9a, b). The model somewhat overestimates total depositions of lead, most probably because of additional dry depositions which are not taken into account in the measurement-based estimates. Computed depositions of mercury are 1.5 – 3 times higher than those estimated from measurements (Figure 9c). The stations, where monitoring of mercury during 1990 – 1995 was performed, were located mainly on the Danish, Swedish and Norwegian coasts, where atmospheric depositions were lower compared to other parts of the Northern Sea (e.g. near the coast of the United Kingdom, Belgium or the Netherlands). Therefore, mercury depositions derived from those measurement data may be underestimated.

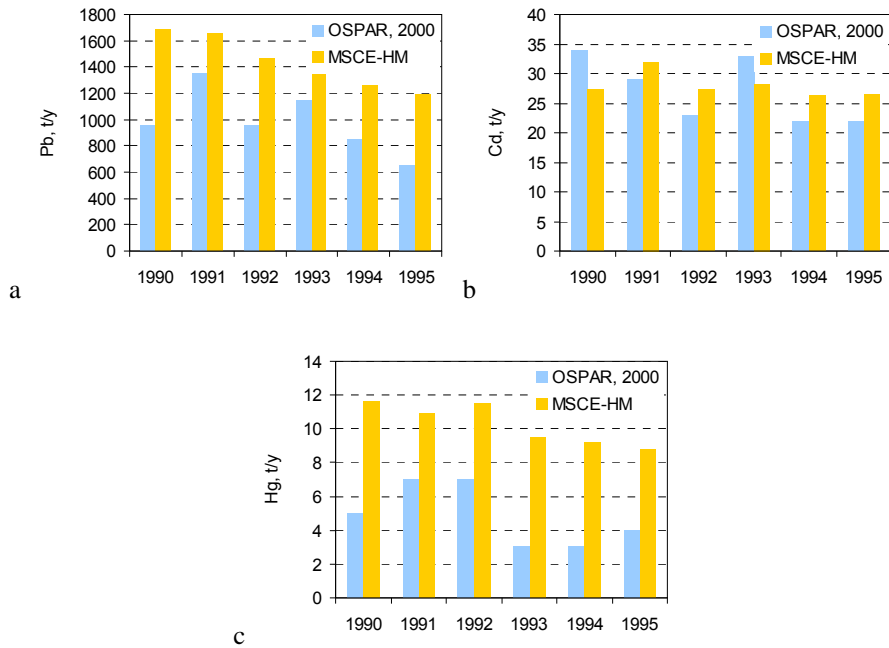


Figure 9. Depositions of lead (a), cadmium (b) and mercury (c) to Region II (Greater North Sea) modelled by MSCE-HM model and derived from monitoring data (OSPAR, Region II, 2000).

According to the estimates presented in this report the net depositions of PCB-153 to the OSPAR maritime area decreased from about 1 t/y to 0.25 t/y in the period 1990 – 2005. To compare these modelling results with other studies, the estimates of PCB deposition presented in OSPAR, Region II (2000) can be used. According to these estimates, the atmospheric input of seven PCBs with precipitation to the OSPAR maritime area is accounted for 3 - 7 t/y in the period 1992 – 1994. Taking into account that the contribution of emissions of PCB-153 in 1992 – 1994 to the total annual emissions of seven PCB congeners (28, 52, 101, 118, 138, 153, and 180) is about 12%, the computed annual net deposition of seven PCBs could be about 6.5 – 7.25 t/y.

The net annual γ -HCH deposition to the Greater North Sea can be compared with the estimates obtained in the framework of the ESQUAD study (van den Hout, 1994). According to this work, annual γ -HCH depositions to the North Sea (area 525 000 km²) for 1990 were estimated to be 6.2 t/y. Net annual γ -HCH depositions to the Greater North Sea obtained using the MSCE-POP model changed from 8.8 t/y in 1990 to 0.9 t/y in 2005. Thus the value of depositions for 1990 is rather close to the estimates presented in the report of ESQUAD project.

8. Conclusions

A model assessment of atmospheric deposition of three heavy metals (lead, cadmium and mercury) and two persistent organic pollutants (PCB and γ -HCH) to the OSPAR maritime area has been performed for the period 1990 – 2005. Annual depositions for each year of the period were calculated for the main Regions of the OSPAR maritime area and for 13 sub-regions of OSPAR Region II (Greater North Sea). Furthermore, the contribution of key emission source categories to the deposition of lead, cadmium and mercury to the OSPAR Regions was assessed. The modelling results were evaluated against available monitoring data from the OSPAR monitoring network (CAMP).

Heavy metals

- Lead, cadmium, and mercury emissions significantly decreased in most OSPAR countries during the period 1990 – 2005. The highest emission reductions were noted for lead (from 61% to 97%). Changes of cadmium emissions varied from reductions of 84% to an increase of 6% in the different OSPAR countries. For mercury, the variation of changes in emissions was even higher, ranging from a 85% reduction to a 55% increase. The total emissions of lead cadmium, and mercury of all OSPAR countries decreased by 93%, 61%, and 68%, respectively. This is higher than the emission decrease in Europe as a whole because of less pronounced emission reductions in Central and Eastern European countries.
- The total depositions of lead and cadmium in 2005 to the OSPAR maritime area demonstrate a pronounced decline from the European coast to the open sea westward and northward (from 1.2 to 0.5 mg/m²/y for lead and from 0.03 to 0.005 mg/m²/y for cadmium). This can be explained by the significant influence of European emission sources. The net deposition flux is considerably lower and exhibits a more marked decline towards the centre of the Wider Atlantic (down to 0.01 and 0.003 mg/m²/y, respectively).
- The spatial distribution of total mercury depositions in 2005 does not exhibit a distinct gradient from the European coast towards the open sea, mainly because of the significant impact of global mercury transport from other continents on the depositions to the OSPAR maritime area. Somewhat elevated depositions to the Northern Atlantic (more than 0.008 mg/m²/y) are caused by relatively high concentrations of the oxidants and elevated precipitation amounts in this Region. The net deposition flux of mercury has a similar spatial pattern but with lower deposition values (mostly below 0.005 mg/m²/y). A distinctive feature of the estimated mercury net flux pattern is the negative values for the coastal waters and regional seas of Europe.
- Both the total depositions and the net atmospheric input of lead and cadmium to the five OSPAR Regions decreased during the period 1990 – 2005, following emission reductions in Europe. The highest decrease of total depositions took place in Region IV (Bay of Biscay) reaching up to 60% for lead and cadmium. The lowest decrease was obtained for Region V (Wider Atlantic) and amounted to 30% for lead and 25% for cadmium. In general, the decrease in depositions was somewhat lower than that in emissions because of the effect of wind re-suspension of previous atmospheric depositions accumulated in soil and seawater.
- A gradual long-term decrease of mercury deposition during the period 1990 – 2005 took place in Region II (Greater North Sea) and Region III (Celtic Seas) amounting to 35% and 25%, respectively. At the same time, the decrease of total deposition in other OSPAR Regions did not exceed 15% because of large contributions from global sources. In all the Regions, net atmospheric input of mercury is significantly lower than total deposition which indicates the significant role of re-emission. In the coastal areas, the estimated net atmospheric input of mercury dropped to a negligible level in the middle of the assessment period and altered around zero during the following years, demonstrating a balance between depositions and re-emission.
- The key emission source category “Combustion in power plants and in industry and industrial processes” was the largest (70 – 90%) contributor to depositions of lead, cadmium and mercury to the OSPAR Regions and the sub-regions of the Greater North Sea. The second most important contributor varies for the different metals: “Transport” for lead, “Commercial, residential and other combustion” for cadmium, and “Waste” for mercury.
- Modelled wet deposition fluxes of lead, cadmium and mercury are in satisfactory agreement with most annual mean measured values. The most reasonable agreement between modelled and observed fluxes was obtained for stations in Denmark, Germany, Norway, France and Iceland.

Model estimates of lead and mercury depositions reproduced well both general values and long-term changes of observations. Calculated cadmium depositions underestimated the measured depositions at a number of stations, which is likely to be linked with uncertainties of available emission data, uncertainties of model parameterisation of wind re-suspension, and inaccuracy of measurements at the very beginning of the assessment period.

Persistent Organic Pollutants

- Annual emissions of PCB-153 from OSPAR countries essentially decreased by 77% in the period 1990 – 2005. Among the OSPAR countries, the most significant decline of emissions can be noted for Norway (88%), the Netherlands (87%), and Denmark (86%), while the lowest changes took place in Belgium (47%). The highest emissions during this period were characteristic for France, Spain, Germany, and United Kingdom.
- According to officially reported emission data and expert estimates, γ -HCH emission to the atmosphere decreased in period 1990 – 2005 by almost 90% in OSPAR countries. The most significant γ -HCH emissions can be noted for France and Germany in 1990 – 1996, as well as for the United Kingdom and Spain during the whole period 1990 – 2005. γ -HCH emissions of the United Kingdom declined by 85% from 1990 to 2005, while they increased in Spain by 25%.
- Highest levels of computed PCB-153 depositions in 2005 to the OSPAR maritime area were calculated for Region II (Greater North Sea) ($5 \cdot 10^{-5}$ mg/m²/y and higher). The lowest values of PCB-153 deposition are characteristic for Region I (Arctic Waters) (about $1 \cdot 10^{-5}$ mg/m²/y and lower). The spatial pattern of γ -HCH depositions in 2005 follows in general that of PCB-153. It is characterised by high values of deposition fluxes in Region II (Greater North Sea) ($1 \cdot 10^{-3}$ – $3 \cdot 10^{-3}$ mg/m²/y). Deposition levels are decreasing to the north up to $1 \cdot 10^{-4}$ – $2 \cdot 10^{-4}$ mg/m²/y in Region I (Arctic Waters) and to the west up to $2 \cdot 10^{-4}$ – $5 \cdot 10^{-4}$ mg/m²/y in Region V (Wider Atlantic).
- For the considered period 1990 – 2005, the decline of PCB-153 total annual deposition, following achieved emission reductions, varies within the OSPAR maritime area from 3.3 to 3.7 times. Highest reductions of PCB-153 total depositions took place in Region V (Wider Atlantic). The reduction of the net deposition flux is more significant and amounts to a factor of four in most of the regions.
- The total annual depositions of γ -HCH to the OSPAR maritime area declined significantly in the period 1990 – 2005 by a factor ranging from 5.5 to 9.3, depending on the Region concerned. The highest decrease of deposition took place in Region II (Greater North Sea) and Region IV (Bay of Biscay). Following the essential reduction or elimination of γ -HCH emissions, a substantial influence of re-emission can be noted for a number of sub-regions of the Greater North Sea.
- A comparison of computed deposition fluxes of PCB-153 with available measurements of the EMEP monitoring network revealed that model predictions reasonably match the variations of observed deposition fluxes for most of the observation sites with the exception for the period 1998 – 2001 where significant differences (more than a factor of 3) were noted. This might be caused by uncertainties in the description of temporal variations of PCB-153 emissions during this period.
- The computed deposition fluxes of γ -HCH reasonably agree with available measurements of the OSPAR monitoring network. For most of the observation sites, the model reproduces reasonably well the temporal variations of measured wet deposition fluxes of γ -HCH. Significant differences were noted between model results and the measurements at the monitoring station in Iceland both for γ -HCH and PCB-153. This is likely to be due to an overestimation of boundary conditions, uncertainties in model parameterisation of removal processes or the representativeness of measurements of this site.

References

- Behrenfeld, M.J. and Falkowski, P.G., 1997. Photosynthetic derived from satellite-based chlorophyll concentration. *Limnol. Oceanogr.*, vol. 42, No.1, pp.1-20.
- Berdowski, J.J.M., Baas, J., Bloos, J.P.J., Visschedijk, A.J.H. and Zandveld, P.Y.J., 1997. The European Emission Inventory of Heavy Metals and Persistent Organic Pollutants for 1990. TNO Institute of Environmental Sciences, Energy Research and Process Innovation, UBA-FB report 104 02 672/03, Apeldoorn, p.239.
- Breivik, K., Sweetman, A., Pacyna, J.M. and Jones, K.C., 2002a. Towards a global historical emission inventory for selected PCB congeners – a mass balance approach. 1. Global production and consumption. *Science of the Total Environment*. vol. 290, pp. 181-198.
- Breivik, K., Sweetman, A., Pacyna, J.M. and Jones, K.C., 2007. Towards a global historical emission inventory for selected PCB congeners - a mass balance approach. 3. An update. *Science of the Total Environment*. vol. 377, No. 2-3, pp. 296-307.
- Breivik, K., Sweetman, A., Pacyna, J.M., Jones, K.C., 2002b. Towards a global historical emission inventory for selected PCB congeners – a mass balance approach. 2. Emissions. *Science of the Total Environment*, vol 290, pp. 199-224.
- Carpi, A. and Lindberg, S.E., 1998. Application of a teflonTM dynamic flux chamber for quantifying soil mercury flux: tests and results over background soil. *Atmos. Environ.*, vol. 32, No.5, pp. 873-882.
- CGEIC, Canadian Global Emissions Interpretation Centre. <http://www.ortech.ca/cgeic/>
- Denier van der Gon, H.A.C., van het Bolscher, M., Visschedijk, A.J.H. and Zandveld, P.Y.J., 2005. Study to the effectiveness of the UNECE Heavy Metals Protocol and costs of possible additional measures. Phase I: Estimation of emission reduction resulting from the implementation of the HM Protocol. TNO-report B&O-A R 2005/193.
- Gomes, L., Rajot, J.L., Alfaro, S.C. and Gaudichet, A., 2003. Validation of a dust production model from measurements performed in semi-arid agricultural areas of Spain and Niger. *Catena*, vol. 52, pp. 257-271.
- Gong, S.L., 2003. A parameterization of sea-salt aerosol source function for sub- and super-micron particles. *Global Biogeochemical Cycles*, vol. 17, No. 4, p.1097.
- Grell, G.A., Dudhia, J., Stauffer, D.R., 1995. A description of the Fifth-Generation Penn State/NCAR Mesoscale Model (MM5). NCAR Technical note TN-398. National Center for Atmospheric Research, Boulder, Colorado.
- Gusev, A., Mantseva, E., Shatalov, V., Strukov, B., 2005a. Regional multicompartment model MSCE-POP EMEP/MSCE-E Technical Report 5/2005, June 2005.
- Gusev, A., Li, Y.-F., Mantseva, E., Shatalov, V., Rozovskaya, O. and Vulykh, N., 2005b. Evaluation of B[a]P and γ -HCH transport from European and North American emission sources and assessment of deposition to the OSPAR region Report was prepared in the framework of EMEP as a contribution to German Canadian Project "Quality of measuring data on atmospheric input of POPs". EMEP/MSCE-E Technical Report 12/2005. June 2005.
- Gusev, A., Ilyin, I., Mantseva, L., Rozovskaya, O., Shatalov, V. and Travnikov, O., 2006. Progress in further development in MSCE-HM and MSCE-POP models (implementation of the model review recommendations). EMEP/MSCE-E Technical report 4/2006, p.114.
- Gustin, M.S., Lindberg, S., Marsik, F., Casimir, A., Ebinghaus, R., Edwards, G., Hubble-Fitzgerald, C., Kemp, R., Kock, H., Leonard, T., London, J., Majewski, M., Montecinos, C., Owens, J., Pilote, M., Poissant, L., Rasmussen, P., Schaedlich, F., Schneeberger, D., Schroeder, W., Sommar, J., Turner, R., Vette, A., Wallschlaeger, D., Xiao, Z., and Zhang, H., 1999. Nevada STORMS project: Measurement of mercury emissions from naturally enriched surfaces. *J. Geophys. Res.*, vol. 104, No.D17, pp.21831-21844.
- Hedgecock, I.M., Pirrone, N., Trunfio, G.A., Sprovieri, F., 2006. Integrated mercury cycling, transport, and air-water exchange (MECAWEx) model. *J. Geophys. Res.*, vol. 111, No. D20, D20302
- Hurrell, J.W., Kushnir, Y., Visbeck, M., and Ottersen, G., 2003. An Overview of the North Atlantic Oscillation. The North Atlantic Oscillation: Climate Significance and Environmental Impact, Hurrell, J.W., Kushnir, Y., Ottersen, G. and Visbeck, M., Eds. Geophysical Monograph Series, vol.134, pp. 1-35.
- Ilyin, I. and Travnikov, O., 2005. Modelling of heavy metal airborne pollution in Europe: Evaluation of the model performance. EMEP/MSCE-E Technical report 8/2005. June 2005.
- Ilyin, I., Rozovskaya, O., Travnikov, O. and Aas, W., 2007. Heavy metals: transboundary pollution of the environment. EMEP Status Report 2/2007, p.54

- Jacobs, C.M.J. and van Pul, W.A.J., 1996. Long-range atmospheric transport of persistent organic pollutants. 1: Description of surface - Atmosphere exchange modules and implementation in EUROS. National Institute of Public Health and the Environment, Bilthoven, The Netherlands. Report No. 722401013.
- Jacobson, M. Z., 1999. Fundamentals of atmospheric modeling. Cambridge University Press. p.656
- Kim, K.-H., Lindberg, S.E. and Meyers, T.P., 1995. Micrometeorological measurements of mercury vapor fluxes over background forest souls in eastern Tennessee. *Atmos. Environ.*, vol. 29, No.2, pp.267-282.
- Lamborg, C.H., Fitzgerald, W.F., O'Donnell, J. and Torgersen, T., 2002. A non-steady-state compartmental model of global-scale mercury biogeochemistry with interhemispheric atmospheric gradients. *Geochimica et Cosmochimica Acta*, vol. 66, No. 7, pp. 1105-1118.
- Li, Y.-F., 2004. Emission Inventories of γ -HCH for North America during 2000 and 2002. June 28.
- Li, Y.-F., Cai, D.J., Shan, Z.J. and Zhu, Z.L., 2001. Gridded usage inventories of technical hexachlorocyclohexane and lindane for China with 1/6° latitude by 1/4° longitude resolution. *Arch.Environ.Contam.Toxicol.*, vol. 41, pp. 261-266.
- Li, Y.-F., McMillan, A. and Scholtz, M.T., 1996. Global HCH usage with 10x10 longitude/latitude resolution. *Environ. Sci. Technol.*, vol. 30, No.12, pp. 3525-3533.
- Macdonald, R.W., Barrie, L.A., Bidleman, T.F., Diamond, M.L., Gregor, D.J., Semkin, R.G., Strachan, W.M., Li, Y.F., Wania, F., Alae, M., Alexeeva, L.V., Backus, S.M., Bailey, R., Bowers, J.M., Gobel, C., Halsall, C.J., Harner T., Hoff, J.T., Jantunen, L.M.M., Lockhart, W.L., Mackay, D., Muir, D.C.G., Pudykiewicz, J., Reimer, K.J., Smith, J.N., Stern, G.A., Schroeder, W.H., Wagemann, R. and Yunker, M.B., 2000. Contaminants in the Canadian Arctic: 5 years of progress in understanding sources, occurrence and pathways. *The Science of the Total Environment*, vol. 254, pp. 93-234.
- Nijenhuis, W.A.S., Van Pul, W.A.J. and De Leeuw, F.A.A.M., 2001. Deposition of heavy metals to the Convention waters of the Oslo and Paris Commissions. *Water, Air and Soil Pollution*, 126, pp. 121-149.
- OSPAR Commission 2000. Quality Status Report 2000. OSPAR Commission, London. 108+vii pp.
- OSPAR Commission 2000. Quality Status Report 2000, Region II-Greater North Sea. OSPAR Commission, London. 136+xiii pp.
- Pacyna, E.G., Pacyna, J.M., Steenhuisen, F. and Wilson S., 2006. Global anthropogenic mercury emission inventory for 2000. *Atmos. Environ.*, vol. 40, No. 22, pp. 4048-4063.
- Pacyna, J. M., Pacyna, E.G., Steenhuisen, F., Wilson, S., 2003. Mapping 1995 global anthropogenic emissions of mercury. *Atmos. Environ.*, vol. 37, Supplement No. 1, pp. 109-117
- Pacyna, J.M. *et al.*, 1999. Final report for Project POPCYCLING-Baltic. EU DGXII, Environment and Climate Program ENV4-CT96-0214. Available on CD-rom including technical report, the emission and environmental databases as well as the POPCYCLING-Baltic model. NILU, P.O. Box 100, N-2027 Kjeller, Norway.
- Petersen, G., Munthe, J., Pleijel, K., Bloxam, R. and Kumar, A.V., 1998. A comprehensive Eulerian modeling framework for airborne mercury species: Development and testing of the tropospheric chemistry module (TCM). *Atmos. Environ.*, vol. 32, No.5, pp. 829-843.
- Poissant, L. and Casimir, A., 1998. Water-air and soil-air exchange rate of total gaseous mercury measured at background sites. *Atmos. Environ.*, vol. 32, No. 5, pp. 883-893.
- Ruijgrok, W., Tieben, H. and Eisinga, P., 1997. The dry deposition of particles to a forest canopy: a comparison of model and experimental results. *Atmospheric Environment*, vol. 31, pp. 399-415.
- Shatalov, V., Gusev, A., Dutchak, S., Holoubek, I., Mantseva, E., Rozovskaya, O., Sweetman, A., Strukov, B. and Vulykh N., 2005. Modelling of POP Contamination in European Region: Evaluation of the Model Performance. Technical Report 7/2005.
- Shatalov, V., Mantseva, E., Fedynin, M., Strukov, B. and Vulykh N., 2003. Persistent Organic Pollutants in the environment. MSC-E Technical Report 4/2003.
- Slinn, W.G.N., 1982. Predictions for particle deposition to vegetative canopies. *Atmos. Environ.*, vol. 16, pp. 1785-1794.
- Travnikov, O. and Ilyin, I., 2005. Regional Model MSCE-HM of Heavy Metal Transboundary Air Pollution in Europe. EMEP/MSCE Technical Report 6/2005.
- Travnikov, O., Ryaboshapko, A., 2002. Modelling of mercury hemispheric transport and depositions. EMEP/MSCE Technical Report 6/2002, Meteorological Synthesizing Centre - East, Moscow, Russia.
- Uggerud, H. and Hjellbrekke, A-G., 2007. Analytical intercomparison of heavy metals in precipitation 2005 and 2006. EMEP/CCC-Report 4/2007.

- van den Hout, K.D. (ed.), 1994. The impact of atmospheric deposition of non-acidifying pollutants on the quality of European forest soils and the North Sea. Main report of the ESQUAD project. IMW-TNO report 93/329, Delft, The Netherlands
- Wesely, M.L., Cook, D.R., Hart, R.L., 1985. Measurements and parameterization of particulate sulfur dry deposition over grass. *Journal of Geophysical Research*, vol. 90, No. D1, pp. 2131-2143.
- Wesely, M. L. and Hicks, B.B., 2000. A review of the current status of knowledge on dry deposition, *Atmos. Environ.*, vol. 34, pp. 2261–2282
- Williams, R.M., 1982. A model for the dry deposition of particles to natural water surfaces. *Atmos. Environ.*, vol.16, pp.1933-1938.
- Zender, C.S., Bian, H. and Newman, D., 2003. Mineral dust entrainment and deposition (DEAD) model: description and 1990s dust climatology. *Journal of Geophysical Research*, vol. 108, No. D14, p. 4416.
- Zhang, H., Lindberg, S.E., Marsik, F.J. and Keeler, G.J., 2001. Mercury air/surface exchange kinetics of background soils of the Tahquamenon River watershed in the Michigan upper peninsula. *WASP 126*, pp.151-169.

Abbreviations

MSC-E	EMEP Meteorological Synthesizing Centre (East)
MSCE-HM	Heavy metal model developed by MSC-E
MSCE-HM-Hem	Heavy metal hemispheric model developed by MSC-E
MSCE-POP	POP model developed by MSC-E
POP	Persistent Organic Pollutant
EMEP	Co-operative Programme for Monitoring and Evaluation of the Long-Range Transport of Air Pollutants in Europe
TFMM	EMEP Task Force on Measurements and Modelling
MM5	Fifth Generation Penn State/NCAR Mesoscale Model
NCAR	US National Centre for Atmospheric Research
NCEP	US National Centres for Environmental Prediction
ECMWF	European Centre for Medium-Range Weather Forecasts
UNECE	United Nations Economic Commission for Europe
LRTP Convention	UNECE Convention on Long-Range Transboundary Air Pollution
ICES	International Council for the Exploration of the Sea
WEBDAB	EMEP WEB-published emission DATAbase
OSPAR countries	State Contracting Parties to the OSPAR Convention: Belgium, Denmark, Finland, France, Germany, Iceland, Ireland, Luxembourg, the Netherlands, Norway, Portugal, Spain, Sweden, Switzerland, and the UK. Note that the European Community is also Contracting Party to the OSPAR Convention but not covered by the term of "OSPAR countries".
TNO	The Netherlands Organisation for Applied Scientific Research (<i>Nederlandse Organisatie voor Toegepast Natuurwetenschappelijk Onderzoek</i>)
NFR	EMEP Nomenclature For Reporting of emission sources
SNAP	EMEP/CORINAIR Selected Nomenclature for Air Pollutants
CORINAIR	CORe INventory of AIR emissions, a project for data collection on air emissions of the European Topic Centre on Air Emissions of the European Environment Agency
CGEIS	Canadian Global Emissions Interpretation Centre.
CAMP	OSPAR Comprehensive Atmospheric Monitoring Programme
ESPREME	Project for the Estimation of willingness-to-pay to reduce the risks of exposure to heavy metals and cost-benefit analysis for reducing heavy metals occurrence in Europe
CCC	Chemical Co-ordination Centre of EMEP
ESQUAD	Project on European Soil and sea Quality due to Atmospheric Deposition

Annex A: Data products for heavy metals

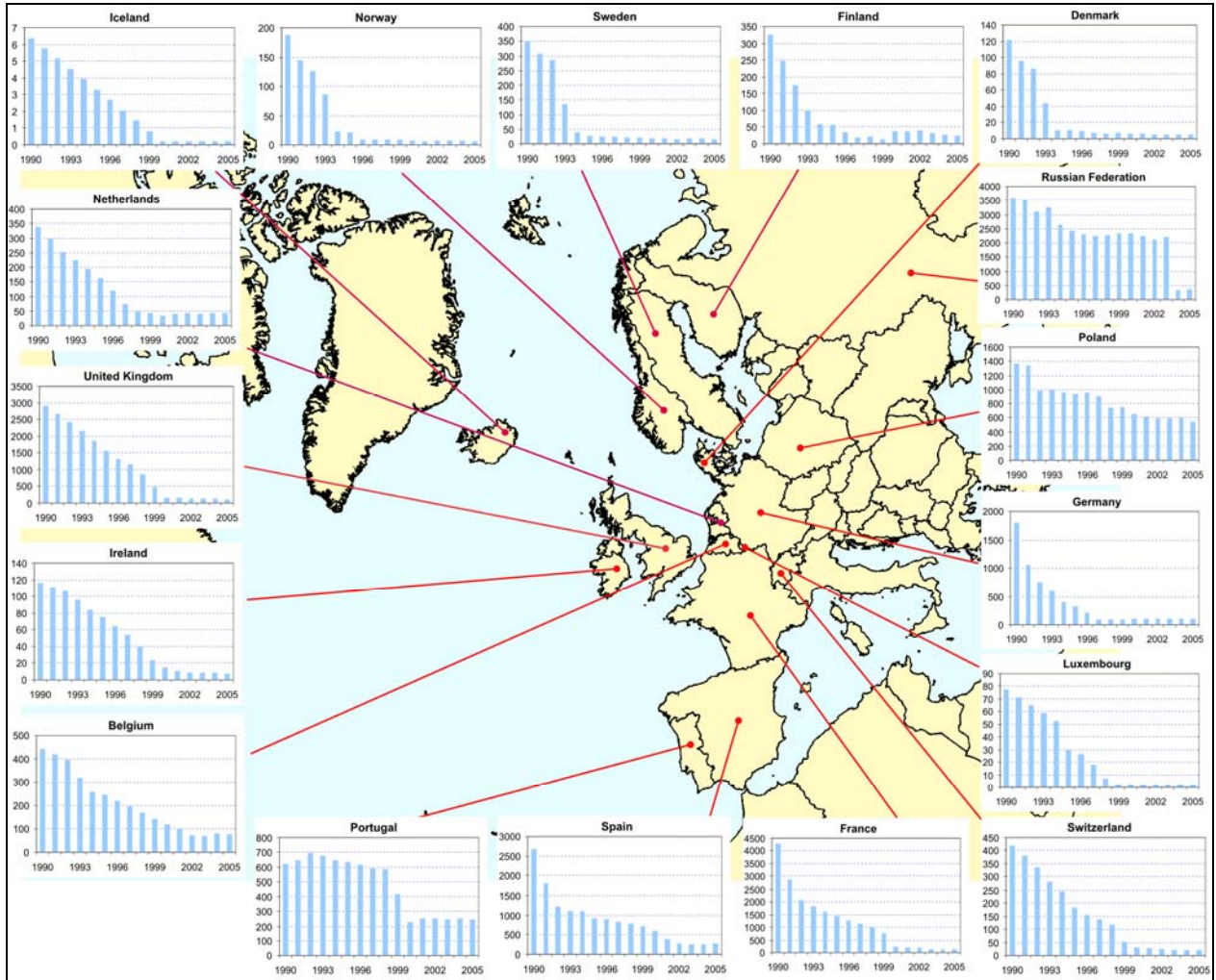


Figure A.1. Time series of lead emissions from the OSPAR Contracting Parties and selected countries with large contribution to deposition to the OSPAR maritime area (Poland and European part of the Russian Federation). Units: t/y.

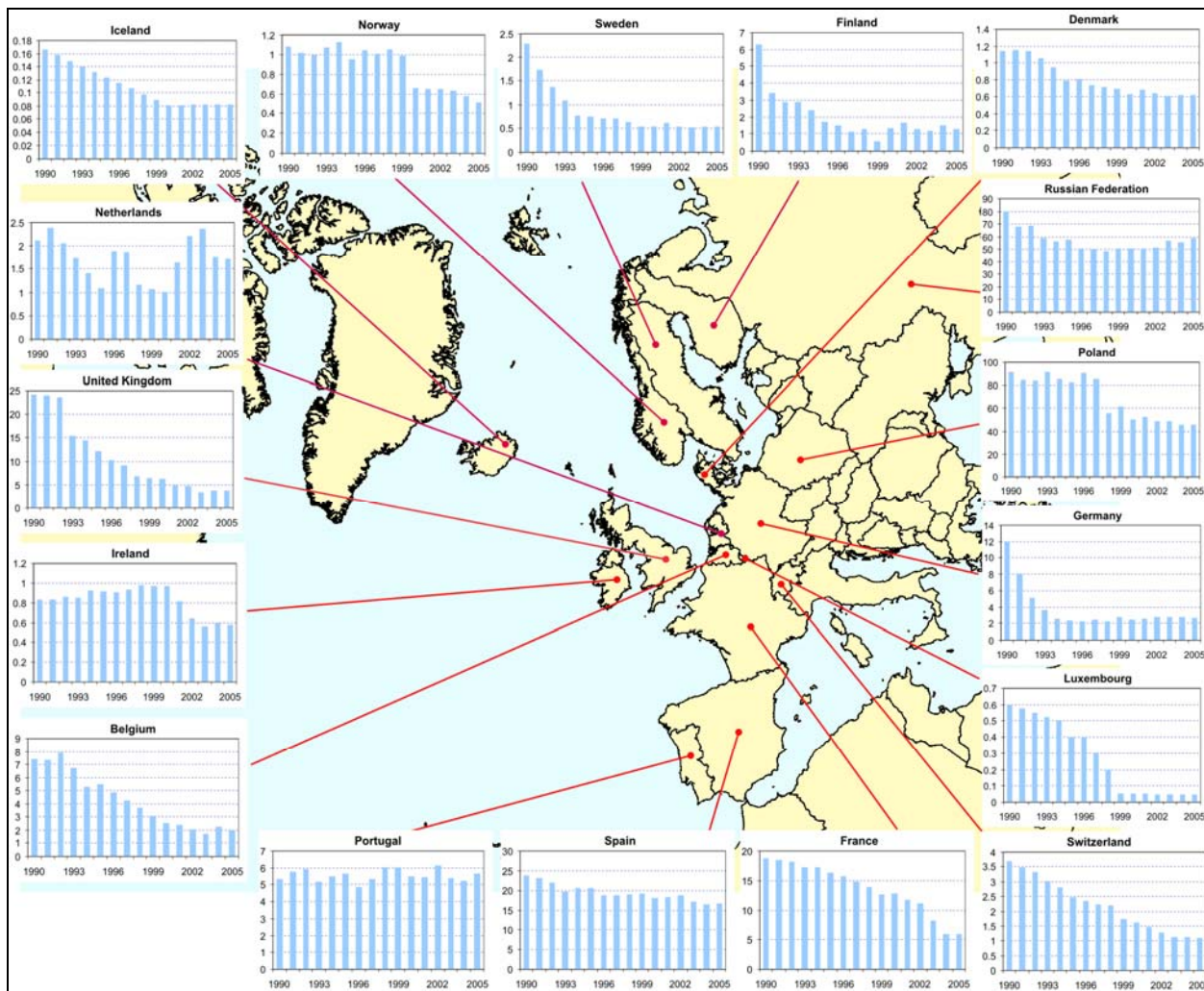


Figure A.2. Time series of **cadmium** emissions from the OSPAR Contracting Parties and selected countries with large contribution to deposition to the OSPAR maritime area (Poland and European part of the Russian Federation). Units: t/y.

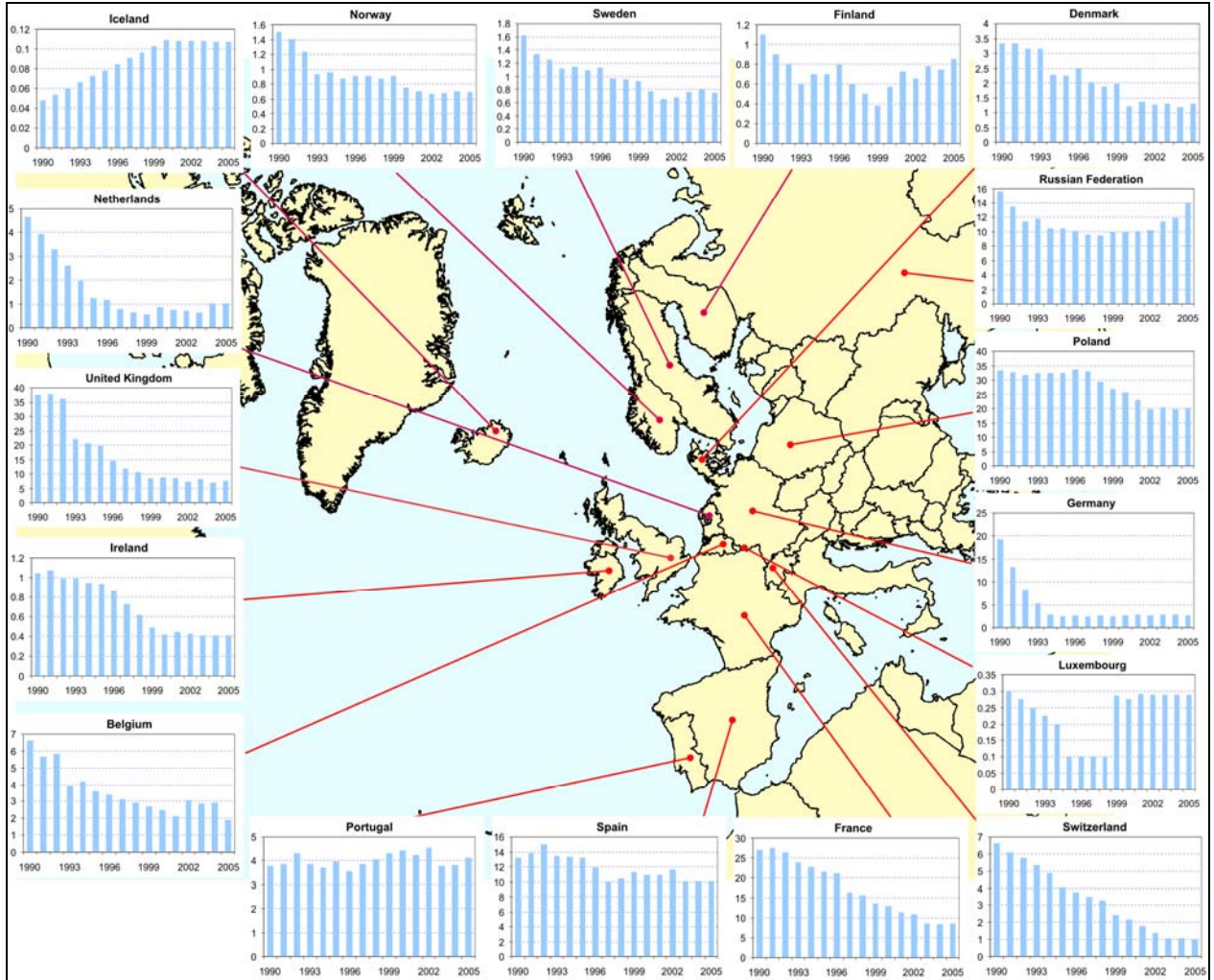


Figure A.3. Time series of mercury emissions from the OSPAR Contracting Parties and selected countries with large contribution to deposition to the OSPAR maritime area (Poland and European part of the Russian Federation). Units: t/y.

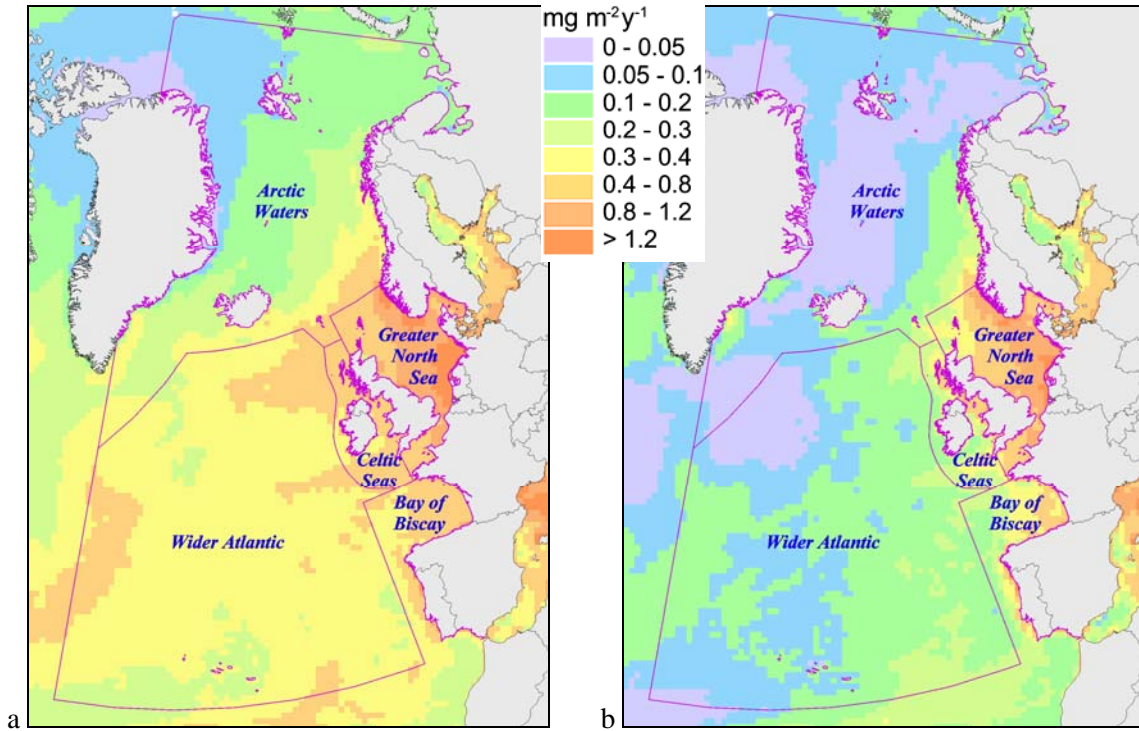


Figure A.4. Spatial distribution of annual total deposition flux (a) and net deposition flux (b) of lead over the five main OSPAR regions in 2005. Units: $\text{mg m}^{-2} \text{y}^{-1}$

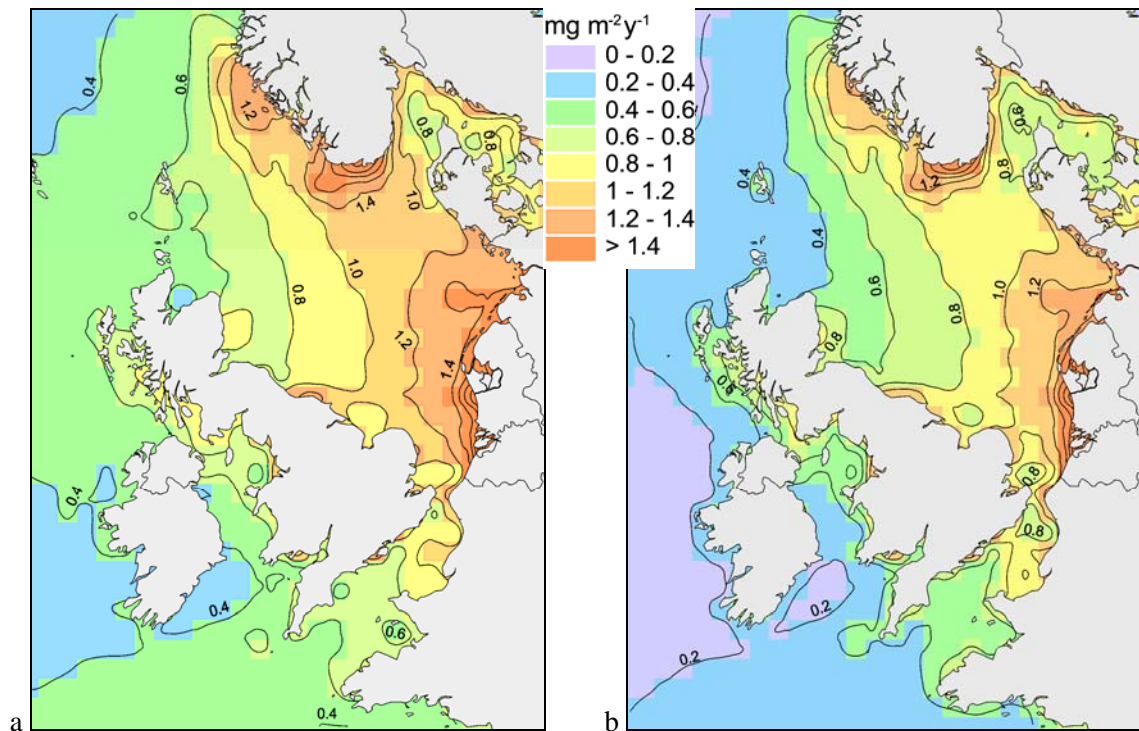


Figure A.5. Spatial distribution of annual total deposition flux (a) and net deposition flux (b) of lead over the OSPAR Region II (Greater North Sea) in 2005. Units: $\text{mg m}^{-2} \text{y}^{-1}$

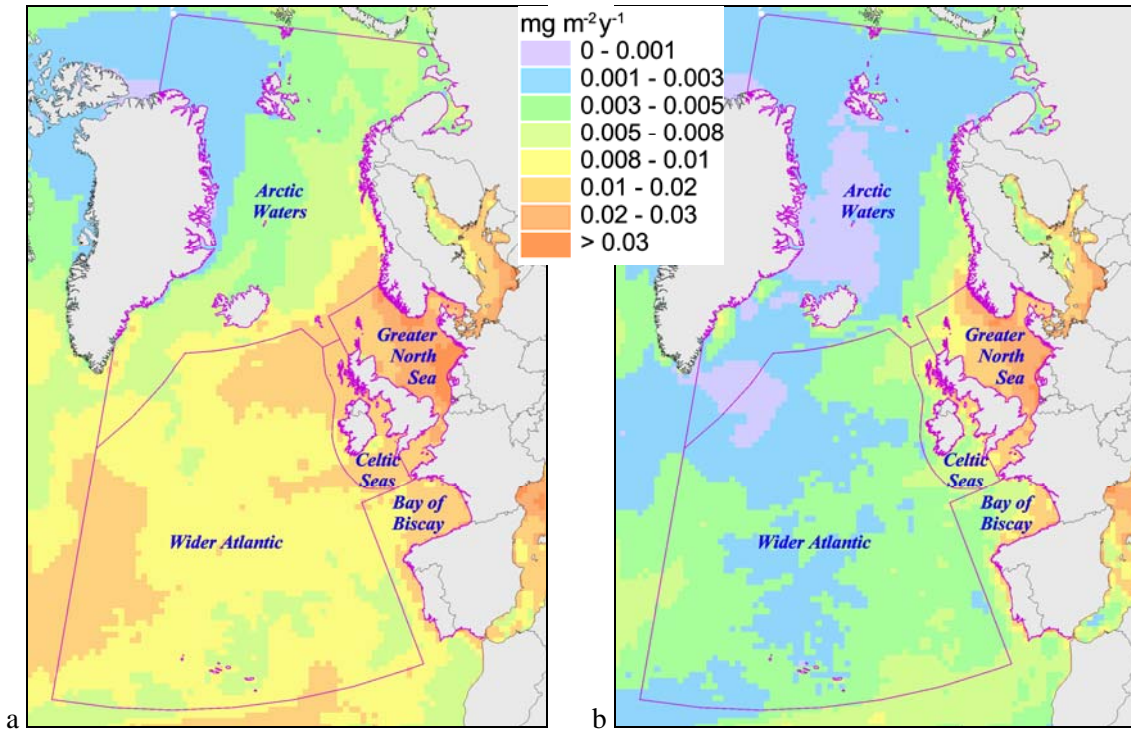


Figure A.6. Spatial distribution of annual total deposition flux (a) and net deposition flux (b) of **cadmium** over the five main OSPAR regions in 2005. Units: $\text{mg m}^{-2} \text{y}^{-1}$

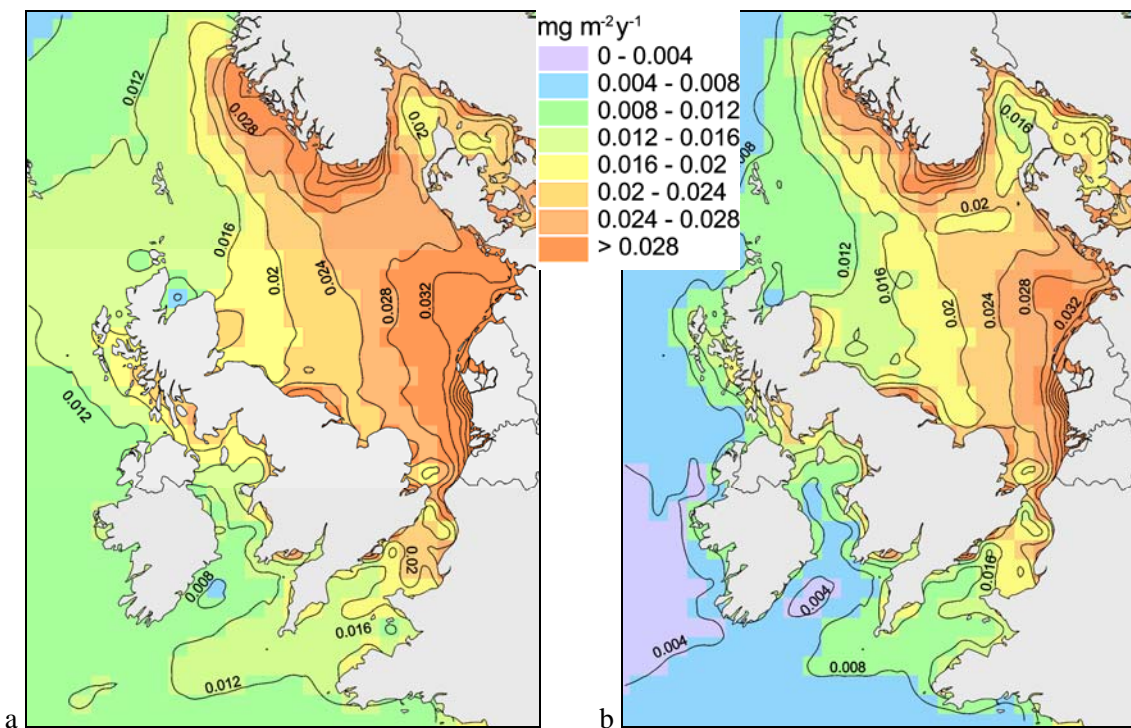


Figure A.7. Spatial distribution of annual total deposition flux (a) and net deposition flux (b) of **cadmium** over the OSPAR Region II (Greater North Sea) in 2005. Units: $\text{mg m}^{-2} \text{y}^{-1}$

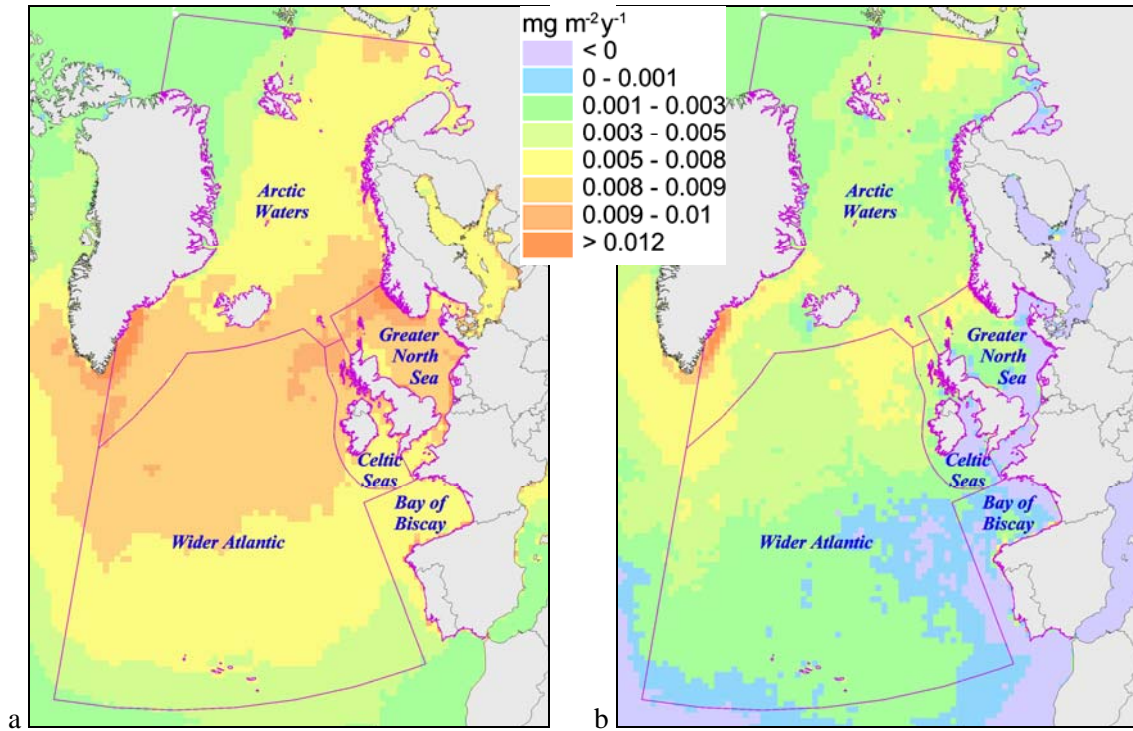


Figure A.8. Spatial distribution of annual total deposition flux (a) and net deposition flux (b) of **mercury** over the five main OSPAR regions in 2005. Units: $\text{mg m}^{-2} \text{y}^{-1}$

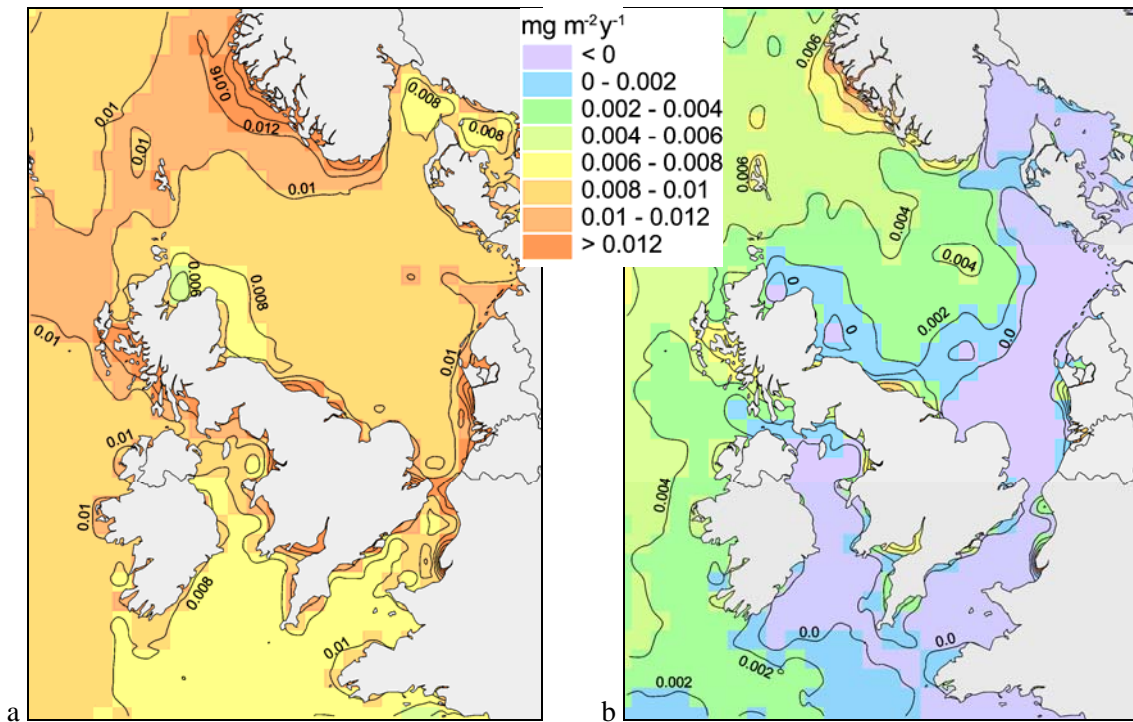


Figure A.9. Spatial distribution of annual total deposition flux (a) and net deposition flux (b) of **mercury** over the OSPAR Region II (Greater North Sea) in 2005. Units: $\text{mg m}^{-2} \text{y}^{-1}$

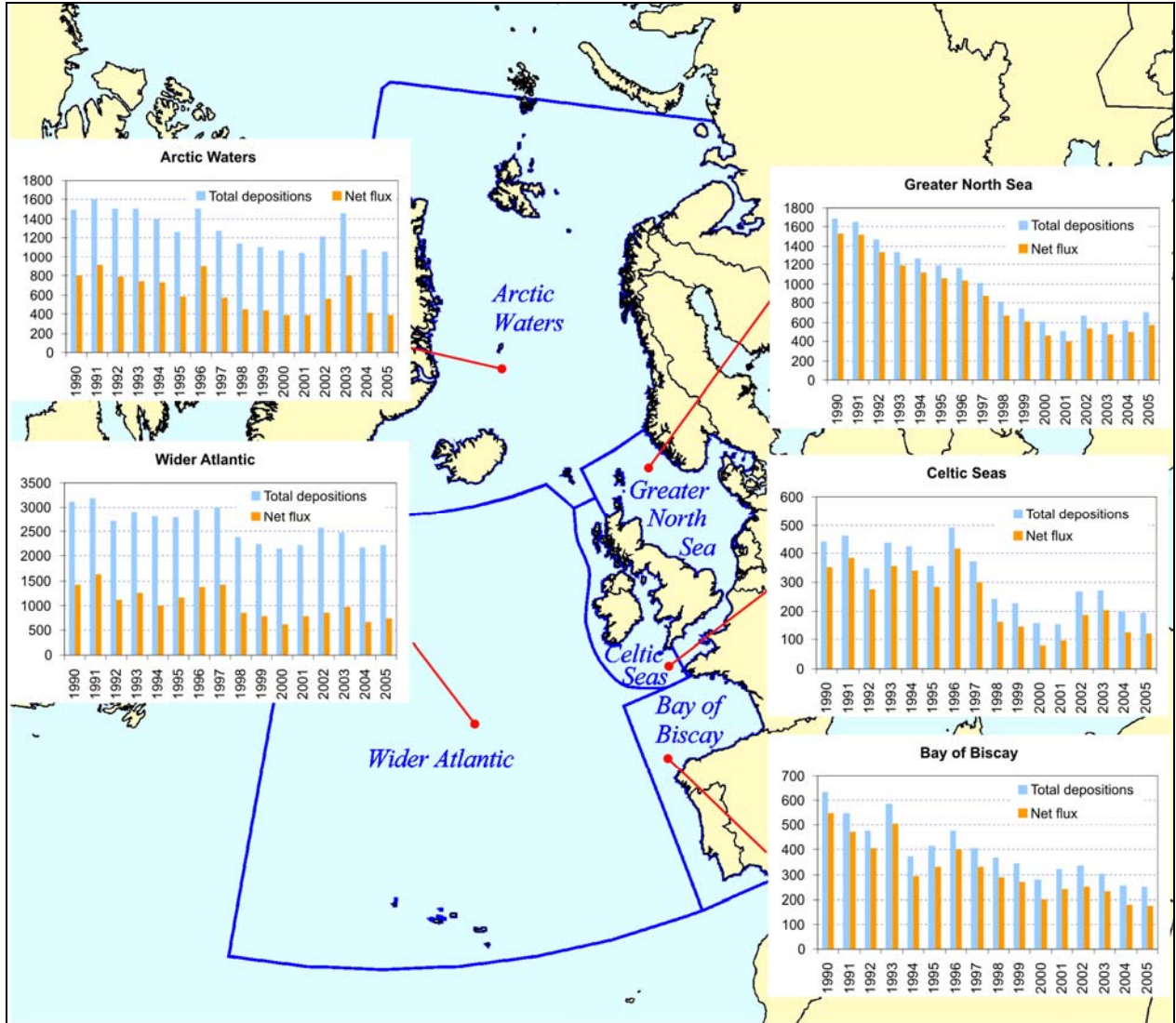


Figure A.10. Time series of modelled total annual deposition and net atmospheric input of lead to the five main OSPAR regions. Units: t/y.

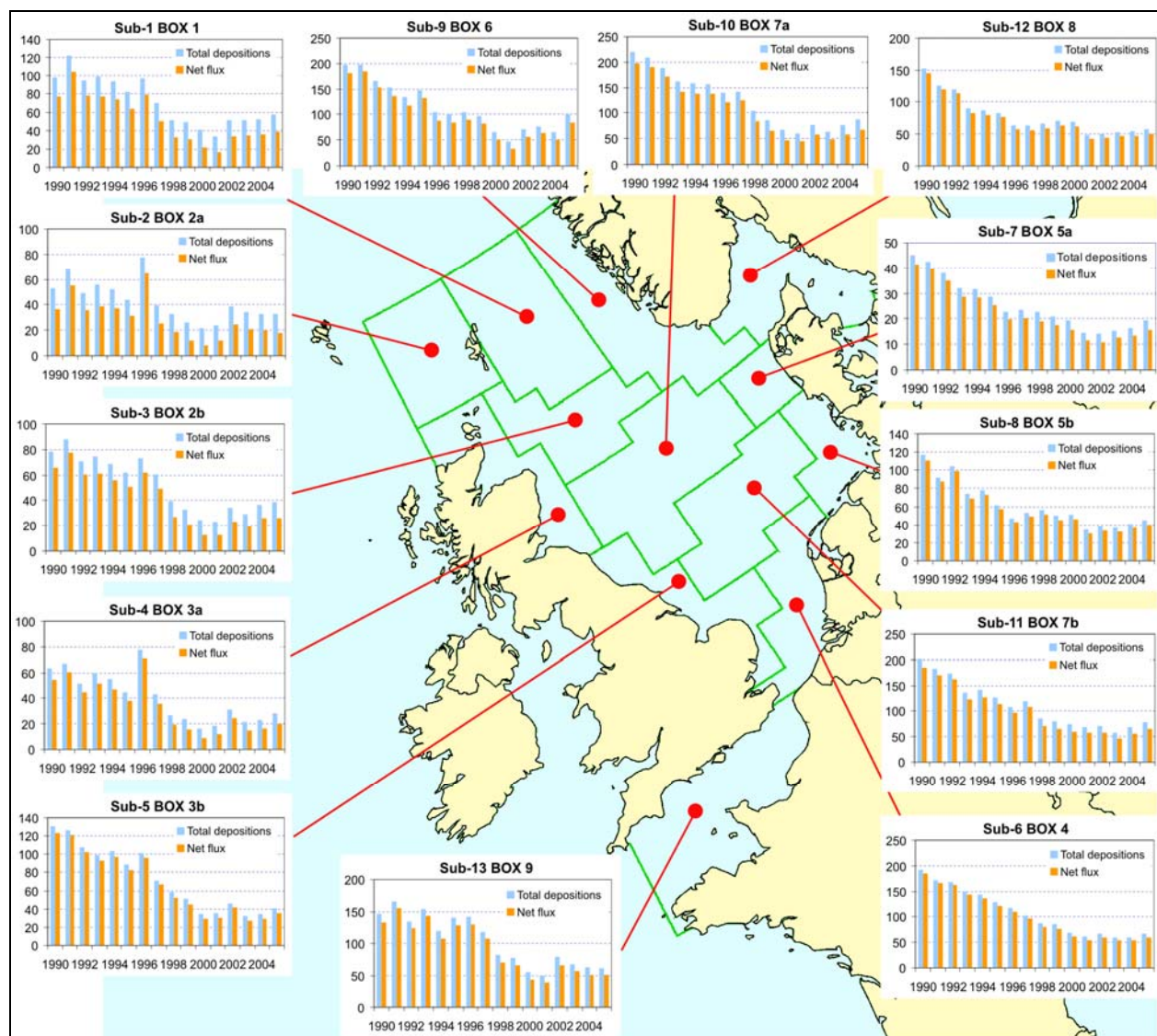


Figure A.11. Time series of modelled total annual deposition and net atmospheric input of lead to 13 sub-regions of the OSPAR Region II (Greater North Sea). Units: t/y.

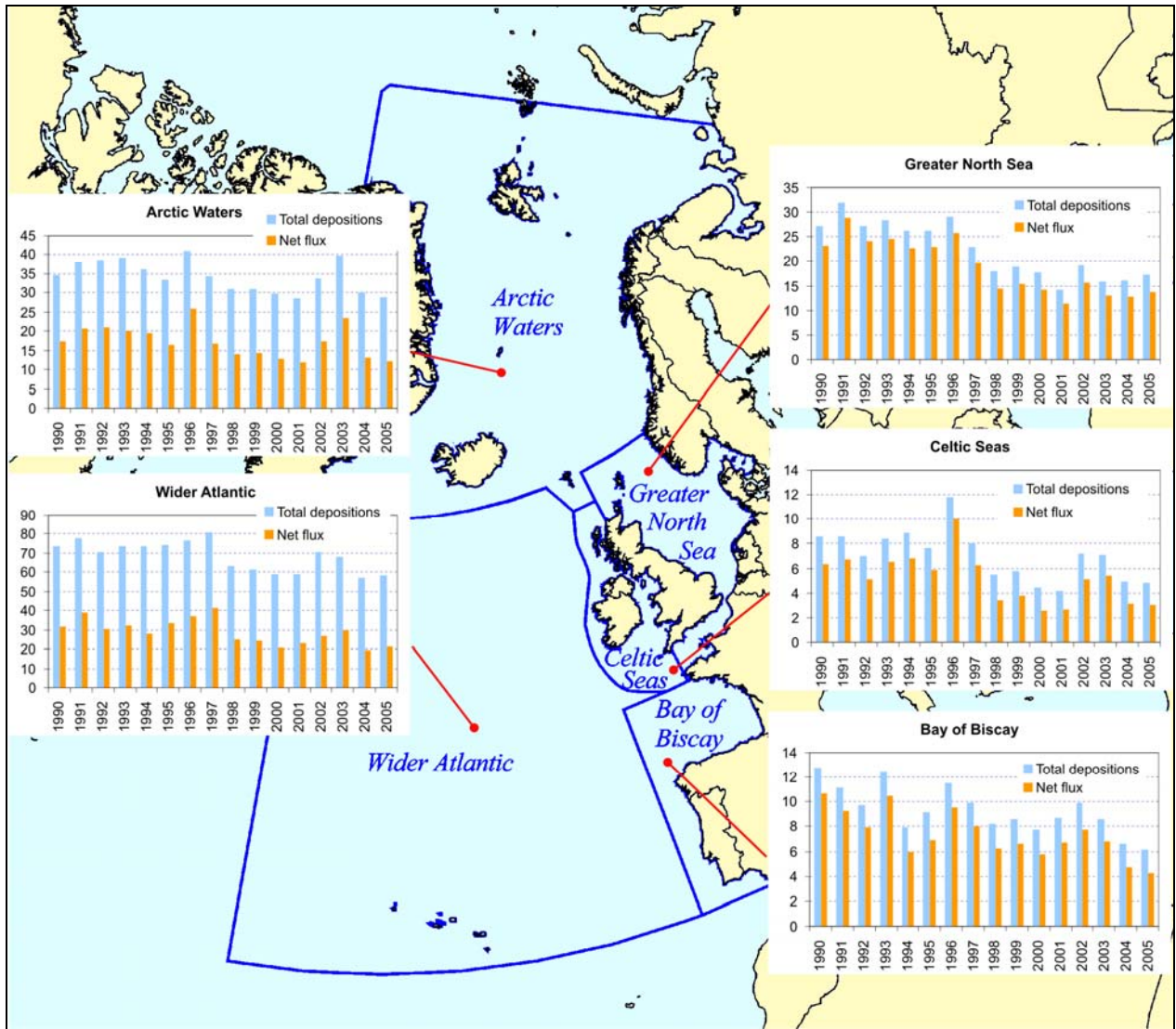


Figure A.12. Time series of modelled total annual deposition and net atmospheric input of cadmium to the five main OSPAR regions. Units: t/y.

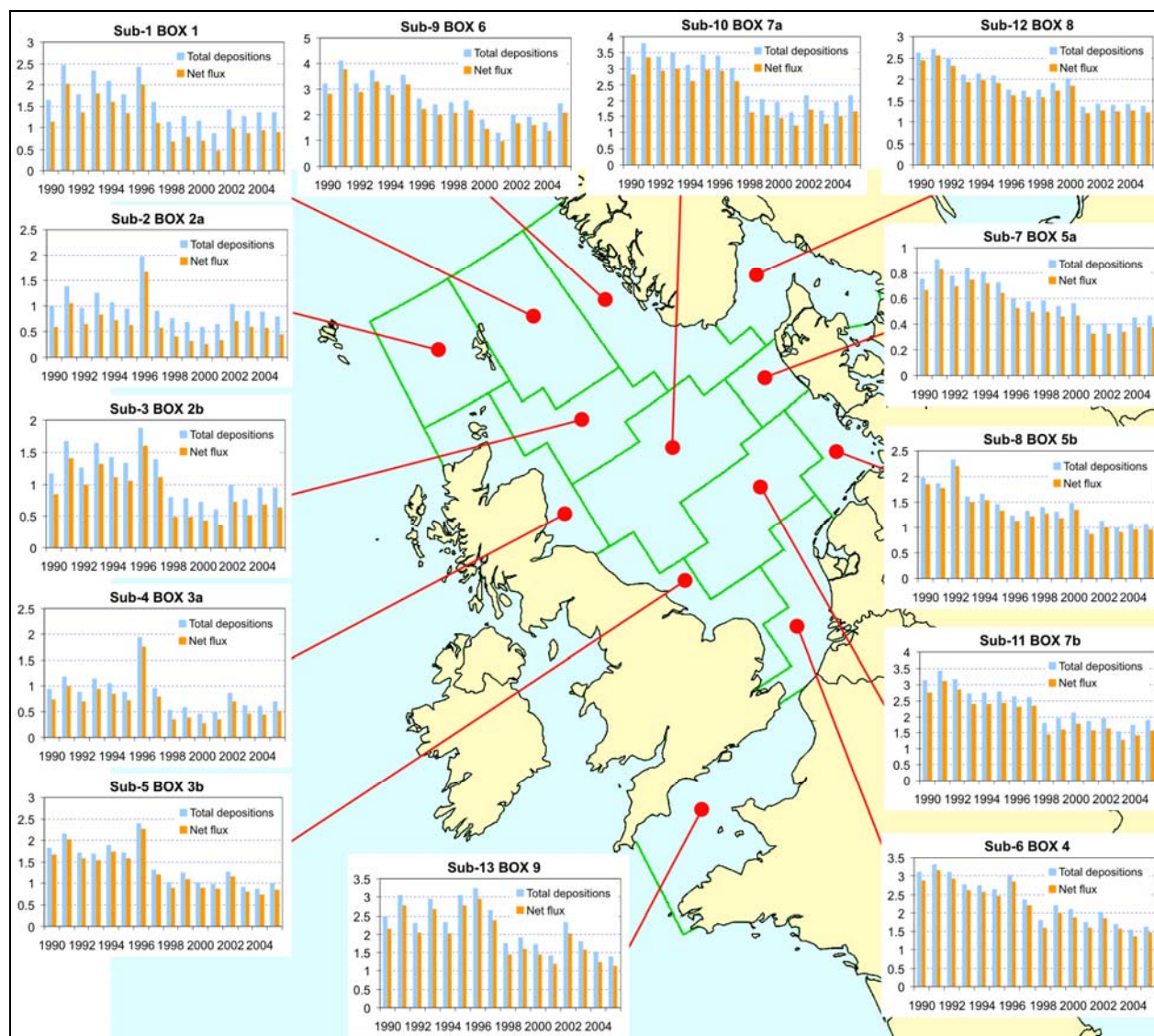


Figure A.13. Time series of modelled total annual deposition and net atmospheric input of **cadmium** to 13 sub-regions of the OSPAR Region II (Greater North Sea). Units: t/y

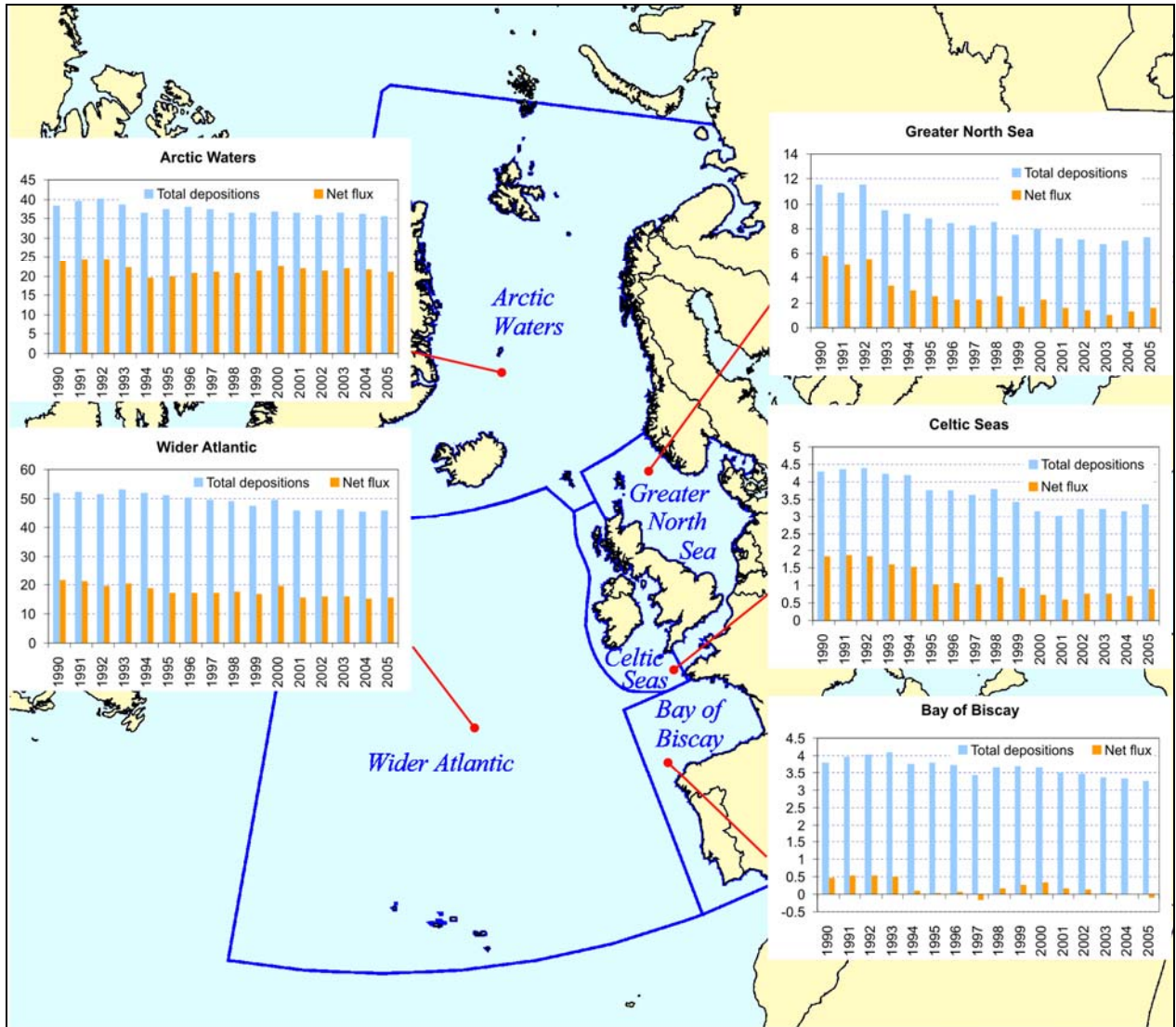


Figure A.14. Time series of modelled total annual deposition and net atmospheric input of **mercury** to the five main OSPAR regions. Units: t/y.

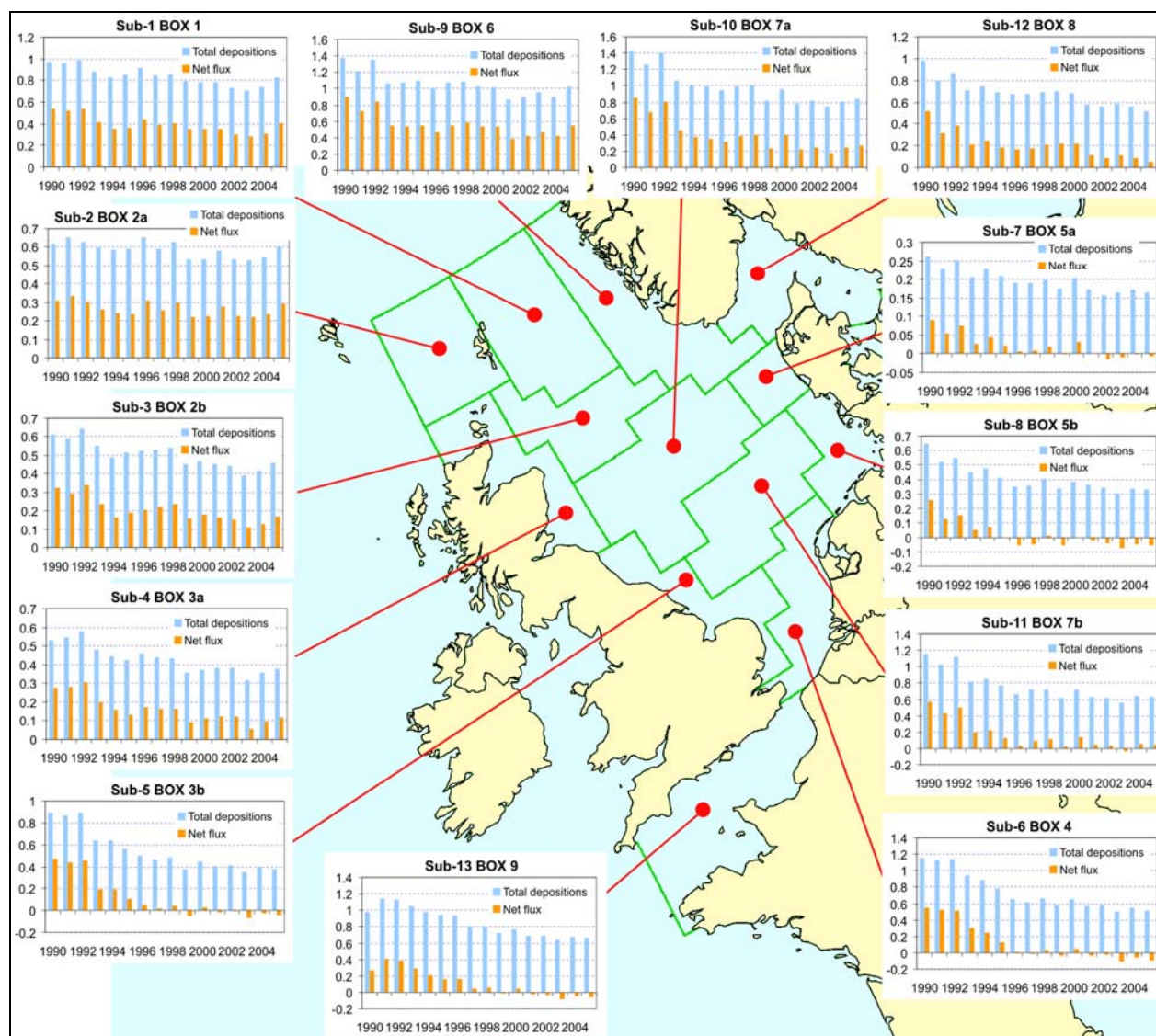


Figure A.15. Time series of modelled total annual deposition and net atmospheric input of mercury to 13 sub-regions of the OSPAR Region II (Greater North Sea). Units: t/y

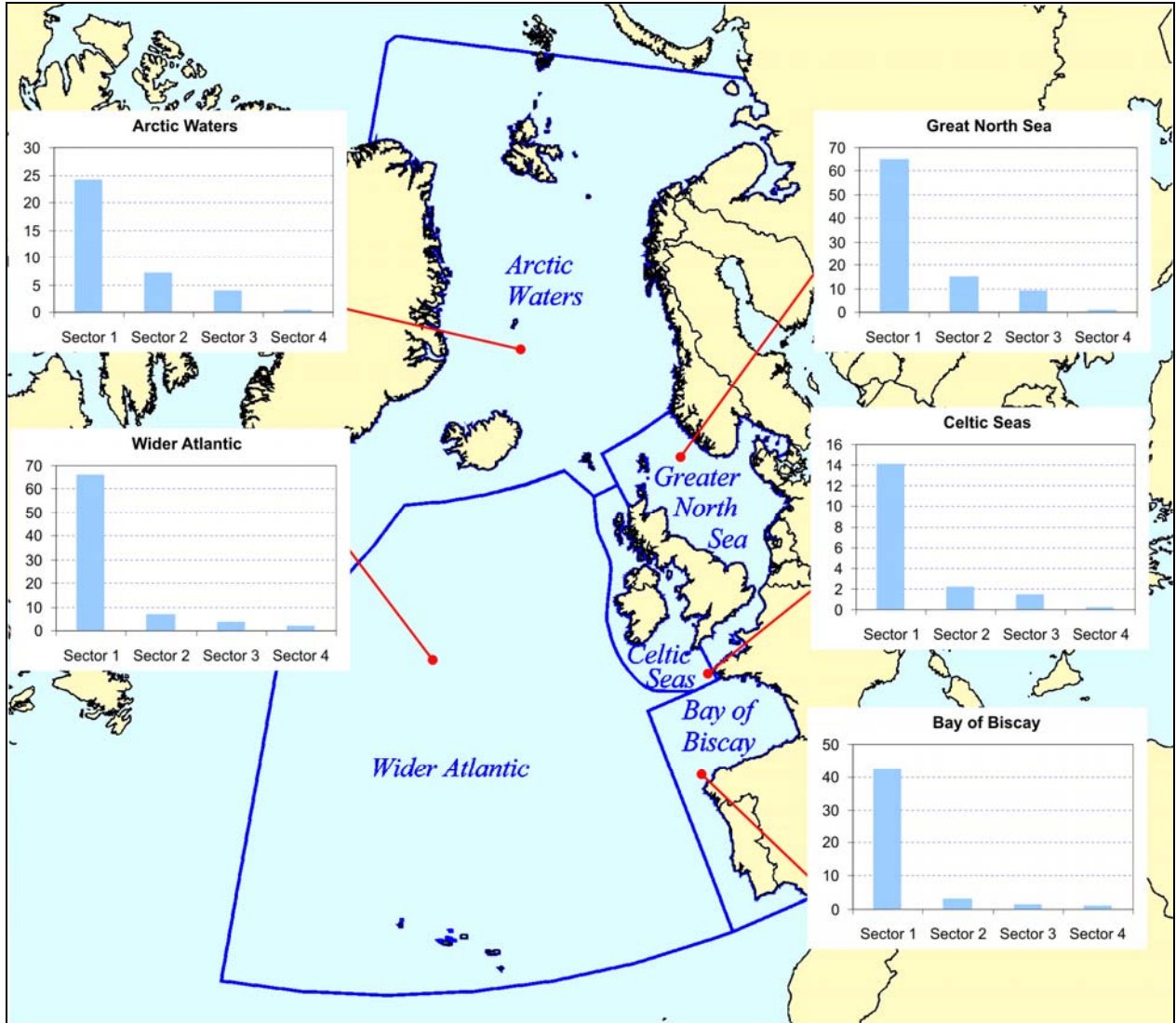


Figure A.16. Contribution of four key source categories (1 – combustion in power plants and industry and industrial processes; 2 – transport; 3 - commercial, residential and other combustion; 4 - waste) to **lead** depositions to the five main OSPAR regions in 2005. Units: t/y

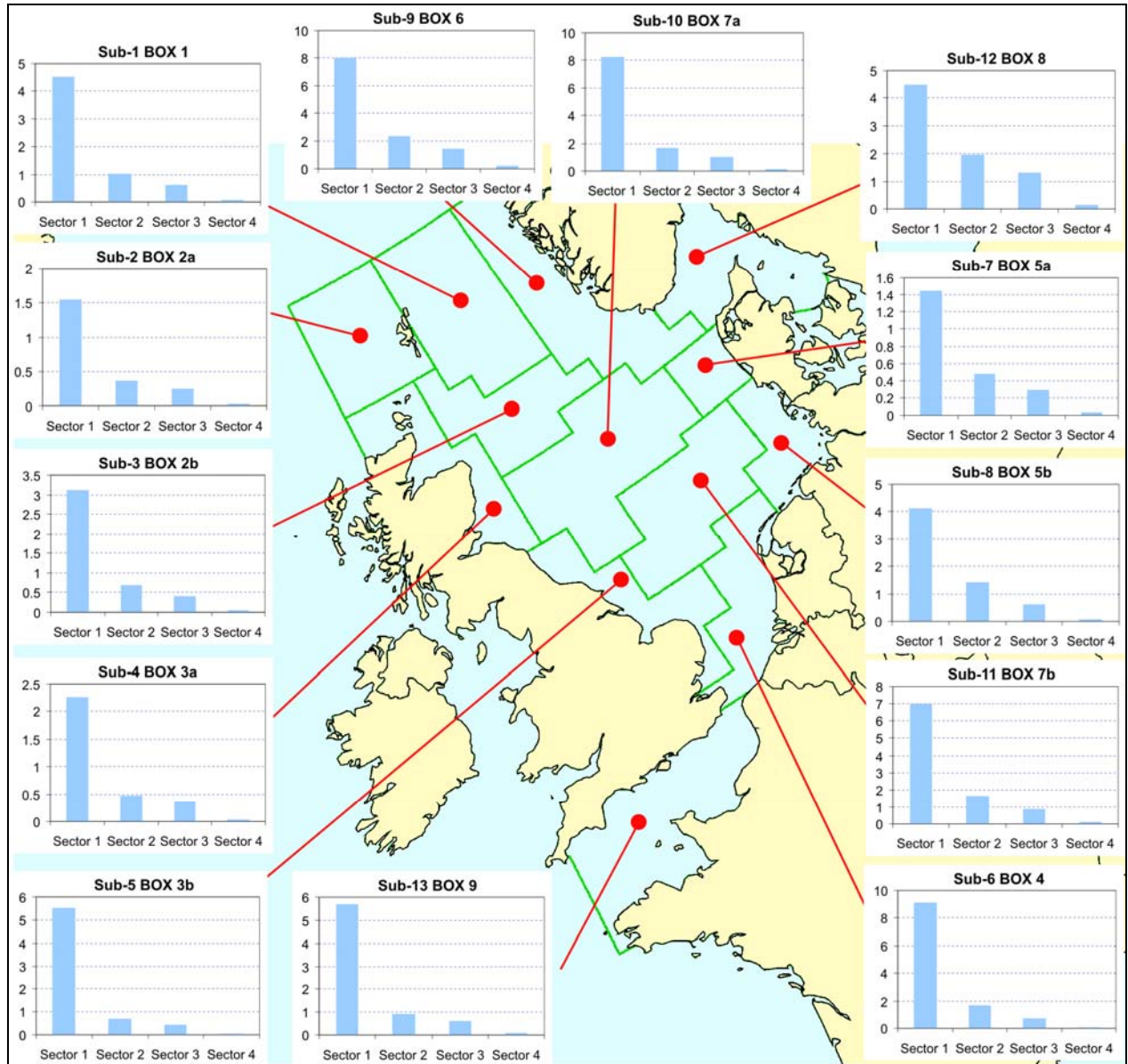


Figure A.17. Contribution of four key source categories (1 – combustion in power plants and industry and industrial processes; 2 – transport; 3 - commercial, residential and other combustion; 4 - waste) to **lead** depositions to 13 sub-regions of the OSPAR Region II (Greater North Sea) in 2005. Units: t/y

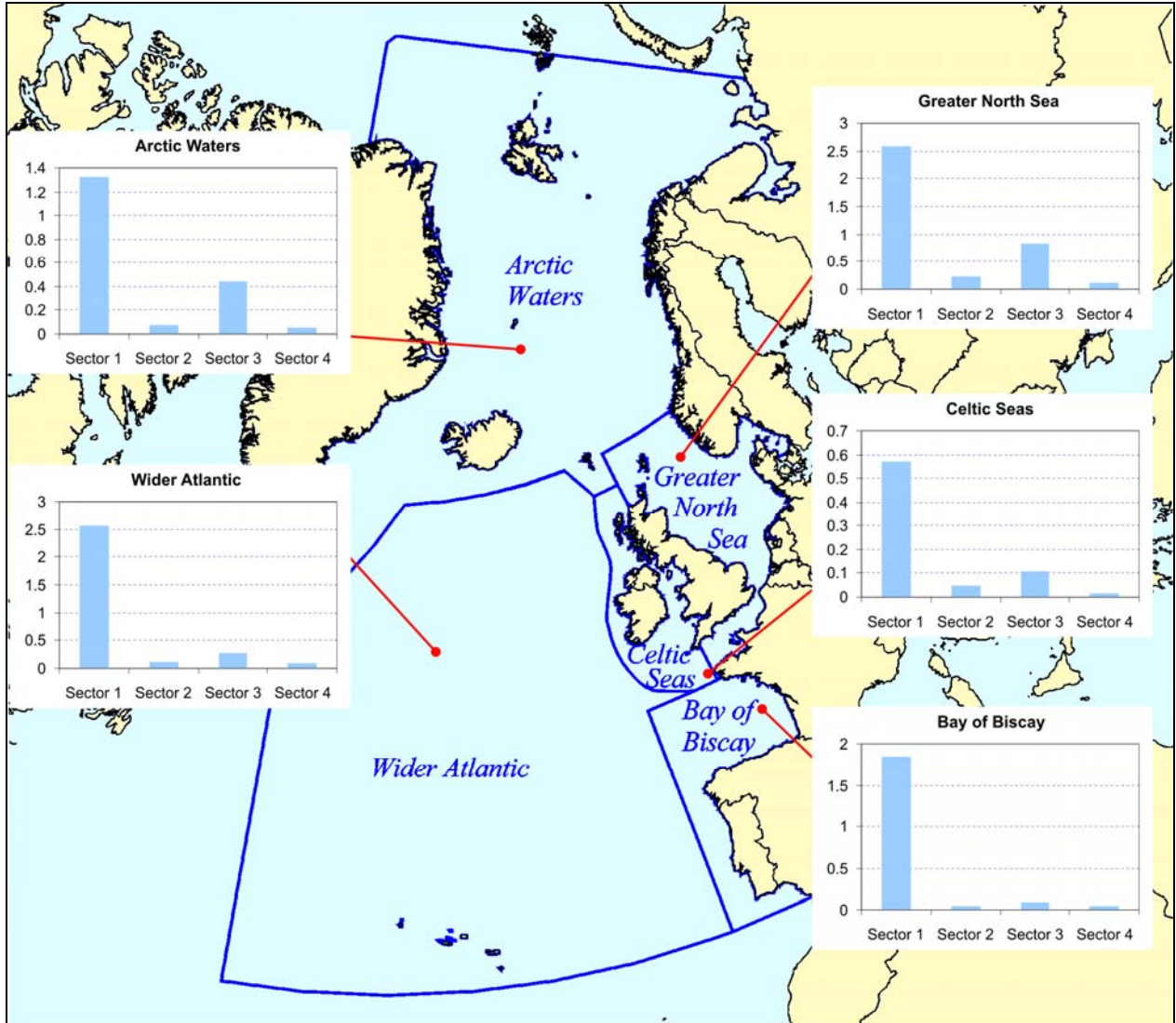


Figure A.18. Contribution of four key source categories (1 – combustion in power plants and industry and industrial processes; 2 – transport; 3 - commercial, residential and other combustion; 4 - waste) to **cadmium** depositions to the five main OSPAR regions in 2005. Units: t/y

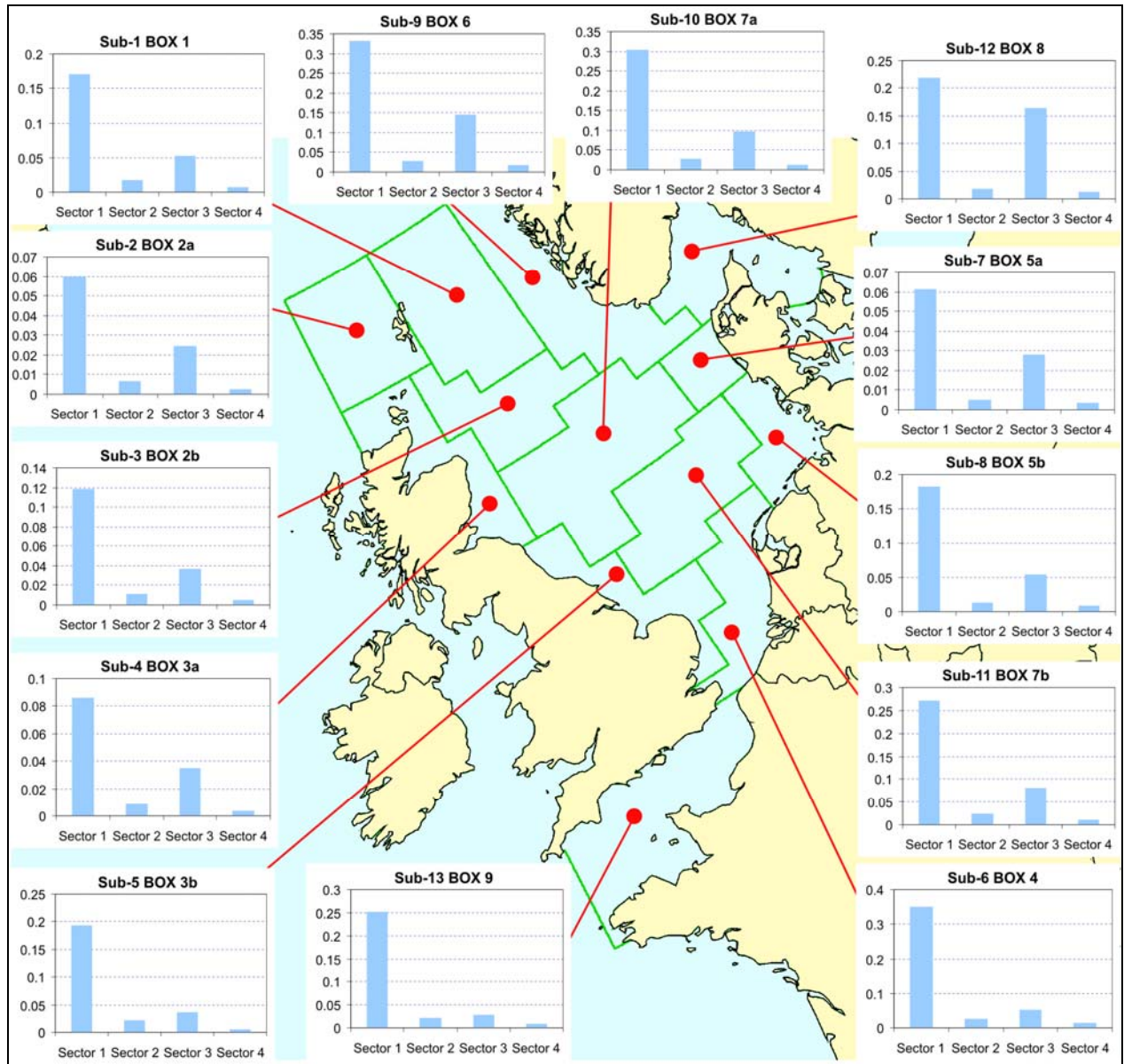


Figure A.19. Contribution of four key source categories (1 – combustion in power plants and industry and industrial processes; 2 – transport; 3 - commercial, residential and other combustion; 4 - waste) to **cadmium** depositions to 13 sub-regions of the OSPAR Region II (Greater North Sea) in 2005. Units: t/y

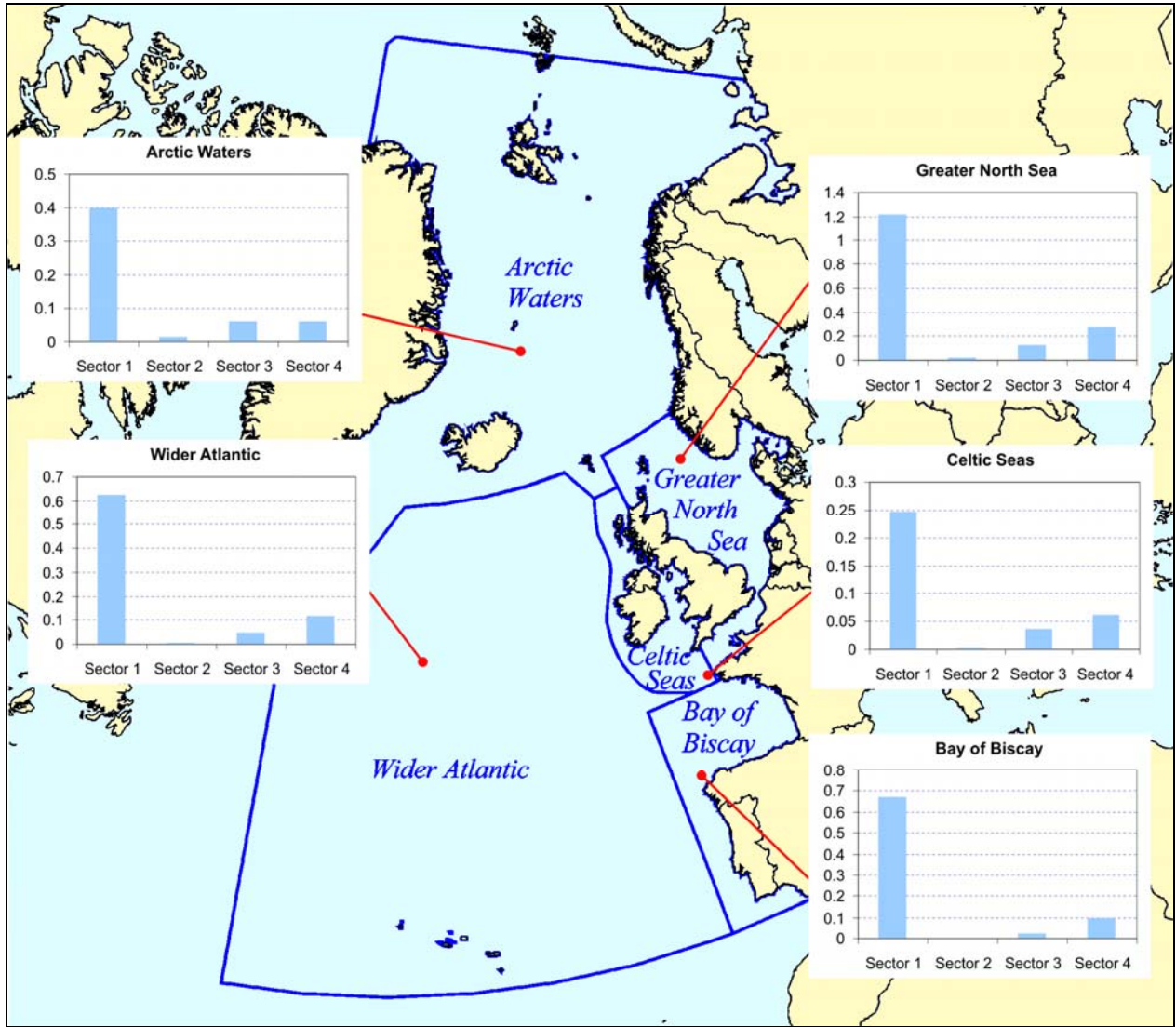


Figure A.20. Contribution of four key source categories (1 – combustion in power plants and industry and industrial processes; 2 – transport; 3 - commercial, residential and other combustion; 4 - waste) to **mercury** depositions to the five main OSPAR regions in 2005. Units: t/y

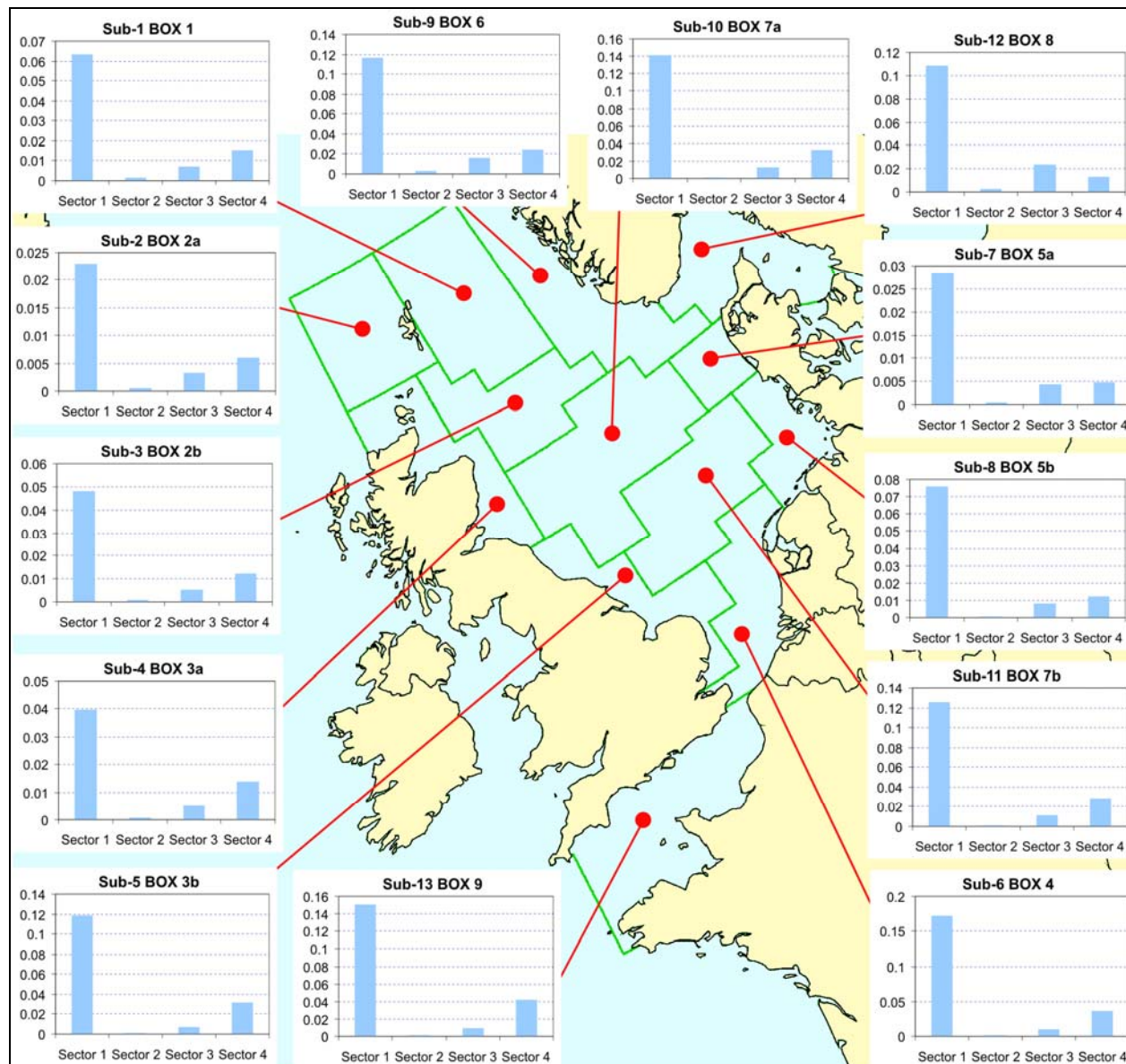
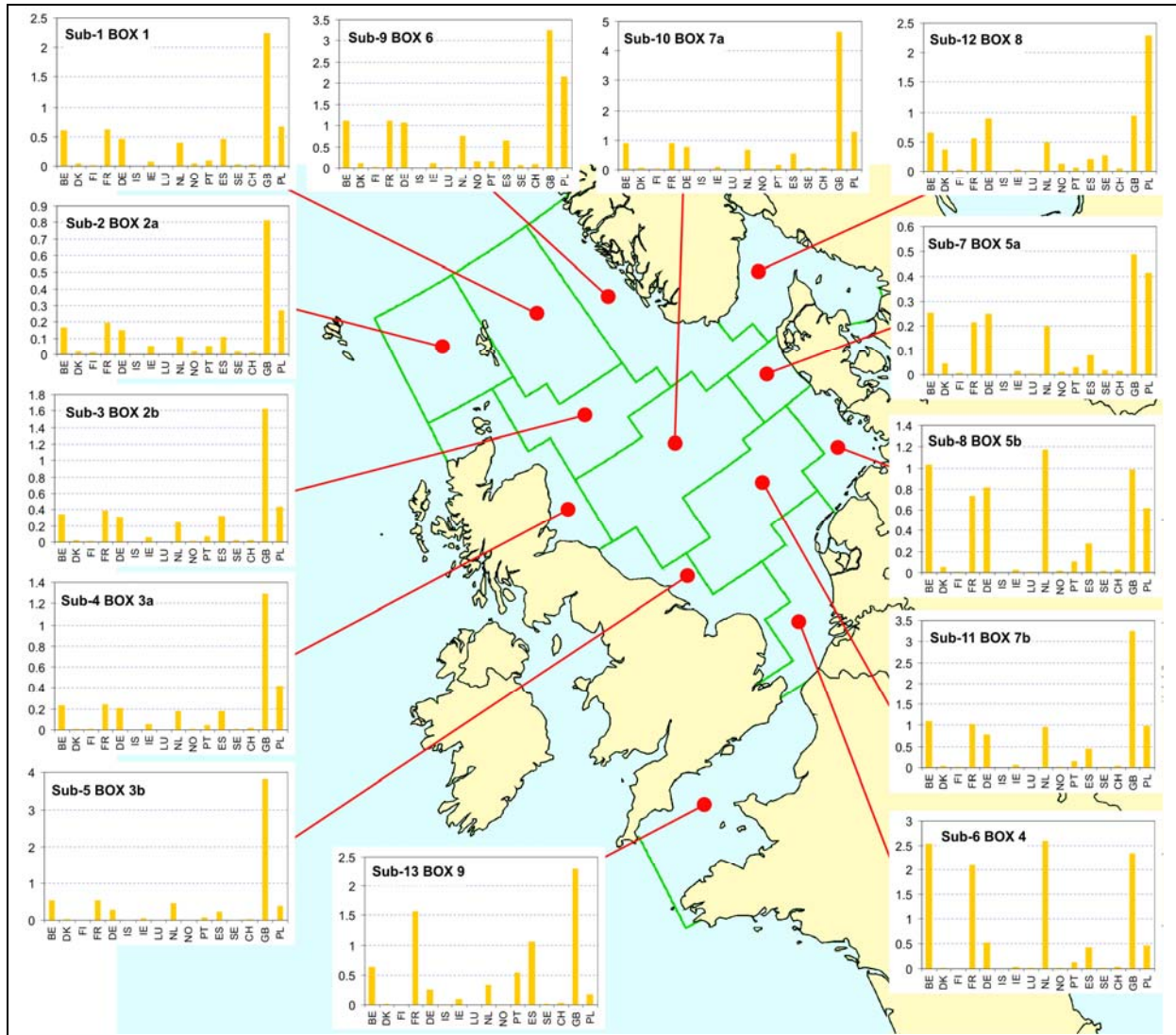


Figure A.21. Contribution of four key source categories (1 – combustion in power plants and industry and industrial processes; 2 – transport; 3 - commercial, residential and other combustion; 4 - waste) to **mercury** depositions to 13 sub-regions of the OSPAR Region II (Greater North Sea) in 2005. Units: t/y



BE	Belgium
DK	Denmark
FI	Finland
FR	France
DE	Germany
IS	Iceland
IE	Ireland
LU	Luxembourg
NL	Netherlands
NO	Norway
PT	Portugal
ES	Spain
SE	Sweden
CH	Switzerland
GB	United Kingdom
PL	Poland

Figure A.22. Contribution of the OSPAR Contracting Parties and one other selected country (Poland) to lead anthropogenic depositions to 13 sub-regions of the OSPAR Region II (Greater North Sea) in 2005. Units: $\mu\text{g}/\text{m}^2/\text{y}$

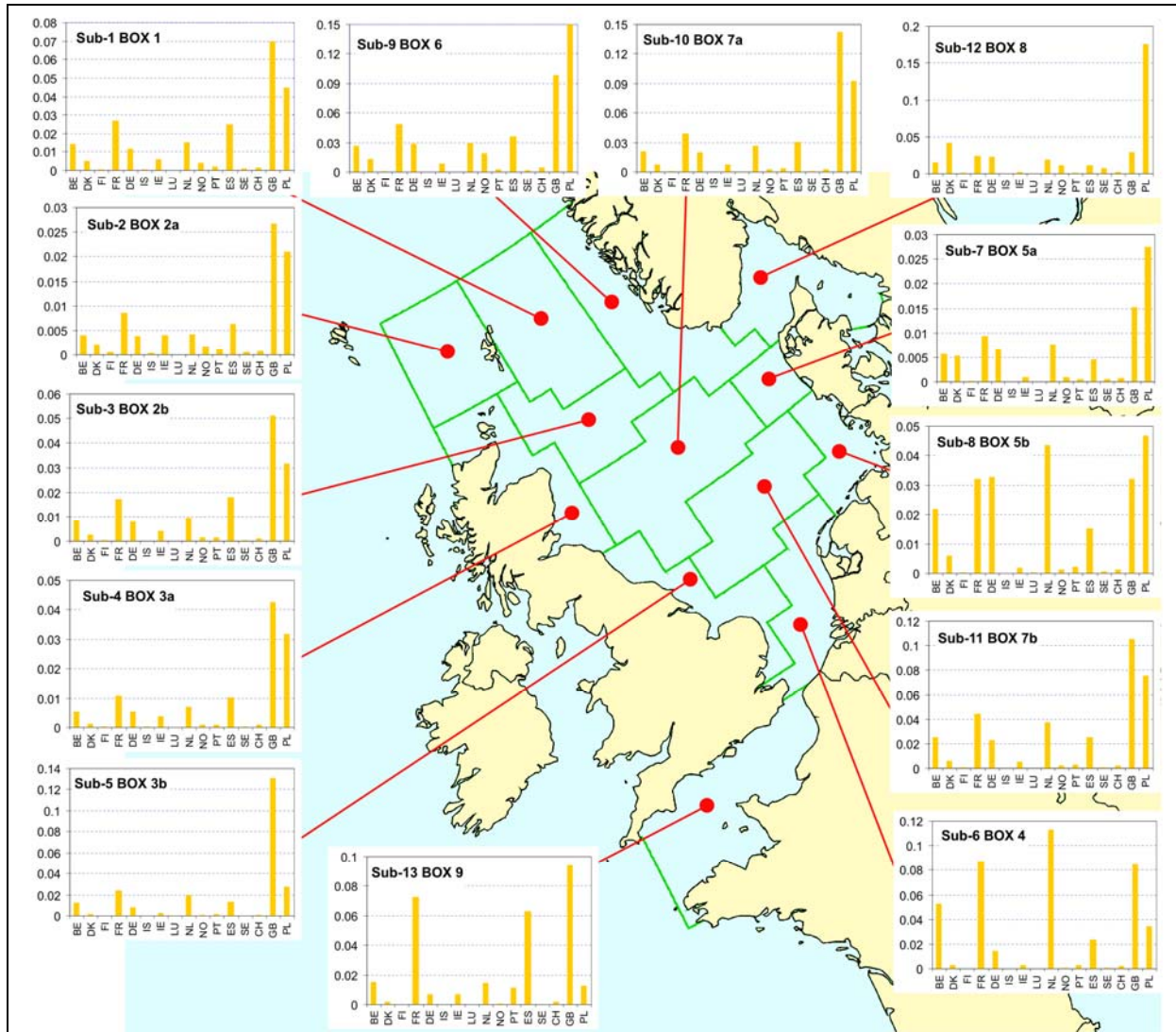
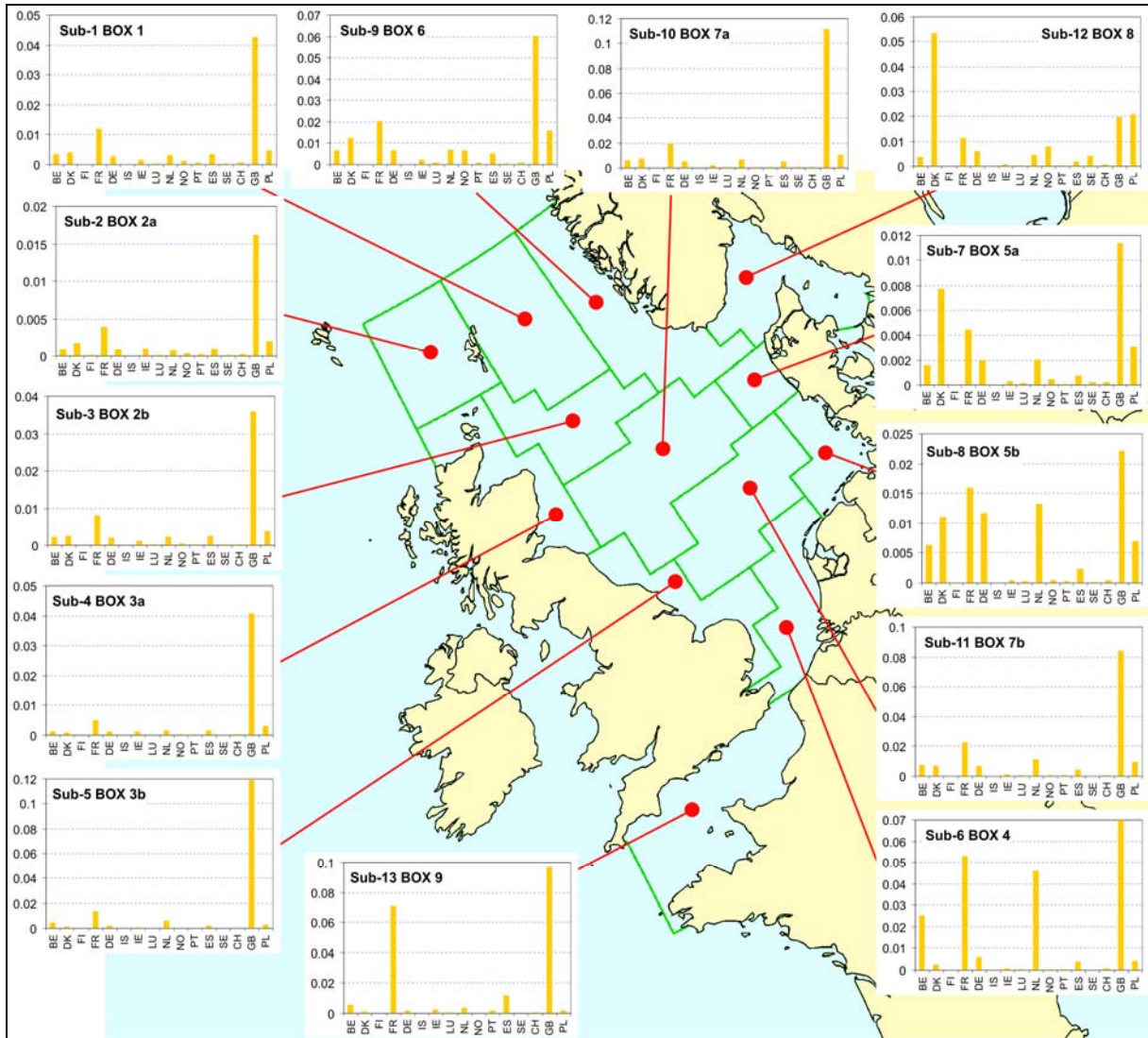


Figure A.23. Contribution of the OSPAR Contracting Parties and one other selected country (Poland) to **cadmium** anthropogenic depositions to 13 sub-regions of the OSPAR Region II (Greater North Sea) in 2005. Units: t/y



BE	Belgium
DK	Denmark
FI	Finland
FR	France
DE	Germany
IS	Iceland
IE	Ireland
LU	Luxembourg
NL	Netherlands
NO	Norway
PT	Portugal
ES	Spain
SE	Sweden
CH	Switzerland
GB	United Kingdom
PL	Poland

Figure A.24. Contribution of the OSPAR Contracting Parties and one other selected country (Poland) to **mercury** anthropogenic depositions to 13 sub-regions of the OSPAR Region II (Greater North Sea) in 2005. Units: t/y

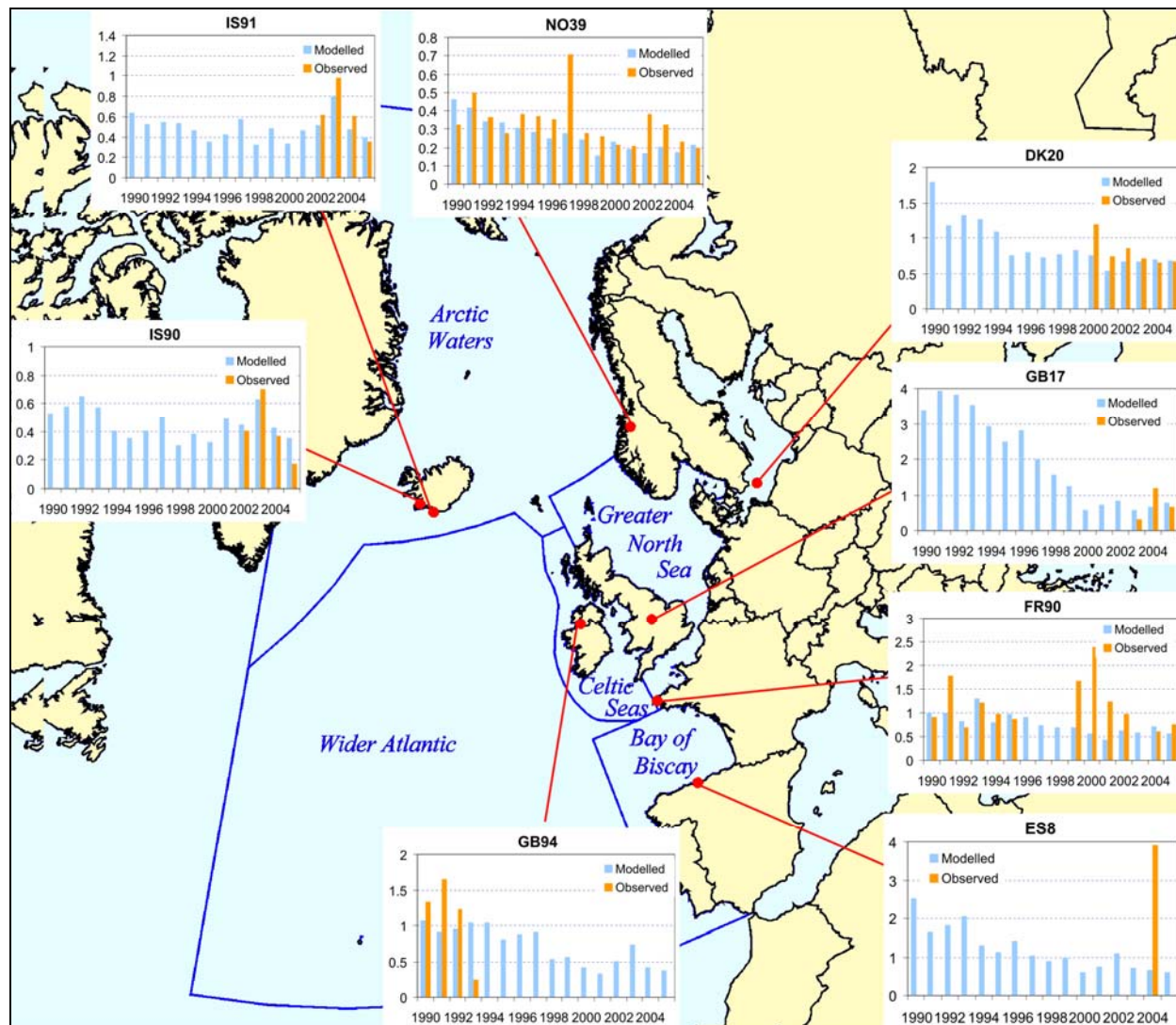


Figure A.25. Comparison of modelled and measured annual wet deposition flux of lead at the monitoring stations in the five main OSPAR regions. Units: mg/m²/y

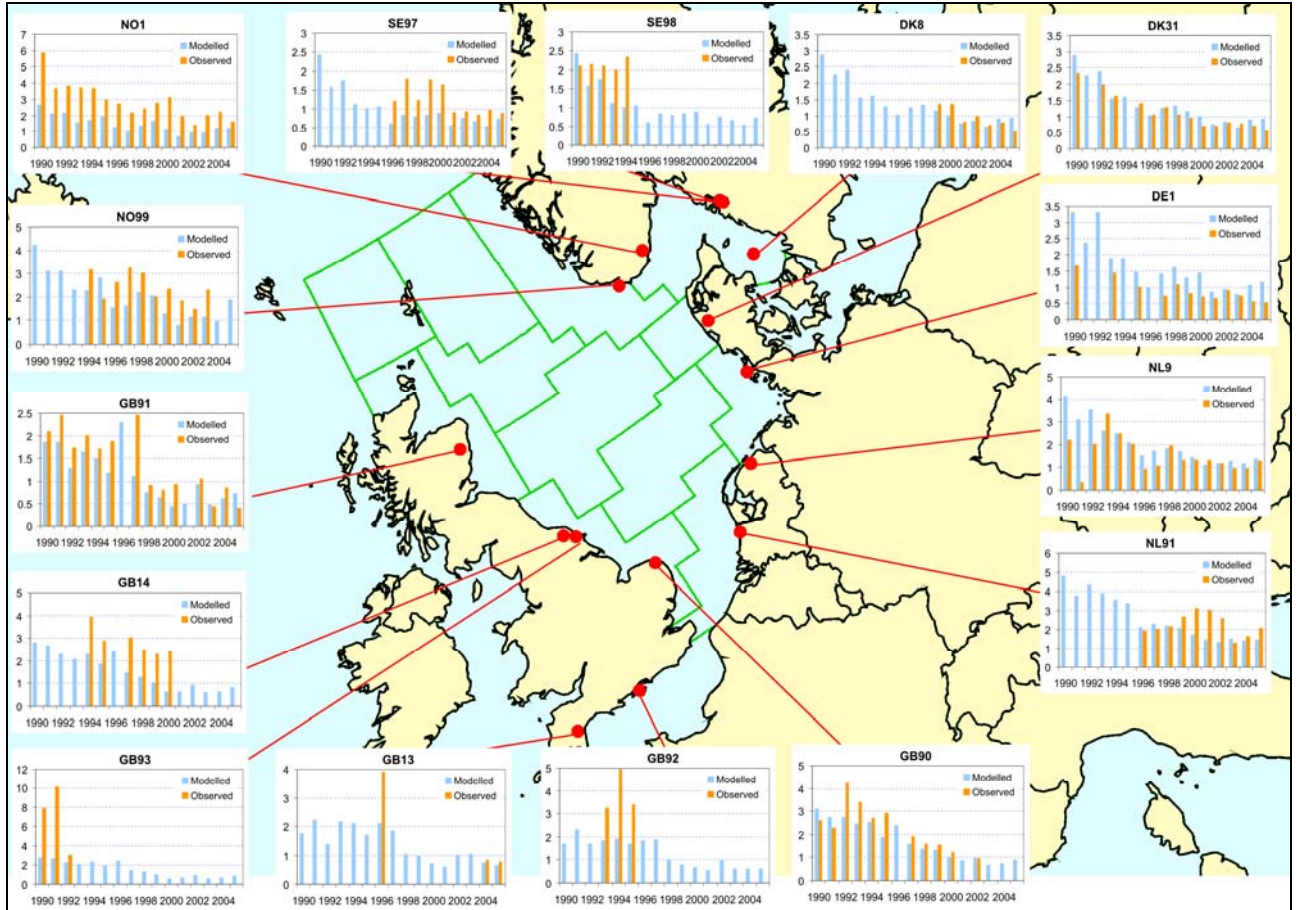


Figure A.26. Comparison of modelled and measured annual wet deposition flux of lead at the monitoring stations in the OSPAR Region II (Greater North Sea). Units: mg/m²/y

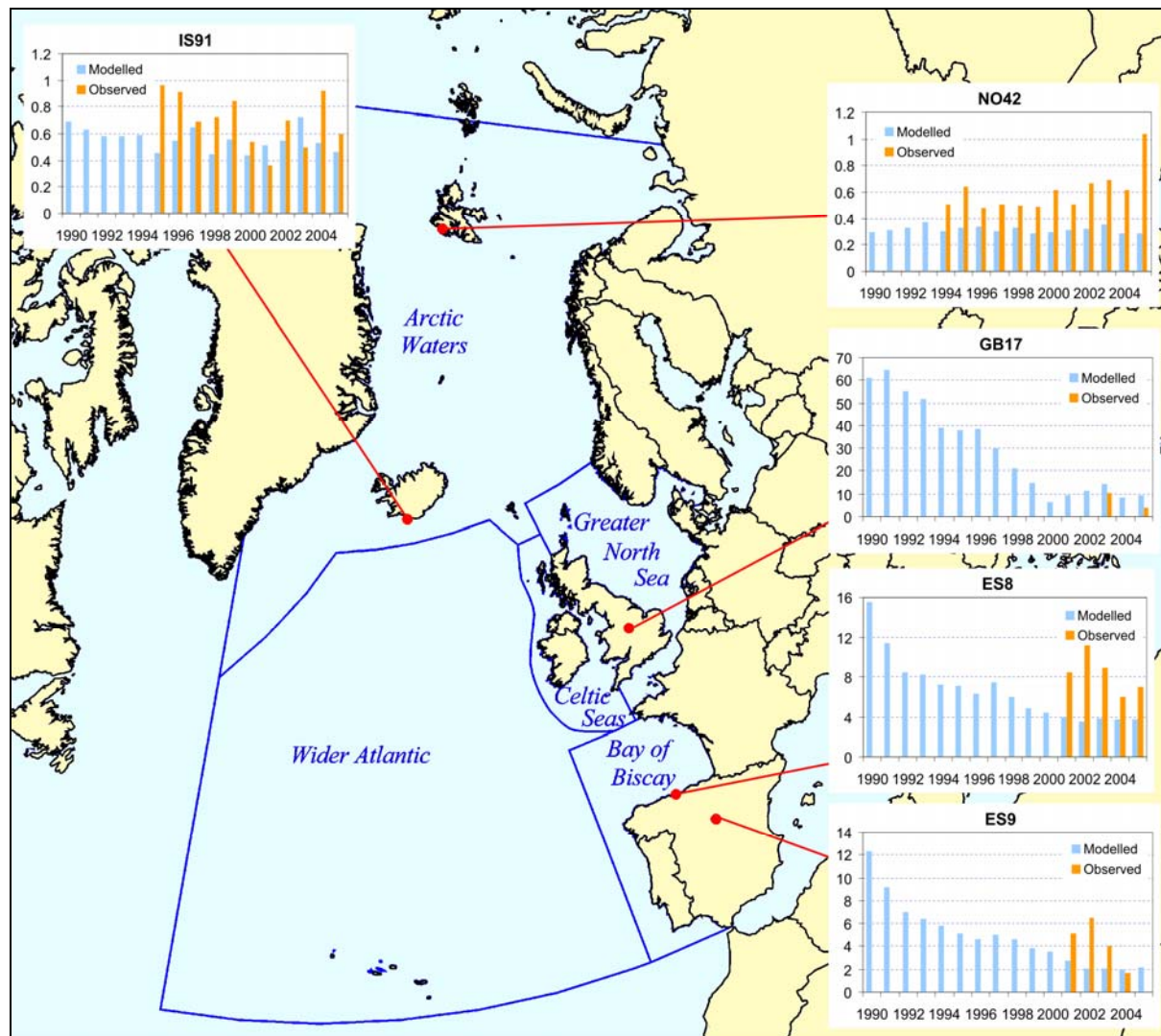


Figure A.27. Comparison of modelled and measured annual air concentrations of lead at the monitoring stations in the five main OSPAR regions. Units: ng/m³

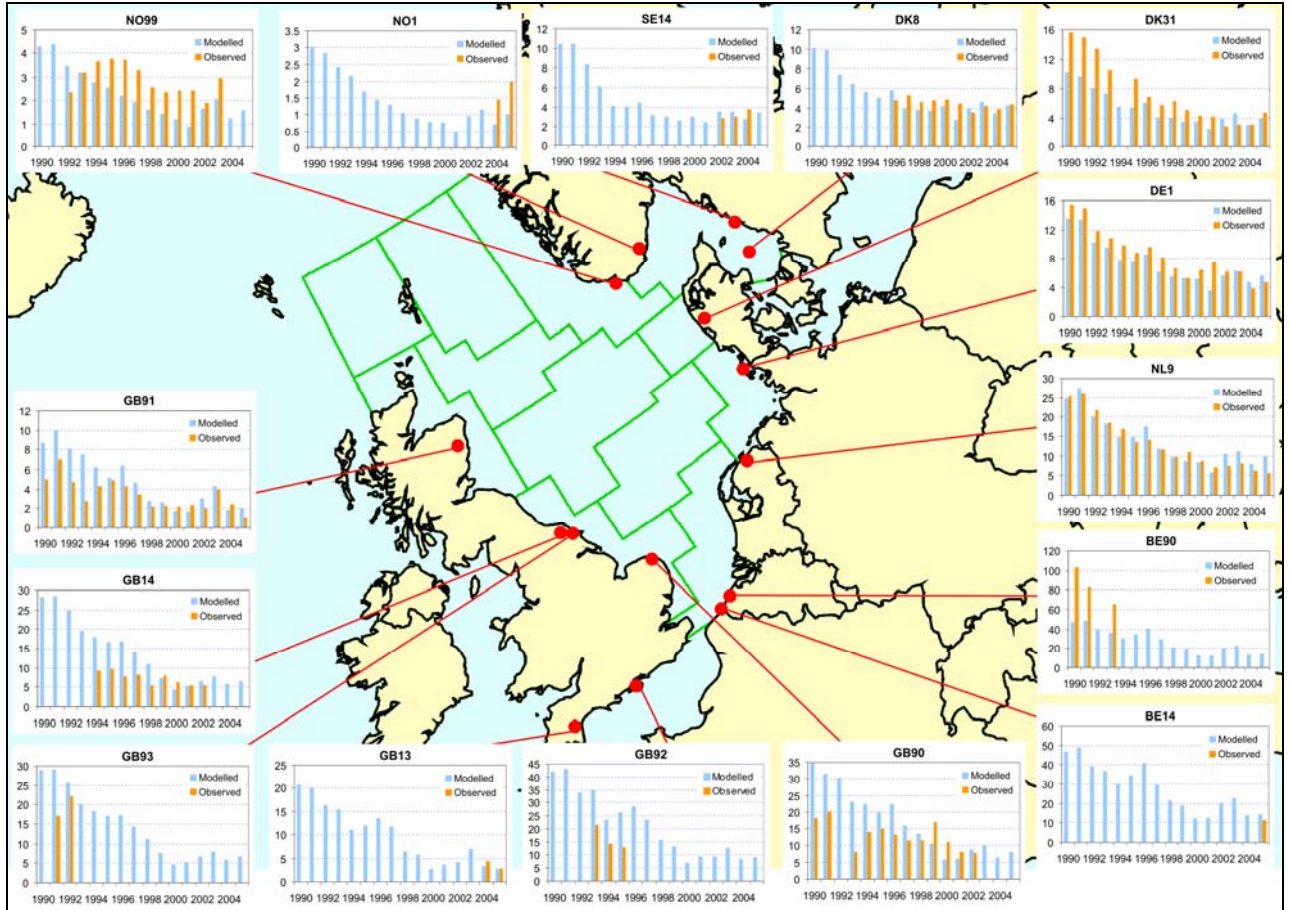


Figure A.28. Comparison of modelled and measured annual air concentrations of lead at the monitoring stations in the OSPAR Region II (Greater North Sea). Units: ng/m³

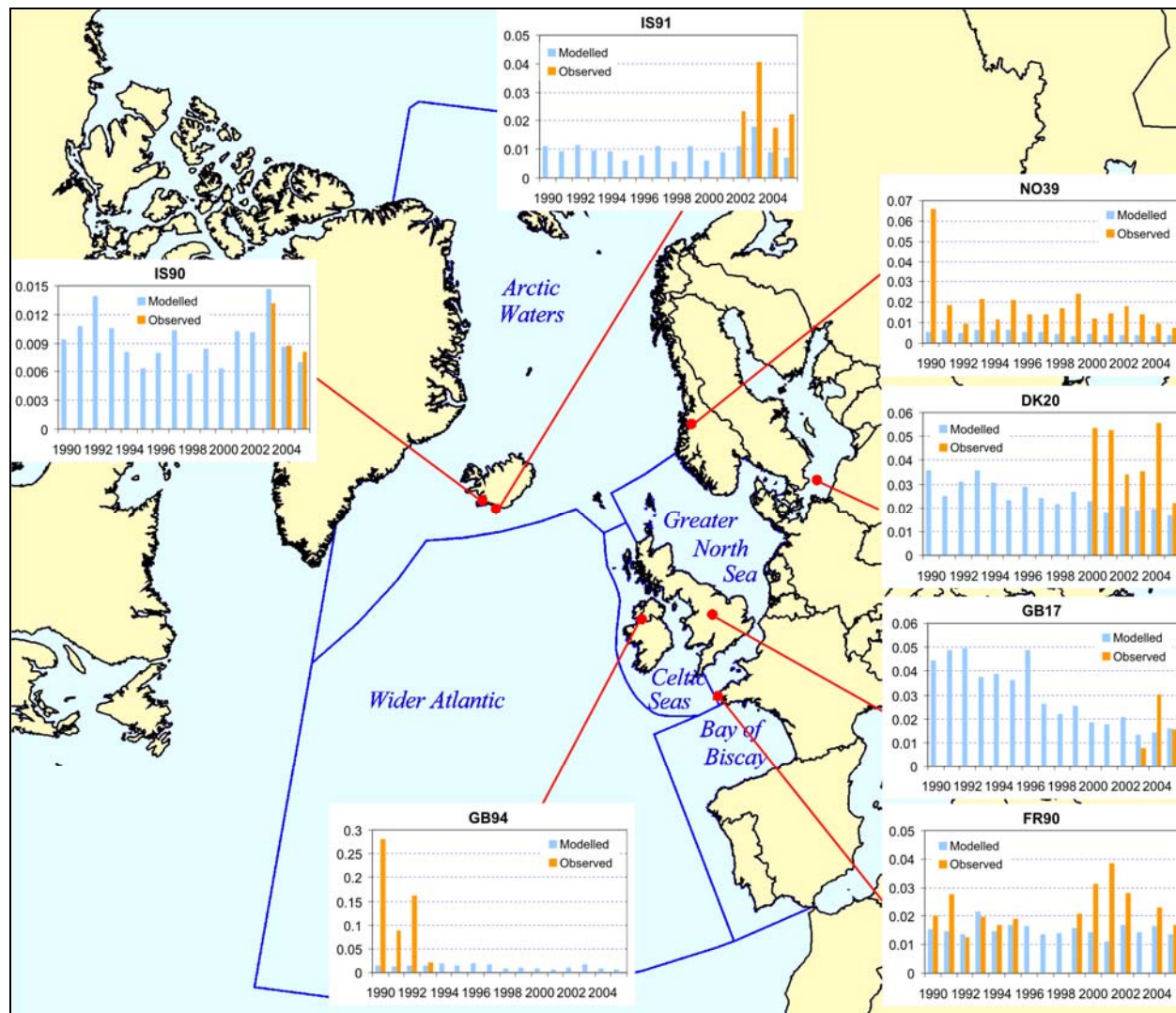


Figure A.29. Comparison of modelled and measured annual wet deposition flux of cadmium at the monitoring stations in the five main OSPAR regions. Units: mg/m²/y

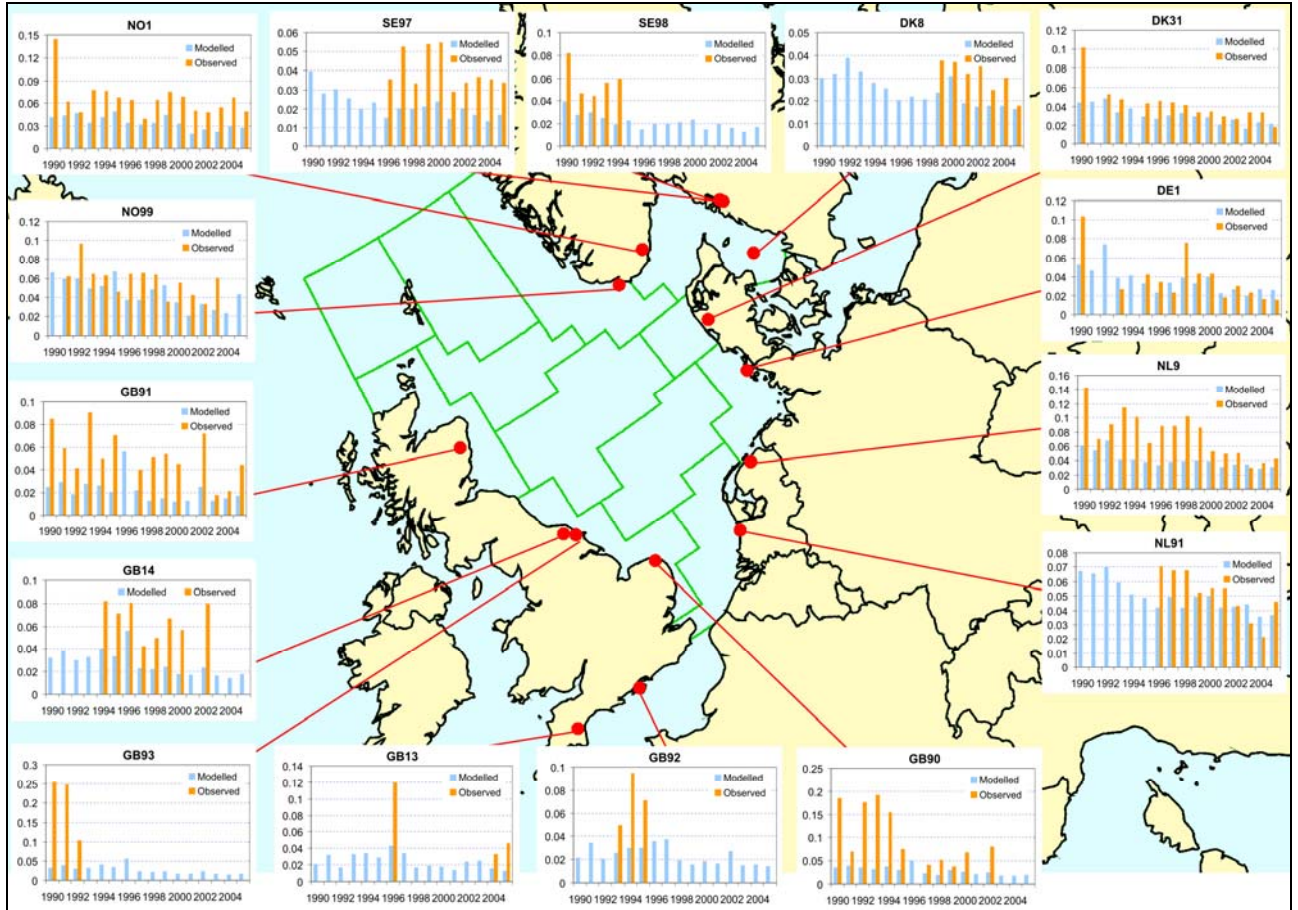


Figure A.30. Comparison of modelled and measured annual wet deposition flux of cadmium at the monitoring stations in the OSPAR Region II (Greater North Sea). Units: mg/m²/y

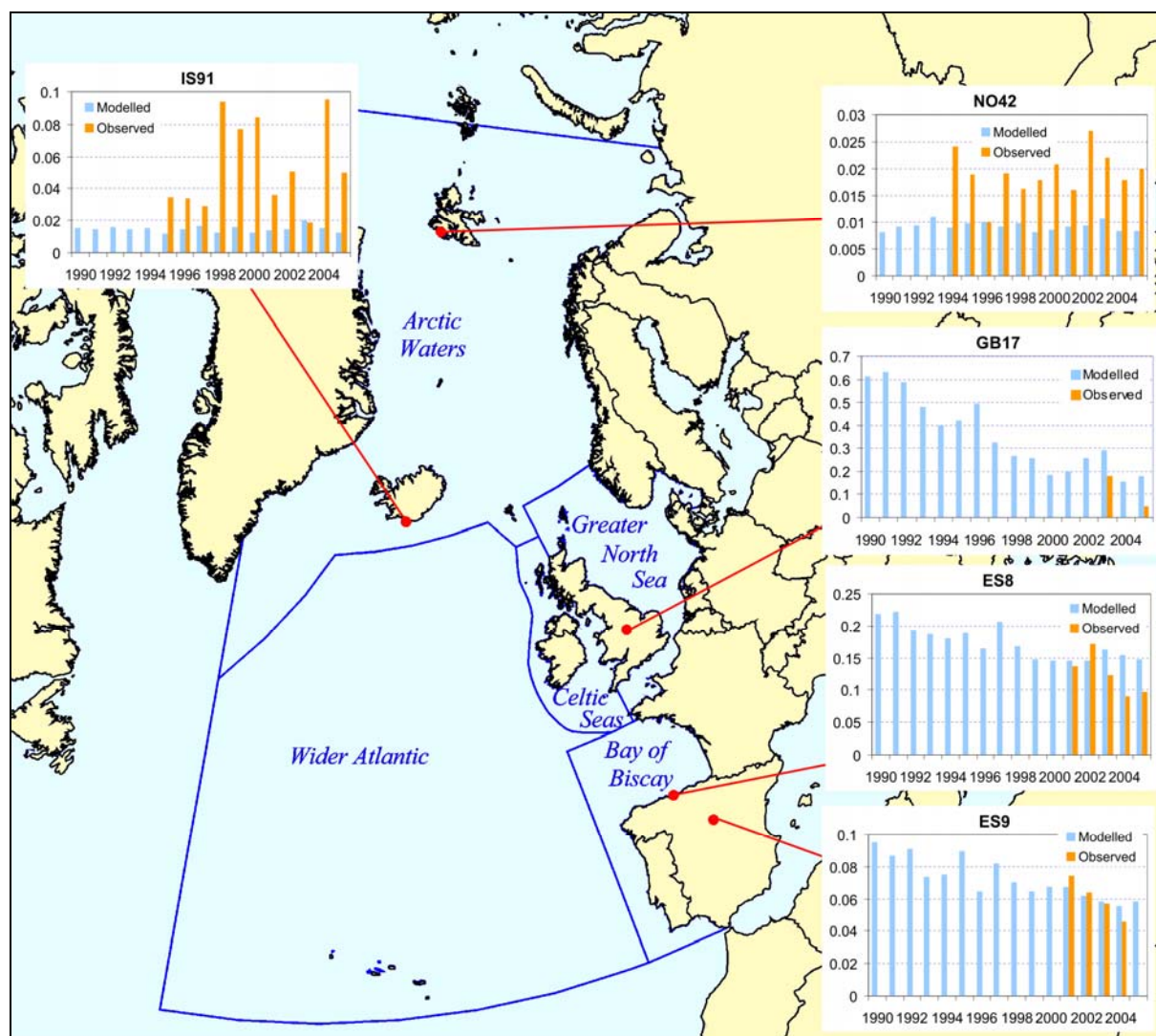


Figure A.31. Comparison of modelled and measured annual air concentrations of cadmium at the monitoring stations in the five main OSPAR regions. Units: ng/m³

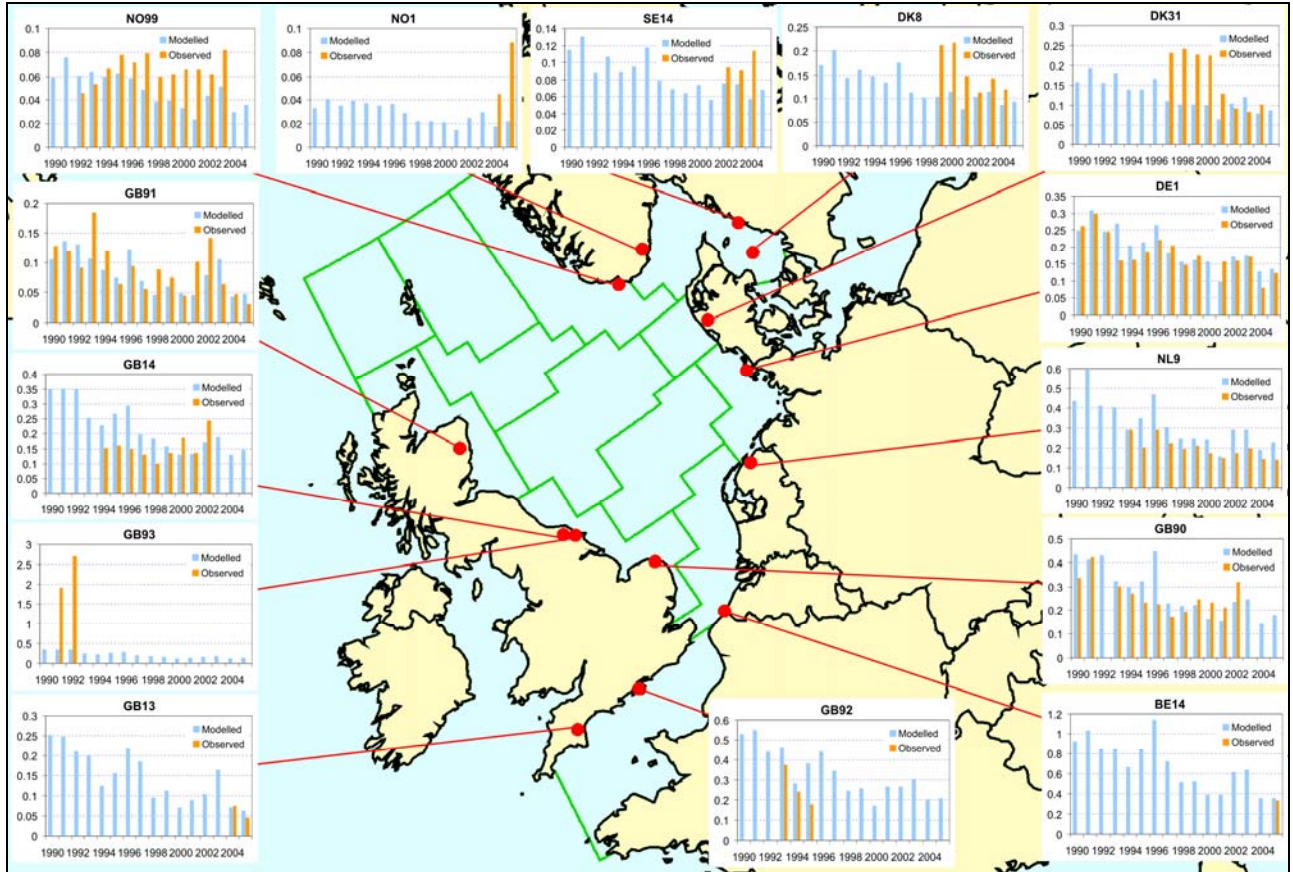


Figure A.32. Comparison of modelled and measured annual air concentrations of cadmium at the monitoring stations in the OSPAR Region II (Greater North Sea). Units: ng/m³

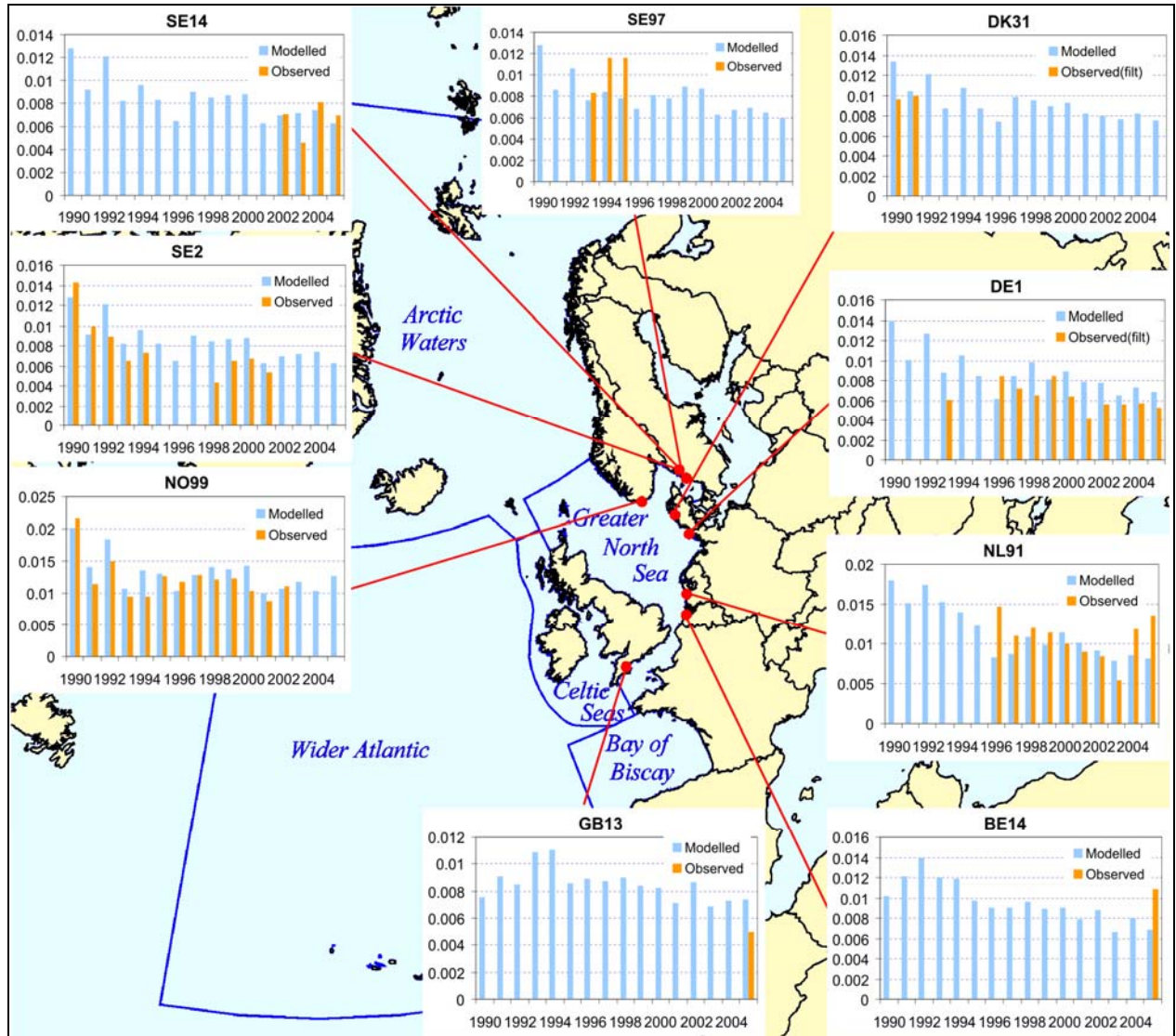


Figure A.33. Comparison of modelled and measured annual wet deposition flux of mercury at the monitoring stations in the OSPAR maritime area. Units: mg/m²/y

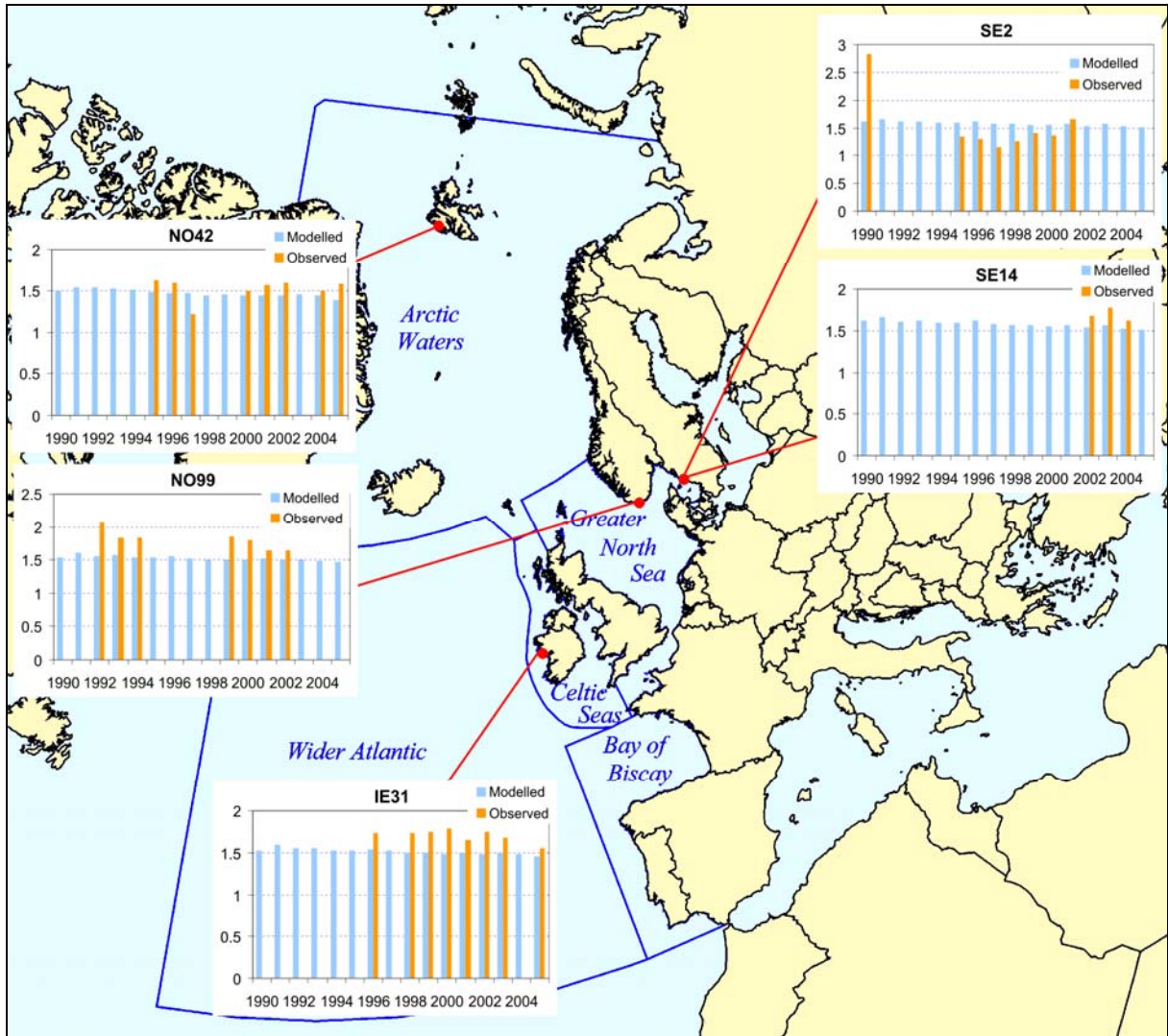


Figure A.34. Comparison of modelled and measured annual air concentrations of total gaseous mercury at the monitoring stations in the five main OSPAR regions. Units: ng/m3

Table A.1. Annual lead anthropogenic emissions from the OSPAR Contracting Parties and two main contributors to deposition. Units: t/y.

Country	Year															
	1990	1991	1992	1993	1994	1995	1996	1997	1998	1999	2000	2001	2002	2003	2004	2005
Belgium	442	418	397	320	259	247	221	195	169	144	118	102	72	68	81	78
Denmark	122	95	86	44	11	10	10	8	7	7	7	6	5	5	5	6
Finland	326	247	175	100	60	57	35	19	20	14	38	38	40	34	27	24
France	4283	2876	2090	1833	1630	1450	1276	1127	1010	776	250	213	206	145	135	134
Germany	1801	1055	761	606	405	330	222	96	94	96	102	105	106	107	109	107
Iceland	6	6	5	5	4	3	3	2	1	1	0.2	0.2	0.2	0.2	0.2	0.2
Ireland	116	111	107	96	84	76	65	54	39	24	15	11	9	8	8	8
Luxembourg	77	71	65	59	53	30	26	18	7	2	2	2	2	2	2	2
Netherlands	340	299	251	225	193	164	120	73	50	42	35	39	43	40	44	44
Norway	187	144	127	87	24	22	10	9	9	9	7	6	8	7	8	6
Portugal	621	646	694	674	649	631	615	591	586	417	228	250	253	248	252	244
Spain	2681	1809	1220	1115	1104	932	902	839	779	709	589	389	268	265	261	266
Sweden	352	307	287	135	41	27	23	24	23	21	19	19	17	18	18	17
Switzerland	420	380	335	281	247	184	156	137	117	52	30	27	24	21	20	20
UK	2912	2657	2434	2159	1859	1549	1314	1151	849	495	165	156	143	130	134	118
OSPAR, kt	14.7	11.1	9	7.7	6.6	5.7	5	4.3	3.8	2.8	1.6	1.4	1.2	1.1	1.1	1.1
Poland	1372	1336	986	997	966	937	960	896	736	745	647	610	588	596	600	536
Russia	3591	3553	3095	3276	2643	2426	2304	2247	2262	2339	2352	2235	2118	2207	330	355
EMEP, kt	35	29.2	24.4	22.5	19.9	17.7	16.1	14.6	13.3	11.8	9.7	8.7	7.1	6.9	4.9	4.7
ReNat ^(*), kt	2.7	2.5	2.6	2.7	2.8	2.6	2.5	2.6	2.5	2.5	2.5	2.4	2.7	2.4	2.4	2.5

(*) Total re-emission and natural emission from the OSPAR maritime area

Table A.2. Annual cadmium anthropogenic emissions from the OSPAR Contracting Parties and two main contributors to deposition. Units: t/y.

Country	Year															
	1990	1991	1992	1993	1994	1995	1996	1997	1998	1999	2000	2001	2002	2003	2004	2005
Belgium	7.4	7.3	7.9	6.7	5.3	5.5	4.9	4.3	3.7	3.1	2.5	2.4	2.1	1.7	2.3	2.0
Denmark	1.1	1.2	1.1	1.1	1.0	0.8	0.8	0.7	0.7	0.7	0.6	0.7	0.6	0.6	0.6	0.6
Finland	6.3	3.4	2.9	2.9	2.4	1.7	1.5	1.1	1.3	0.6	1.4	1.6	1.3	1.2	1.5	1.3
France	18.8	18.5	18.2	17.3	17.2	16.3	15.8	14.8	13.9	12.6	12.9	11.7	11.2	8.2	6.0	5.9
Germany	12.0	8.0	5.2	3.7	2.6	2.3	2.2	2.4	2.2	2.7	2.4	2.6	2.7	2.7	2.7	2.7
Iceland	0.2	0.2	0.1	0.1	0.1	0.1	0.1	0.1	0.1	0.1	0.1	0.1	0.1	0.1	0.1	0.1
Ireland	0.8	0.8	0.9	0.8	0.9	0.9	0.9	0.9	1.0	1.0	1.0	0.8	0.6	0.6	0.6	0.6
Luxembourg	0.6	0.6	0.6	0.5	0.5	0.4	0.4	0.3	0.2	0.1	0.1	0.1	0.05	0.05	0.05	0.05
Netherlands	2.1	2.4	2.1	1.7	1.4	1.1	1.9	1.9	1.2	1.1	1.0	1.6	2.2	2.4	1.8	1.7
Norway	1.1	1.0	1.0	1.1	1.1	1.0	1.0	1.0	1.1	1.0	0.7	0.7	0.7	0.6	0.6	0.5
Portugal	5.3	5.8	5.9	5.2	5.5	5.7	4.9	5.3	6.0	6.0	5.5	5.4	6.1	5.4	5.3	5.7
Spain	23.8	23.2	22.0	19.7	20.7	20.7	18.8	18.7	19.0	19.3	18.2	18.2	18.9	17.2	16.6	16.7
Sweden	2.3	1.7	1.4	1.1	0.8	0.7	0.7	0.7	0.6	0.5	0.5	0.6	0.5	0.5	0.5	0.5
Switzerland	3.7	3.5	3.3	3.0	2.8	2.5	2.4	2.2	2.2	1.8	1.6	1.5	1.3	1.1	1.1	1.1
UK	24.3	24.0	23.6	15.4	14.4	12.2	10.3	9.2	6.8	6.5	6.3	5.0	4.8	3.4	3.7	3.8
OSPAR	110	102	96	80	77	72	67	64	60	57	55	53	53	46	43	43
Poland	91.6	85.0	84.1	91.9	85.8	82.6	91.2	85.8	55.4	61.7	50.4	52.5	48.7	48.5	46.0	46.0
Russia	79.4	68.2	68.8	59.0	56.6	57.4	51.0	50.4	49.0	50.9	50.5	51.0	51.5	57.3	55.4	59.4
EMEP	484	449	429	399	375	361	351	338	295	293	269	264	250	276	242	244
ReNat ^(*)	68	63	65	68	70	65	62	64	63	61	63	59	67	61	61	61

(*) Total re-emission and natural emission from the OSPAR maritime area

Table A.3. Annual mercury anthropogenic emissions from the OSPAR Contracting Parties and two main contributors to deposition. Units: t/y.

Country	Year															
	1990	1991	1992	1993	1994	1995	1996	1997	1998	1999	2000	2001	2002	2003	2004	2005
Belgium	6.6	5.7	5.8	3.9	4.2	3.6	3.4	3.2	2.9	2.7	2.5	2.1	3.1	2.8	2.9	1.9
Denmark	3.3	3.3	3.2	3.2	2.3	2.2	2.5	2.0	1.9	2.0	1.2	1.4	1.3	1.3	1.2	1.3
Finland	1.1	0.9	0.8	0.6	0.7	0.7	0.8	0.6	0.5	0.4	0.6	0.7	0.7	0.8	0.7	0.9
France	27.0	27.5	26.4	23.8	22.8	21.6	21.0	16.3	15.6	13.7	13.0	11.4	10.8	8.7	8.5	8.6
Germany	19.2	13.3	8.4	5.3	2.8	2.4	2.6	2.5	2.6	2.5	2.7	2.7	2.7	2.9	2.8	2.7
Iceland	0.05	0.1	0.1	0.1	0.1	0.1	0.1	0.1	0.1	0.1	0.1	0.1	0.1	0.1	0.1	0.1
Ireland	1.0	1.1	1.0	1.0	0.9	0.9	0.9	0.7	0.6	0.5	0.4	0.4	0.4	0.4	0.4	0.4
Luxembourg	0.3	0.3	0.3	0.2	0.2	0.1	0.1	0.1	0.1	0.3	0.3	0.3	0.3	0.3	0.3	0.3
Netherlands	4.7	3.9	3.3	2.6	2.0	1.2	1.2	0.8	0.6	0.5	0.9	0.7	0.7	0.7	1.0	1.0
Norway	1.5	1.4	1.2	0.9	1.0	0.9	0.9	0.9	0.9	0.9	0.8	0.7	0.7	0.7	0.7	0.7
Portugal	3.8	3.9	4.3	3.9	3.7	4.0	3.6	3.9	4.1	4.3	4.4	4.2	4.5	3.8	3.8	4.1
Spain	13.2	13.9	15.0	13.5	13.4	13.2	11.9	9.9	10.4	11.3	10.9	10.9	11.6	10.1	10.1	10.0
Sweden	1.6	1.3	1.3	1.1	1.1	1.1	1.1	1.0	0.9	0.9	0.8	0.7	0.7	0.8	0.8	0.7
Switzerland	6.6	6.1	5.8	5.4	4.9	4.1	3.8	3.5	3.3	2.4	2.1	1.8	1.4	1.0	1.0	1.0
UK	37.7	37.9	36.1	22.2	20.6	19.7	14.7	11.8	10.7	8.6	8.7	8.4	7.4	8.1	7.0	7.6
OSPAR	128	120	113	88	81	76	68	57	55	51	49	47	46	42	41	41
Poland	33.3	32.7	31.9	32.5	32.4	32.3	33.6	33.0	29.5	27.1	25.6	23.2	19.8	20.2	19.8	20.1
Russia	15.6	13.4	11.4	11.8	10.4	10.4	10.1	9.6	9.4	9.9	10.0	10.1	10.2	11.4	11.9	14.0
EMEP	334	317	299	269	255	249	236	222	215	204	202	196	172	194	170	172
ReNat ^(*)	57	56	54	53	52	50	52	53	54	56	57	55	57	57	58	57

(*) Total re-emission and natural emission from the OSPAR maritime area

Table A.4. Lead emissions by aggregated source categories for the OSPAR Contracting Parties and two main contributors to deposition in 2005. Units: t/y.

Country	Source category			
	Combustion in power plants and industry & Industrial processes	Transport	Commercial, residential and other combustion	Waste
Belgium	66	11	0.8	1.0
Denmark	3.9	1.4	0.2	--
Finland	19	2.1	2.6	0.02
France	95	17	20.3	2.1
Germany	14	82	10.3	7.4E-06
Iceland	0.1	0.003	0.08	0.01
Ireland	3.8	2.3	1.8	0.01
Luxembourg	1.5	0.3	0.05	0.05
Netherlands	25	14	4.5	--
Norway	2.6	3.0	0.2	0.04
Portugal	219	7.3	6.2	11.7
Spain	238	25	0.8	1.5
Sweden	9.2	6.6	0.8	0.03
Switzerland	9.4	5	0.3	5.5
United Kingdom	109	2.9	5.2	0.2
OSPAR	815	181	54	22
Poland	242	60	225	9.6
Russian Federation	355	--	--	--
EMEP	2473	1786	347	80

Table A.5. Cadmium emissions by aggregated source categories for the OSPAR Contracting Parties and two main contributors to deposition in 2005. Units: t/y.

Country	Source category			
	Combustion in power plants and industry & Industrial processes	Transport	Commercial, residential and other combustion	Waste
Belgium	1.35	0.14	0.20	0.30
Denmark	0.37	0.04	0.21	--
Finland	1.05	0.0005	0.25	0.005
France	5.33	0.002	0.33	0.29
Germany	1.75	0.30	0.65	1.3E-06
Iceland	0.06	0.002	0.02	0.0017
Ireland	0.36	0.03	0.18	0.0004
Luxembourg	0.02	0.005	0.02	0.0002
Netherlands	1.55	0.07	0.10	--
Norway	0.27	0.09	0.12	0.02
Portugal	4.86	0.17	0.32	0.33
Spain	16.02	0.36	0.24	0.09
Sweden	0.37	0.02	0.14	0.004
Switzerland	0.54	0.06	0.23	0.29
United Kingdom	2.92	0.59	0.29	0.01
OSPAR	37	1.9	3.3	1.3
Poland	10.85	0.36	34.08	0.73
Russian Federation	59.4	--	--	--
EMEP	190	4	44	6.3

Table A.6. Mercury emissions by aggregated source categories for the OSPAR Contracting Parties and two main contributors to deposition in 2005. Units: t/y.

Country	Source category			
	Combustion in power plants and industry & Industrial processes	Transport	Commercial, residential and other combustion	Waste
Belgium	1.56	--	0.16	0.20
Denmark	1.01	0.01	0.27	--
Finland	0.80	0.02	0.03	0.0029
France	7.18	--	0.23	1.20
Germany	2.55	0.11	0.0006	0.0004
Iceland	0.08	0.0002	0.01	0.02
Ireland	0.21	0.0011	0.18	0.03
Luxembourg	0.28	--	0.0018	0.0014
Netherlands	0.82	--	0.03	0.17
Norway	0.23	0.20	0.17	0.09
Portugal	2.80	0.0013	0.20	1.11
Spain	9.71	0.01	0.15	0.16
Sweden	0.60	0.0002	0.03	0.12
Switzerland	0.33	--	0.10	0.60
United Kingdom	5.30	0.07	0.33	1.88
OSPAR	33	0.42	1.9	5.6
Poland	2.80	0.001	0.21	1.11
Russian Federation	14	--	--	--
EMEP	144	0.48	17	11

Table A.7. Annual modelled lead total depositions to the main regions of the OSPAR maritime area. Units: t/y.

Year	OSPAR Region				
	I. Arctic Waters	II. Greater North Sea	III. Celtic Seas	IV. Bay of Biscay	V. Wider Atlantic
1990	1491	1689	442	633	3111
1991	1608	1656	460	548	3183
1992	1506	1468	350	480	2725
1993	1509	1338	436	587	2900
1994	1398	1265	424	373	2813
1995	1265	1195	355	417	2801
1996	1514	1171	490	480	2946
1997	1272	1005	371	408	3000
1998	1140	817	242	368	2382
1999	1111	747	228	348	2256
2000	1068	609	159	279	2149
2001	1043	516	156	322	2228
2002	1217	666	268	335	2589
2003	1457	595	273	303	2486
2004	1081	622	199	255	2164
2005	1060	710	193	248	2224

Table A.8. Annual modelled lead net atmospheric input to the main regions of the OSPAR maritime area. Units: t/y.

Year	OSPAR Region				
	I. Arctic Waters	II. Greater North Sea	III. Celtic Seas	IV. Bay of Biscay	V. Wider Atlantic
1990	800	1533	352	550	1421
1991	916	1526	385	471	1622
1992	795	1339	277	408	1117
1993	747	1191	358	507	1249
1994	728	1120	340	291	1004
1995	579	1058	284	329	1162
1996	900	1039	417	400	1370
1997	566	875	300	332	1417
1998	455	671	161	289	851
1999	443	603	147	270	771
2000	385	465	81	199	615
2001	384	396	96	243	791
2002	555	532	187	249	854
2003	801	479	203	230	967
2004	408	493	126	180	674
2005	385	570	121	175	730

Table A.9. Annual modelled cadmium total depositions to the main regions of the OSPAR maritime area. Units: t/y.

Year	OSPAR Region				
	I. Arctic Waters	II. Greater North Sea	III. Celtic Seas	IV. Bay of Biscay	V. Wider Atlantic
1990	34.6	27.2	8.6	12.8	73.7
1991	38.1	32.0	8.6	11.2	77.8
1992	38.7	27.3	7.0	9.7	70.7
1993	39.1	28.3	8.4	12.5	73.3
1994	36.2	26.3	8.9	8.0	73.3
1995	33.5	26.4	7.6	9.1	74.2
1996	41.2	29.2	11.8	11.5	76.7
1997	34.2	22.9	8.0	10.0	81.1
1998	31.0	18.0	5.5	8.2	63.3
1999	31.1	19.0	5.8	8.6	61.5
2000	29.9	17.8	4.5	7.8	58.9
2001	28.5	14.3	4.2	8.7	59.2
2002	33.7	19.0	7.1	10.0	70.4
2003	39.9	16.0	7.1	8.6	68.1
2004	30.0	16.1	5.0	6.6	56.9
2005	28.9	17.2	4.8	6.1	58.4

Table A.10. Annual modelled cadmium net atmospheric input to the main regions of the OSPAR maritime area. Units: t/y.

Year	OSPAR Region				
	I. Arctic Waters	II. Greater North Sea	III. Celtic Seas	IV. Bay of Biscay	V. Wider Atlantic
1990	17.3	23.3	6.3	10.7	31.5
1991	20.8	28.8	6.8	9.2	38.8
1992	21.0	24.1	5.1	7.9	30.5
1993	20.0	24.6	6.5	10.5	32.0
1994	19.5	22.6	6.8	5.9	28.1
1995	16.3	23.0	5.9	7.0	33.2
1996	25.8	25.9	10.0	9.5	37.3
1997	16.6	19.6	6.2	8.1	41.5
1998	13.9	14.3	3.4	6.2	25.1
1999	14.4	15.4	3.8	6.7	24.4
2000	12.9	14.2	2.5	5.8	20.6
2001	12.0	11.3	2.7	6.7	23.3
2002	17.2	15.7	5.1	7.8	27.0
2003	23.5	13.0	5.4	6.8	30.1
2004	13.2	12.8	3.1	4.8	19.6
2005	12.0	13.7	3.0	4.3	21.0

Table A.11. Annual modelled mercury total depositions to the main regions of the OSPAR maritime area. Units: t/y.

Year	OSPAR Region				
	I. Arctic Waters	II. Greater North Sea	III. Celtic Seas	IV. Bay of Biscay	V. Wider Atlantic
1990	38.4	11.6	4.3	3.8	51.9
1991	39.5	10.9	4.4	4.0	52.2
1992	40.1	11.5	4.4	4.0	51.4
1993	38.8	9.5	4.2	4.1	53.0
1994	36.5	9.2	4.2	3.8	52.0
1995	37.5	8.8	3.8	3.8	51.0
1996	37.9	8.5	3.8	3.7	50.2
1997	37.5	8.3	3.6	3.4	49.5
1998	36.5	8.5	3.8	3.7	49.2
1999	36.6	7.5	3.4	3.7	47.6
2000	37.0	8.0	3.2	3.7	49.6
2001	36.6	7.3	3.0	3.5	45.7
2002	35.9	7.2	3.2	3.5	46.0
2003	36.5	6.7	3.2	3.4	46.3
2004	36.2	7.1	3.2	3.3	45.6
2005	35.7	7.3	3.3	3.2	45.9

Table A.12. Annual modelled mercury net atmospheric input to the main regions of the OSPAR maritime area. Units: t/y.

Year	OSPAR Region				
	I. Arctic Waters	II. Greater North Sea	III. Celtic Seas	IV. Bay of Biscay	V. Wider Atlantic
1990	23.95	5.87	1.85	0.47	21.76
1991	24.41	5.08	1.87	0.54	21.35
1992	24.35	5.57	1.83	0.53	19.89
1993	22.4	3.37	1.61	0.52	20.73
1994	19.48	3.03	1.53	0.1	19.02
1995	19.84	2.51	1.03	0.04	17.31
1996	20.93	2.27	1.09	0.06	17.25
1997	21.15	2.22	1.03	-0.16	17.3
1998	20.8	2.55	1.23	0.17	17.62
1999	21.54	1.65	0.93	0.28	16.76
2000	22.53	2.27	0.73	0.34	19.53
2001	22.18	1.55	0.6	0.17	15.61
2002	21.41	1.44	0.78	0.12	15.92
2003	22	1.02	0.78	0.03	16.25
2004	21.74	1.36	0.72	-0.01	15.49
2005	21.29	1.6	0.92	-0.08	15.84

Table A.13. Annual modelled lead total deposition to the sub-regions of the Region II (Greater North Sea) of the OSPAR maritime area. Units: t/y.

Year	Sub-regions of the OSPAR Region II												
	1	2	3	4	5	6	7	8	9	10	11	12	13
1990	98.0	52.8	78.5	63.1	130.1	192.7	45.0	116.6	197.4	220.6	200.9	152.9	145.5
1991	122.2	68.2	88.0	67.1	126.4	171.7	42.5	91.8	198.2	208.8	183.0	124.9	165.2
1992	95.5	49.2	71.2	51.8	107.5	168.8	38.2	104.5	166.9	189.0	174.3	119.5	134.5
1993	99.3	55.9	74.3	59.6	99.0	149.8	32.1	74.1	153.5	161.7	135.6	89.5	154.4
1994	93.6	52.1	68.6	55.1	103.5	143.7	31.7	77.9	133.7	157.9	141.4	86.1	120.1
1995	82.2	43.8	62.1	45.1	88.9	129.5	28.8	61.8	147.9	157.4	126.8	82.3	140.5
1996	96.9	77.4	73.3	77.7	101.3	116.6	22.8	47.5	103.7	140.2	108.8	62.5	141.6
1997	69.7	39.3	60.1	43.0	71.0	102.6	23.4	53.7	100.7	142.1	119.5	62.1	117.8
1998	51.5	33.0	39.3	27.1	58.3	88.2	22.6	56.5	104.6	104.3	85.6	65.3	82.2
1999	49.6	26.5	32.8	23.5	50.7	85.3	20.8	49.9	96.6	85.5	79.6	69.5	78.1
2000	41.1	21.6	25.0	16.2	34.4	68.5	19.4	51.7	65.6	67.0	74.7	69.2	54.7
2001	33.2	24.2	22.8	18.6	35.5	60.8	14.5	34.7	47.0	60.3	68.7	47.6	48.7
2002	51.4	38.5	34.6	31.5	46.5	67.4	14.0	38.1	70.0	75.6	70.4	49.6	78.8
2003	51.1	34.0	29.2	21.6	32.4	59.9	15.3	36.2	76.4	63.6	57.0	52.2	67.2
2004	52.5	32.6	36.6	23.4	34.5	60.6	16.6	41.0	64.6	76.2	68.4	53.1	62.5
2005	57.4	32.5	38.5	28.2	40.9	66.6	19.2	44.6	100.1	88.4	78.9	56.1	60.8

Table A.14. Annual modelled lead net atmospheric input to the sub-regions of the Region II (Greater North Sea) of the OSPAR maritime area. Units: t/y.

Year	Sub-regions of the OSPAR Region II												
	1	2	3	4	5	6	7	8	9	10	11	12	13
1990	77.5	36.5	65.6	54.4	123.4	184.0	41.4	111.2	181.7	198.5	185.3	145.5	132.6
1991	104.8	55.2	77.3	60.2	121.1	165.2	39.4	87.4	184.0	190.4	170.5	118.7	154.7
1992	78.6	36.2	60.7	44.7	102.3	162.2	35.1	99.7	153.2	171.1	161.7	113.0	124.0
1993	77.5	39.1	61.5	51.2	93.5	143.2	28.8	69.5	136.8	141.8	122.7	82.5	143.6
1994	74.0	37.7	56.2	47.0	97.7	136.3	28.4	73.0	118.0	137.6	127.7	79.4	108.1
1995	64.1	31.0	51.0	38.3	83.0	121.9	25.5	57.0	133.0	138.1	113.3	75.5	128.9
1996	79.3	64.9	62.3	70.7	95.6	109.8	19.6	43.1	88.6	121.6	96.1	56.7	130.1
1997	50.3	25.5	49.0	36.1	66.6	96.9	20.3	49.5	84.7	124.8	108.3	55.9	107.4
1998	32.8	18.7	27.1	19.4	52.2	80.4	18.9	51.3	89.0	83.6	71.3	57.9	69.9
1999	30.6	12.0	20.5	15.4	44.5	77.4	17.4	45.0	81.9	65.3	65.7	62.6	65.6
2000	22.3	8.2	13.0	8.7	28.8	60.8	15.5	46.0	49.7	46.8	60.6	61.9	43.2
2001	16.7	11.9	12.8	12.2	30.6	54.5	11.6	30.4	33.9	44.0	57.4	41.2	39.2
2002	33.5	25.0	23.5	24.7	41.3	60.3	10.8	33.4	55.9	57.6	57.8	43.3	65.8
2003	35.0	21.2	19.4	14.9	27.6	54.3	12.7	32.5	63.7	47.9	46.7	46.7	57.4
2004	35.4	20.1	26.0	16.7	29.0	53.5	13.4	36.5	50.8	58.2	55.7	46.7	51.2
2005	38.8	18.2	26.3	20.3	35.0	59.7	15.9	39.9	84.8	68.0	65.4	49.5	50.4

Table A.15. Annual modelled cadmium total deposition to the sub-regions of the Region II (Greater North Sea) of the OSPAR maritime area. Units: t/y.

Year	Sub-regions of the OSPAR Region II												
	1	2	3	4	5	6	7	8	9	10	11	12	13
1990	1.64	1.00	1.16	0.95	1.83	3.11	0.76	1.99	3.21	3.37	3.14	2.62	2.48
1991	2.46	1.38	1.68	1.18	2.15	3.33	0.91	1.88	4.12	3.80	3.44	2.72	3.05
1992	1.79	0.97	1.26	0.89	1.70	3.10	0.78	2.33	3.23	3.38	3.17	2.48	2.30
1993	2.34	1.25	1.64	1.15	1.68	2.78	0.83	1.61	3.73	3.50	2.72	2.12	2.95
1994	2.08	1.07	1.43	1.06	1.88	2.76	0.81	1.67	3.16	3.13	2.75	2.14	2.33
1995	1.78	0.94	1.33	0.90	1.72	2.65	0.72	1.46	3.55	3.45	2.78	2.09	3.06
1996	2.43	1.97	1.87	1.94	2.40	3.02	0.60	1.24	2.61	3.41	2.64	1.77	3.23
1997	1.61	0.91	1.39	0.96	1.31	2.35	0.58	1.33	2.41	3.03	2.61	1.73	2.65
1998	1.14	0.77	0.80	0.54	1.03	1.80	0.58	1.40	2.47	2.13	1.82	1.77	1.77
1999	1.26	0.68	0.79	0.59	1.25	2.20	0.54	1.31	2.54	2.04	1.95	1.91	1.93
2000	1.15	0.59	0.73	0.47	1.03	2.09	0.56	1.49	1.83	1.95	2.12	2.03	1.74
2001	0.87	0.64	0.61	0.50	0.99	1.77	0.40	0.97	1.28	1.63	1.87	1.36	1.42
2002	1.43	1.04	1.00	0.88	1.27	2.03	0.41	1.12	2.00	2.16	1.96	1.43	2.34
2003	1.28	0.91	0.77	0.63	0.92	1.71	0.40	1.00	1.92	1.68	1.55	1.39	1.82
2004	1.35	0.90	0.95	0.60	0.86	1.54	0.45	1.08	1.70	1.97	1.74	1.42	1.52
2005	1.36	0.80	0.94	0.71	0.99	1.64	0.47	1.08	2.45	2.17	1.91	1.38	1.39

Table A.16. Annual modelled cadmium net atmospheric input to the sub-regions of the Region II (Greater North Sea) of the OSPAR maritime area. Units: t/y.

Year	Sub-regions of the OSPAR Region II												
	1	2	3	4	5	6	7	8	9	10	11	12	13
1990	1.13	0.59	0.84	0.73	1.66	2.89	0.67	1.85	2.82	2.82	2.75	2.44	2.16
1991	2.02	1.06	1.41	1.00	2.02	3.17	0.83	1.77	3.77	3.34	3.13	2.56	2.78
1992	1.36	0.64	1.00	0.71	1.57	2.93	0.70	2.21	2.89	2.93	2.86	2.32	2.04
1993	1.79	0.83	1.32	0.94	1.54	2.62	0.75	1.49	3.31	3.00	2.40	1.94	2.68
1994	1.59	0.71	1.12	0.86	1.74	2.58	0.72	1.55	2.76	2.62	2.41	1.97	2.03
1995	1.33	0.62	1.05	0.73	1.57	2.46	0.64	1.34	3.17	2.96	2.44	1.92	2.77
1996	1.99	1.66	1.60	1.77	2.26	2.85	0.52	1.13	2.23	2.94	2.32	1.62	2.94
1997	1.12	0.57	1.12	0.79	1.20	2.21	0.50	1.23	2.01	2.59	2.33	1.57	2.40
1998	0.67	0.41	0.50	0.35	0.88	1.61	0.49	1.27	2.08	1.62	1.46	1.58	1.46
1999	0.78	0.32	0.48	0.39	1.09	2.00	0.46	1.19	2.18	1.54	1.61	1.74	1.62
2000	0.68	0.25	0.43	0.28	0.89	1.90	0.46	1.35	1.43	1.44	1.77	1.85	1.45
2001	0.46	0.33	0.35	0.34	0.86	1.62	0.32	0.86	0.95	1.22	1.58	1.20	1.18
2002	0.98	0.70	0.72	0.71	1.15	1.86	0.33	1.01	1.65	1.71	1.64	1.27	2.02
2003	0.87	0.59	0.52	0.46	0.80	1.57	0.34	0.91	1.60	1.29	1.29	1.25	1.57
2004	0.93	0.58	0.68	0.44	0.73	1.37	0.37	0.97	1.35	1.52	1.42	1.26	1.24
2005	0.90	0.44	0.64	0.51	0.84	1.47	0.38	0.97	2.07	1.66	1.57	1.21	1.13

Table A.17. Annual modelled mercury total deposition to the sub-regions of the Region II (Greater North Sea) of the OSPAR maritime area. Units: t/y.

Year	Sub-regions of the OSPAR Region II												
	1	2	3	4	5	6	7	8	9	10	11	12	13
1990	0.97	0.62	0.61	0.53	0.89	1.16	0.26	0.65	1.38	1.42	1.15	0.98	0.98
1991	0.96	0.65	0.59	0.55	0.87	1.14	0.23	0.52	1.22	1.26	1.02	0.79	1.14
1992	0.99	0.63	0.64	0.58	0.90	1.14	0.25	0.55	1.35	1.40	1.11	0.87	1.13
1993	0.88	0.60	0.55	0.48	0.64	0.94	0.21	0.45	1.07	1.06	0.82	0.71	1.05
1994	0.83	0.59	0.49	0.45	0.64	0.89	0.23	0.48	1.08	1.00	0.85	0.75	0.98
1995	0.86	0.59	0.52	0.43	0.56	0.78	0.21	0.41	1.09	1.00	0.77	0.69	0.94
1996	0.92	0.65	0.52	0.46	0.50	0.66	0.19	0.35	1.00	0.95	0.66	0.67	0.93
1997	0.85	0.59	0.53	0.44	0.46	0.62	0.19	0.36	1.07	1.00	0.72	0.67	0.81
1998	0.86	0.63	0.54	0.44	0.48	0.66	0.20	0.41	1.09	1.00	0.72	0.69	0.81
1999	0.80	0.54	0.45	0.36	0.38	0.58	0.17	0.34	1.03	0.82	0.62	0.70	0.72
2000	0.78	0.53	0.47	0.37	0.45	0.65	0.20	0.38	1.02	0.96	0.73	0.68	0.76
2001	0.78	0.58	0.45	0.38	0.40	0.57	0.17	0.36	0.87	0.79	0.63	0.58	0.69
2002	0.73	0.53	0.44	0.38	0.42	0.58	0.16	0.35	0.90	0.81	0.62	0.56	0.69
2003	0.71	0.53	0.39	0.32	0.35	0.50	0.16	0.31	0.95	0.75	0.56	0.58	0.64
2004	0.74	0.54	0.42	0.36	0.39	0.55	0.17	0.34	0.90	0.81	0.64	0.56	0.68
2005	0.83	0.60	0.46	0.38	0.38	0.51	0.17	0.33	1.03	0.84	0.63	0.52	0.67

Table A.18. Annual modelled mercury net atmospheric input to the sub-regions of the Region II (Greater North Sea) of the OSPAR maritime area. Units: t/y.

Year	Sub-regions of the OSPAR Region II												
	1	2	3	4	5	6	7	8	9	10	11	12	13
1990	0.54	0.31	0.33	0.27	0.47	0.55	0.09	0.26	0.90	0.86	0.57	0.51	0.26
1991	0.52	0.33	0.29	0.28	0.44	0.52	0.05	0.13	0.72	0.68	0.42	0.32	0.41
1992	0.54	0.30	0.34	0.31	0.46	0.52	0.07	0.15	0.84	0.80	0.50	0.38	0.38
1993	0.41	0.26	0.24	0.20	0.20	0.31	0.03	0.05	0.54	0.45	0.20	0.21	0.29
1994	0.35	0.24	0.17	0.16	0.19	0.25	0.05	0.07	0.54	0.37	0.22	0.24	0.21
1995	0.37	0.24	0.19	0.13	0.10	0.13	0.02	0.00	0.55	0.36	0.12	0.18	0.16
1996	0.44	0.31	0.20	0.17	0.05	0.01	0.01	-0.06	0.47	0.32	0.03	0.17	0.16
1997	0.39	0.26	0.22	0.16	0.02	-0.02	0.01	-0.05	0.55	0.39	0.10	0.18	0.05
1998	0.41	0.30	0.24	0.16	0.05	0.04	0.02	0.01	0.58	0.40	0.11	0.21	0.06
1999	0.36	0.22	0.16	0.09	-0.05	-0.04	0.00	-0.05	0.53	0.24	0.02	0.22	-0.02
2000	0.36	0.23	0.18	0.11	0.03	0.05	0.03	0.00	0.53	0.40	0.14	0.22	0.04
2001	0.36	0.28	0.16	0.12	-0.02	-0.03	0.00	-0.02	0.38	0.22	0.04	0.11	-0.03
2002	0.30	0.23	0.15	0.12	-0.01	-0.02	-0.02	-0.04	0.41	0.25	0.03	0.09	-0.03
2003	0.28	0.22	0.11	0.06	-0.07	-0.11	-0.01	-0.08	0.47	0.18	-0.03	0.12	-0.08
2004	0.31	0.24	0.13	0.10	-0.03	-0.06	0.00	-0.05	0.42	0.24	0.05	0.09	-0.04
2005	0.40	0.30	0.17	0.12	-0.04	-0.10	-0.01	-0.06	0.55	0.27	0.04	0.05	-0.06

Table A.19. Annual modelled lead depositions from individual emission sectors to the main regions of the OSPAR maritime area. Units: t/y.

OSPAR Region	Emission sectors			
	Combustion in power plants and industry & industrial processes	Transport	Commercial, residential and other combustion	Waste
I. Arctic Waters	24.1	7.2	4.0	0.6
II. Greater North Sea	64.9	15.3	9.0	1.1
III. Celtic Seas	14.1	2.2	1.5	0.2
IV. Bay of Biscay	42.7	3.2	1.7	1.2
V. Wider Atlantic	66.4	7.0	4.0	2.0

Table A.20. Annual modelled lead deposition from individual emission sectors to the sub-regions of the Region II (Greater North Sea) of the OSPAR maritime area. Units: t/y.

Sub-regions of the OSPAR Region II	Emission sectors			
	Combustion in power plants and industry & industrial processes	Transport	Commercial, residential and other combustion	Waste
1	4.54	1.02	0.61	0.08
2	1.55	0.36	0.25	0.03
3	3.11	0.68	0.41	0.05
4	2.26	0.48	0.36	0.04
5	5.51	0.71	0.44	0.05
6	9.13	1.70	0.74	0.11
7	1.45	0.48	0.29	0.03
8	4.12	1.43	0.63	0.07
9	8.03	2.34	1.49	0.18
10	8.23	1.69	1.05	0.12
11	7.01	1.64	0.89	0.11
12	4.50	1.97	1.31	0.14
13	5.69	0.92	0.60	0.09

Table A.21. Annual modelled cadmium depositions from individual emission sectors to the main regions of the OSPAR maritime area. Units: t/y.

OSPAR Region	Emission sectors			
	Combustion in power plants and industry & industrial processes	Transport	Commercial, residential and other combustion	Waste
I. Arctic Waters	1.33	0.08	0.44	0.05
II. Greater North Sea	2.59	0.23	0.84	0.12
III. Celtic Sea	0.57	0.05	0.11	0.02
IV. Bay of Biscay	1.84	0.05	0.09	0.05
V. Wider Atlantic	2.56	0.11	0.29	0.08

Table A.22. Annual modelled cadmium deposition from individual emission sectors to the sub-regions of the Region II (Greater North Sea) of the OSPAR maritime area. Units: t/y.

Emission sectors				
Sub-regions of the OSPAR Region II	Combustion in power plants and industry & industrial processes	Transport	Commercial, residential and other combustion	Waste
1	0.171	0.017	0.052	0.008
2	0.060	0.007	0.025	0.003
3	0.119	0.011	0.037	0.005
4	0.086	0.009	0.035	0.004
5	0.194	0.021	0.037	0.005
6	0.350	0.025	0.052	0.014
7	0.061	0.005	0.028	0.003
8	0.182	0.013	0.054	0.008
9	0.333	0.028	0.146	0.019
10	0.304	0.028	0.098	0.013
11	0.272	0.025	0.082	0.012
12	0.219	0.017	0.165	0.014
13	0.253	0.022	0.029	0.008

Table A.23. Annual modelled mercury depositions from individual emission sectors to the main regions of the OSPAR maritime area. Units: t/y.

Emission sectors				
OSPAR Region	Combustion in power plants and industry & industrial processes	Transport	Commercial, residential and other combustion	Waste
I. Arctic Waters	0.40	0.01	0.06	0.06
II. Greater North Sea	1.21	0.02	0.13	0.27
III. Celtic Seas	0.25	0.00	0.04	0.06
IV. Bay of Biscay	0.67	0.00	0.03	0.10
V. Wider Atlantic	0.63	0.00	0.05	0.12

Table A.24. Annual modelled mercury deposition from individual emission sectors to the sub-regions of the Region II (Greater North Sea) of the OSPAR maritime area. Units: t/y.

Sub-regions of the OSPAR Region II	Emission sectors			
	Combustion in power plants and industry & industrial processes	Transport	Commercial, residential and other combustion	Waste
1	0.064	0.001	0.007	0.015
2	0.023	0.000	0.003	0.006
3	0.048	0.001	0.005	0.012
4	0.040	0.001	0.005	0.014
5	0.118	0.001	0.007	0.032
6	0.172	0.001	0.011	0.036
7	0.028	0.000	0.004	0.005
8	0.076	0.001	0.008	0.012
9	0.117	0.003	0.016	0.024
10	0.141	0.002	0.013	0.033
11	0.126	0.001	0.011	0.029
12	0.108	0.002	0.024	0.013
13	0.151	0.001	0.009	0.042

Table A.25. Annual modelled lead deposition from some countries to the sub-regions of the Region II (Greater North Sea) of the OSPAR maritime area. Units: t/y.

Countries	Sub-regions of the OSPAR Region II												
	1	2	3	4	5	6	7	8	9	10	11	12	13
Belgium	0.60	0.17	0.35	0.23	0.55	2.55	0.25	1.03	1.11	0.89	1.10	0.66	0.65
Denmark	0.04	0.02	0.02	0.01	0.02	0.02	0.04	0.06	0.12	0.07	0.06	0.37	0.01
Finland	0.01	0.01	0.01	0.01	0.00	0.01	0.01	0.01	0.02	0.02	0.01	0.03	0.00
France	0.63	0.20	0.40	0.25	0.54	2.09	0.22	0.73	1.12	0.91	1.02	0.57	1.57
Germany	0.47	0.15	0.31	0.20	0.29	0.52	0.25	0.82	1.09	0.77	0.78	0.90	0.26
Iceland	0.00	0.00	0.00	0.00	0.00	0.00	0.00	0.00	0.00	0.00	0.00	0.00	0.00
Ireland	0.08	0.05	0.06	0.05	0.04	0.04	0.01	0.03	0.12	0.10	0.07	0.03	0.10
Luxembourg	0.01	0.00	0.00	0.00	0.00	0.01	0.00	0.01	0.02	0.01	0.01	0.01	0.01
Netherlands	0.40	0.11	0.24	0.18	0.46	2.61	0.20	1.18	0.77	0.69	0.97	0.50	0.34
Norway	0.04	0.02	0.02	0.01	0.01	0.01	0.01	0.01	0.16	0.04	0.02	0.13	0.01
Portugal	0.10	0.05	0.07	0.05	0.08	0.13	0.03	0.11	0.15	0.16	0.15	0.07	0.54
Spain	0.46	0.11	0.33	0.18	0.24	0.43	0.08	0.28	0.65	0.55	0.45	0.20	1.06
Sweden	0.03	0.02	0.02	0.01	0.01	0.02	0.02	0.02	0.06	0.05	0.03	0.28	0.01
Switzerland	0.03	0.01	0.02	0.02	0.02	0.04	0.01	0.03	0.09	0.05	0.05	0.05	0.03
United Kingdom	2.24	0.82	1.63	1.29	3.82	2.35	0.49	0.99	3.25	4.64	3.24	0.95	2.28
Poland	0.68	0.27	0.44	0.42	0.38	0.46	0.42	0.62	2.16	1.30	0.99	2.30	0.18

Table A.26. Annual modelled cadmium deposition from some countries to the sub-regions of the Region II (Greater North Sea) of the OSPAR maritime area. Units: t/y.

Countries	Sub-regions of the OSPAR Region II												
	1	2	3	4	5	6	7	8	9	10	11	12	13
Belgium	0.014	0.004	0.008	0.005	0.013	0.052	0.006	0.022	0.026	0.021	0.025	0.015	0.015
Denmark	0.005	0.002	0.003	0.001	0.002	0.003	0.005	0.006	0.014	0.007	0.006	0.042	0.002
Finland	0.001	0.001	0.001	0.000	0.000	0.000	0.000	0.000	0.001	0.001	0.001	0.001	0.000
France	0.027	0.009	0.017	0.011	0.024	0.087	0.009	0.032	0.048	0.040	0.045	0.025	0.073
Germany	0.012	0.004	0.008	0.005	0.008	0.015	0.007	0.033	0.028	0.021	0.023	0.024	0.007
Iceland	0.000	0.000	0.000	0.000	0.000	0.000	0.000	0.000	0.000	0.000	0.000	0.000	0.000
Ireland	0.006	0.004	0.004	0.004	0.003	0.003	0.001	0.002	0.008	0.007	0.005	0.002	0.007
Luxembourg	0.000	0.000	0.000	0.000	0.000	0.000	0.000	0.000	0.000	0.000	0.000	0.000	0.000
Netherlands	0.015	0.004	0.009	0.007	0.020	0.113	0.008	0.044	0.030	0.027	0.038	0.019	0.014
Norway	0.004	0.002	0.002	0.001	0.001	0.001	0.001	0.001	0.019	0.003	0.002	0.011	0.001
Portugal	0.002	0.001	0.002	0.001	0.002	0.003	0.001	0.002	0.003	0.003	0.003	0.001	0.012
Spain	0.025	0.006	0.018	0.010	0.014	0.024	0.005	0.015	0.036	0.031	0.025	0.011	0.063
Sweden	0.001	0.001	0.001	0.000	0.000	0.000	0.001	0.001	0.002	0.001	0.001	0.007	0.000
Switzerland	0.002	0.001	0.001	0.001	0.001	0.002	0.001	0.001	0.004	0.003	0.002	0.002	0.002
United Kingdom	0.070	0.027	0.051	0.043	0.131	0.085	0.015	0.032	0.098	0.143	0.106	0.029	0.094
Poland	0.045	0.021	0.032	0.032	0.028	0.034	0.028	0.047	0.150	0.093	0.076	0.176	0.013

Table A.27. Annual modelled mercury deposition from some countries to the sub-regions of the Region II (Greater North Sea) of the OSPAR maritime area. Units: t/y.

Countries	Sub-regions of the OSPAR Region II												
	1	2	3	4	5	6	7	8	9	10	11	12	13
Belgium	0.004	0.001	0.002	0.001	0.004	0.025	0.002	0.006	0.007	0.006	0.008	0.004	0.006
Denmark	0.004	0.002	0.003	0.001	0.002	0.003	0.008	0.011	0.012	0.008	0.007	0.053	0.001
Finland	0.000	0.000	0.000	0.000	0.000	0.000	0.000	0.000	0.000	0.000	0.000	0.000	0.000
France	0.012	0.004	0.008	0.005	0.014	0.053	0.004	0.016	0.020	0.020	0.023	0.011	0.071
Germany	0.003	0.001	0.002	0.001	0.002	0.006	0.002	0.012	0.007	0.006	0.007	0.006	0.002
Iceland	0.000	0.000	0.000	0.000	0.000	0.000	0.000	0.000	0.000	0.000	0.000	0.000	0.000
Ireland	0.002	0.001	0.001	0.001	0.001	0.001	0.000	0.001	0.002	0.002	0.002	0.001	0.002
Luxembourg	0.000	0.000	0.000	0.000	0.000	0.001	0.000	0.000	0.001	0.001	0.001	0.000	0.000
Netherlands	0.003	0.001	0.002	0.001	0.006	0.046	0.002	0.013	0.007	0.007	0.011	0.005	0.004
Norway	0.001	0.000	0.001	0.000	0.000	0.000	0.000	0.000	0.006	0.001	0.001	0.008	0.000
Portugal	0.000	0.000	0.000	0.000	0.000	0.000	0.000	0.000	0.001	0.001	0.001	0.000	0.002
Spain	0.004	0.001	0.003	0.001	0.002	0.004	0.001	0.002	0.005	0.005	0.004	0.002	0.012
Sweden	0.000	0.000	0.000	0.000	0.000	0.000	0.000	0.000	0.001	0.000	0.000	0.004	0.000
Switzerland	0.000	0.000	0.000	0.000	0.000	0.001	0.000	0.001	0.001	0.001	0.001	0.001	0.001
United Kingdom	0.043	0.016	0.036	0.041	0.119	0.070	0.011	0.022	0.060	0.111	0.084	0.020	0.097
Poland	0.005	0.002	0.004	0.003	0.003	0.004	0.003	0.007	0.016	0.011	0.010	0.021	0.002

Annex B: Data products for Persistent organic pollutants

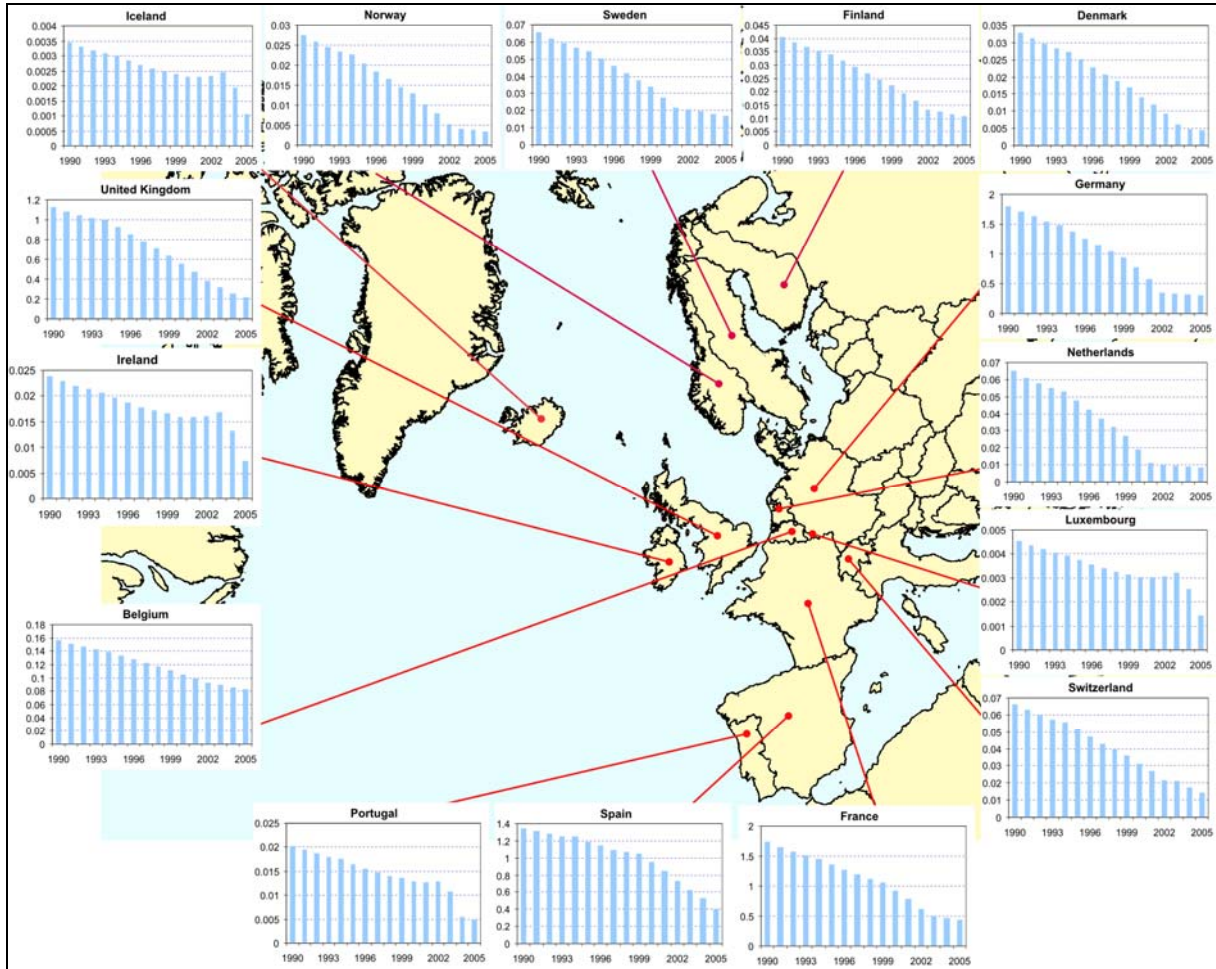


Figure B.1. Time series of PCB-153 emissions from the OSPAR Contracting Parties. Units: t/y.

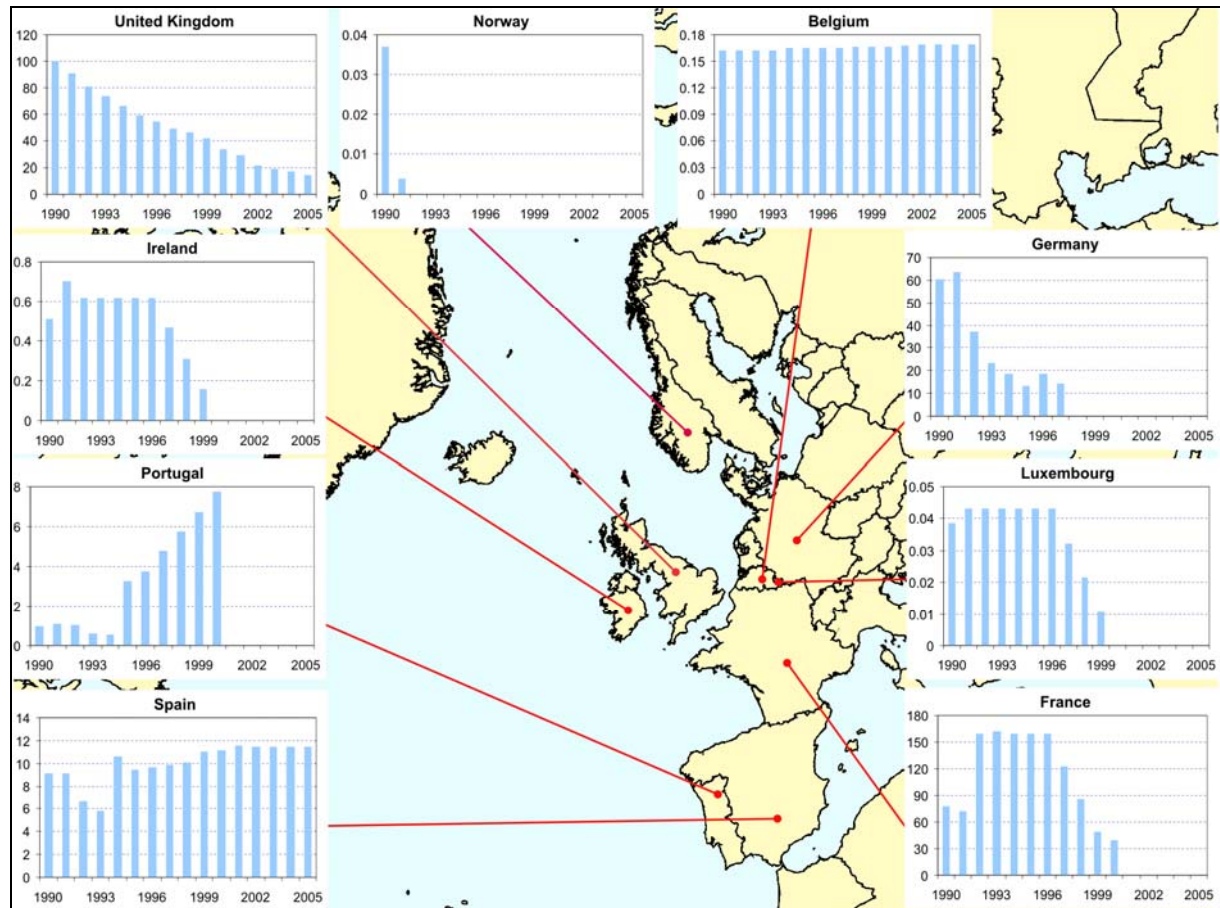


Figure B.2. Time series of γ -HCH emissions from the OSPAR Contracting Parties. Units: t/y.

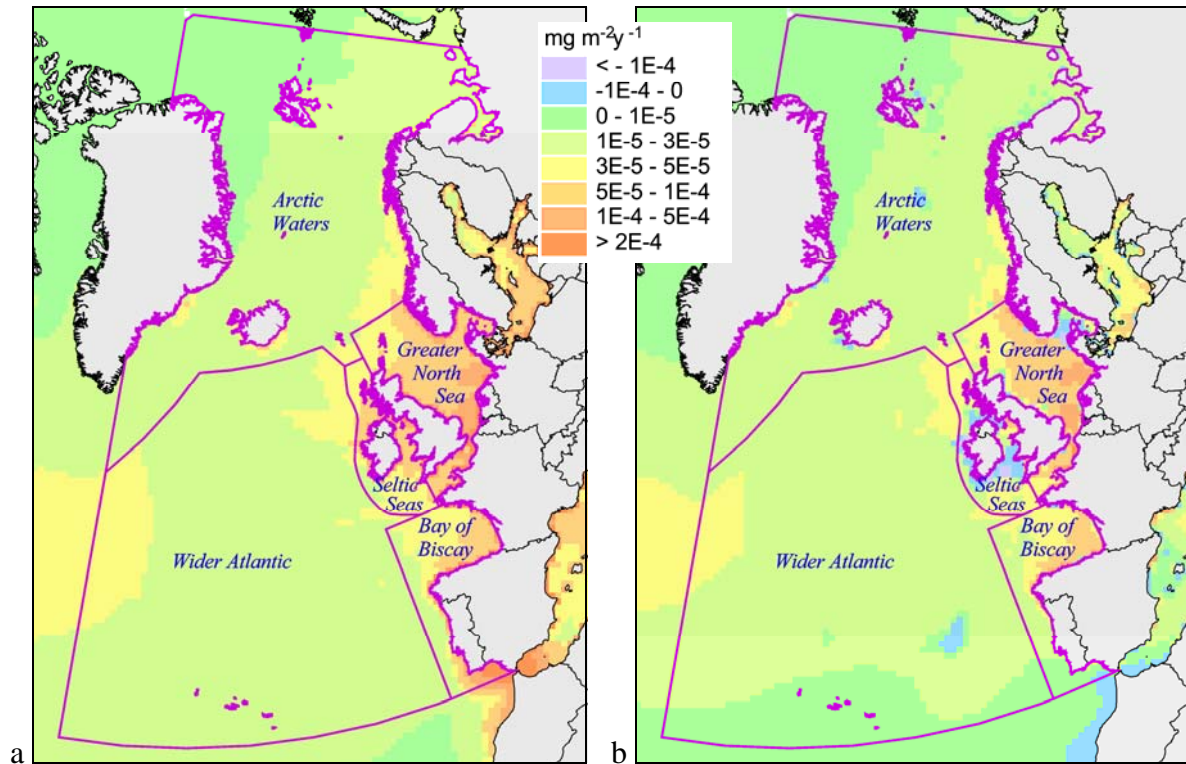


Figure B.3. Spatial distribution of annual total deposition flux (a) and net deposition flux (b) of PCB-153 over the five main OSPAR regions in 2005. Units: $\text{mg m}^{-2} \text{y}^{-1}$

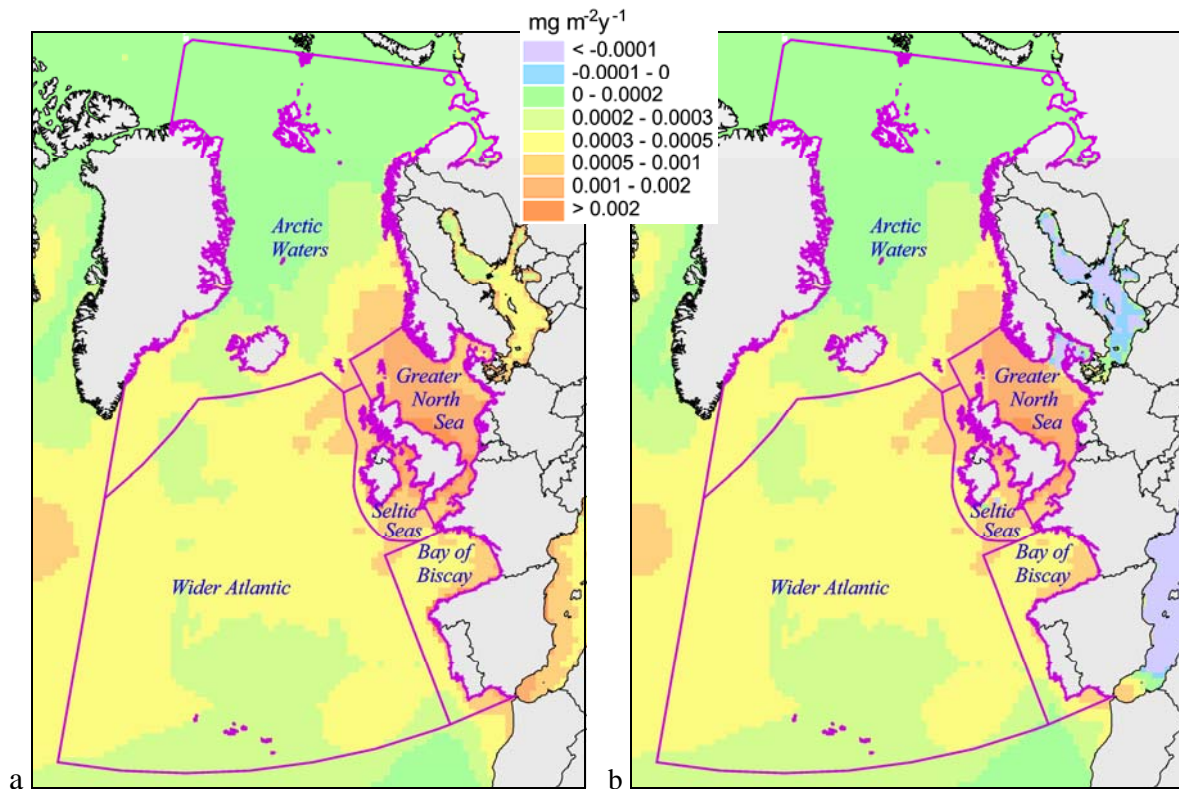


Figure B.4. Spatial distribution of annual total deposition flux (a) and net deposition flux (b) of γ -HCH over the OSPAR region 2 (Greater North Sea) in 2005. Units: $\text{mg m}^{-2} \text{y}^{-1}$

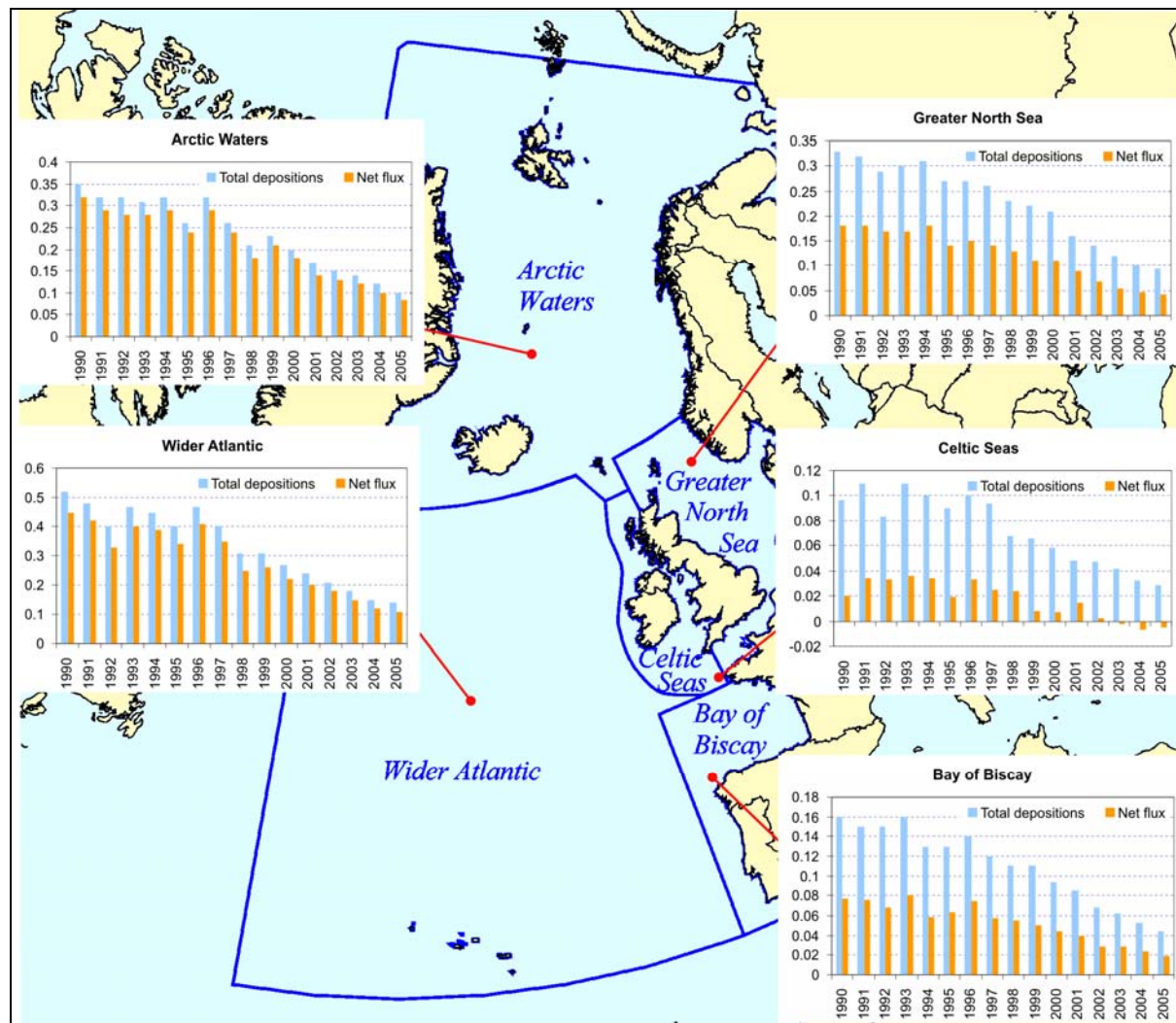


Figure B.5. Time series of modelled total annual deposition and net deposition flux of PCB-153 to the five main OSPAR regions. Units: t/y.

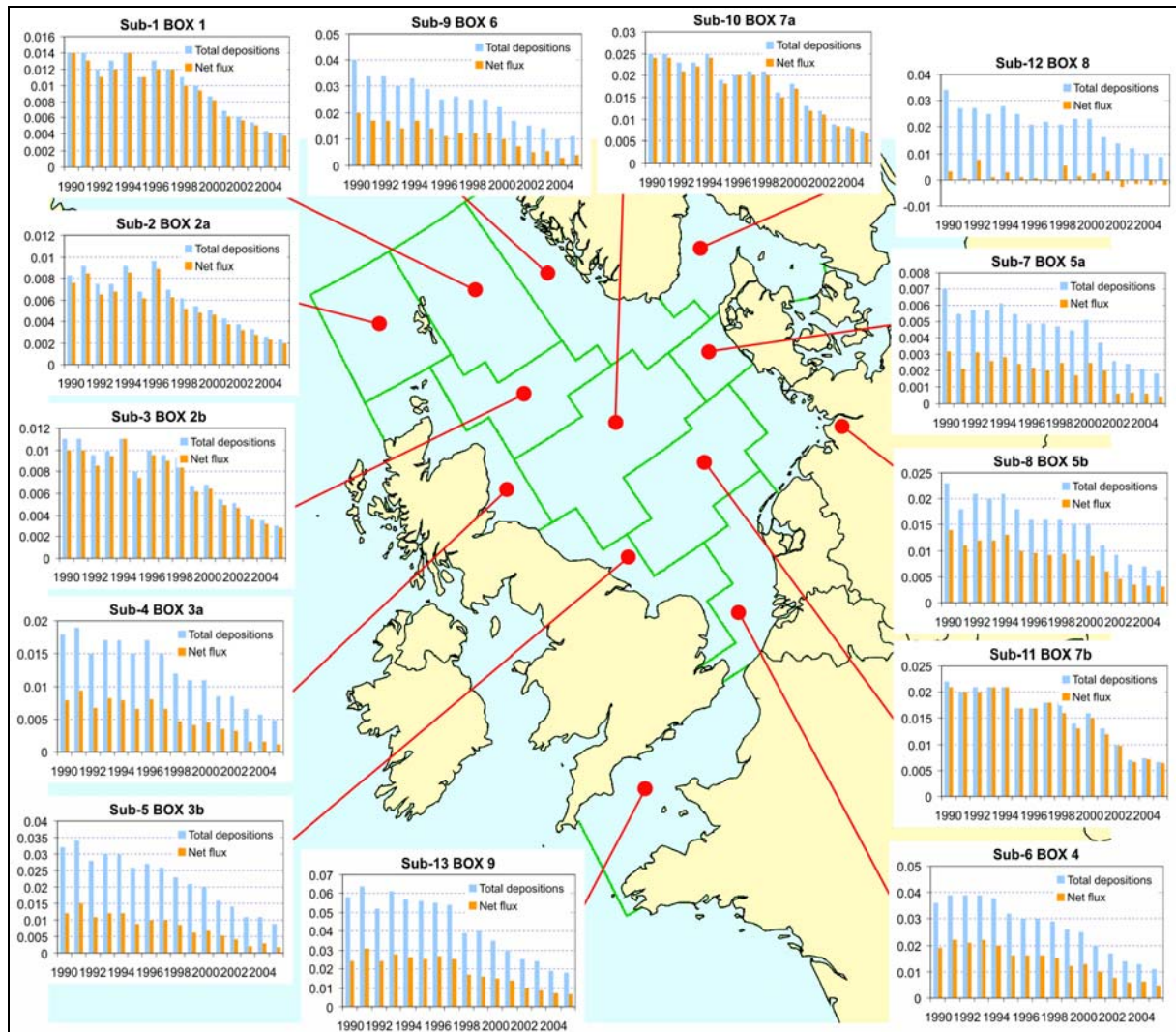


Figure B.6. Time series of modelled total annual deposition and net deposition flux of PCB-153 to 13 sub-regions of the OSPAR region 2 (Greater North Sea). Units: t/y.

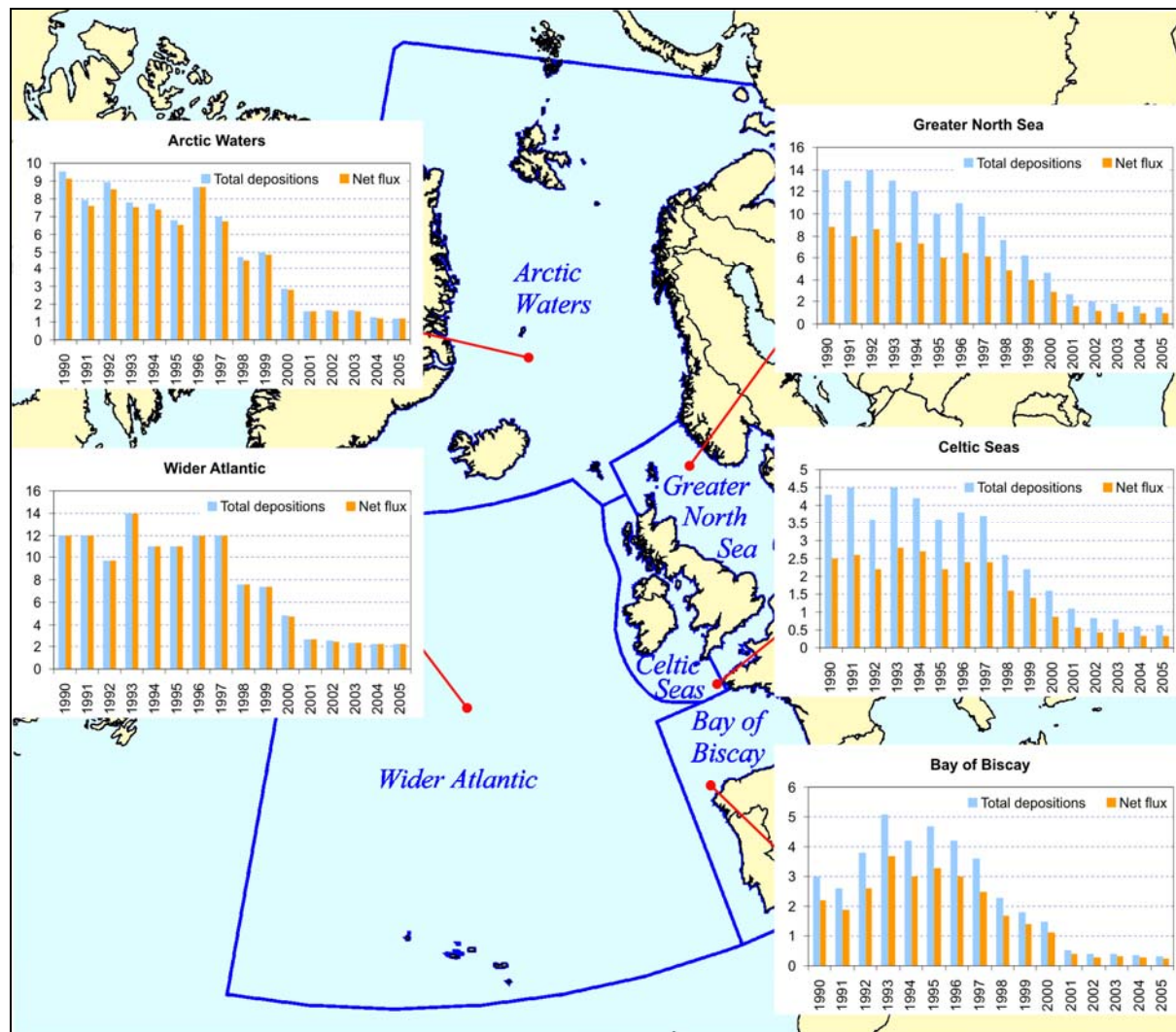


Figure B.7. Time series of modelled total annual deposition and net deposition flux of γ -HCH to the five main OSPAR regions. Units: t/y.

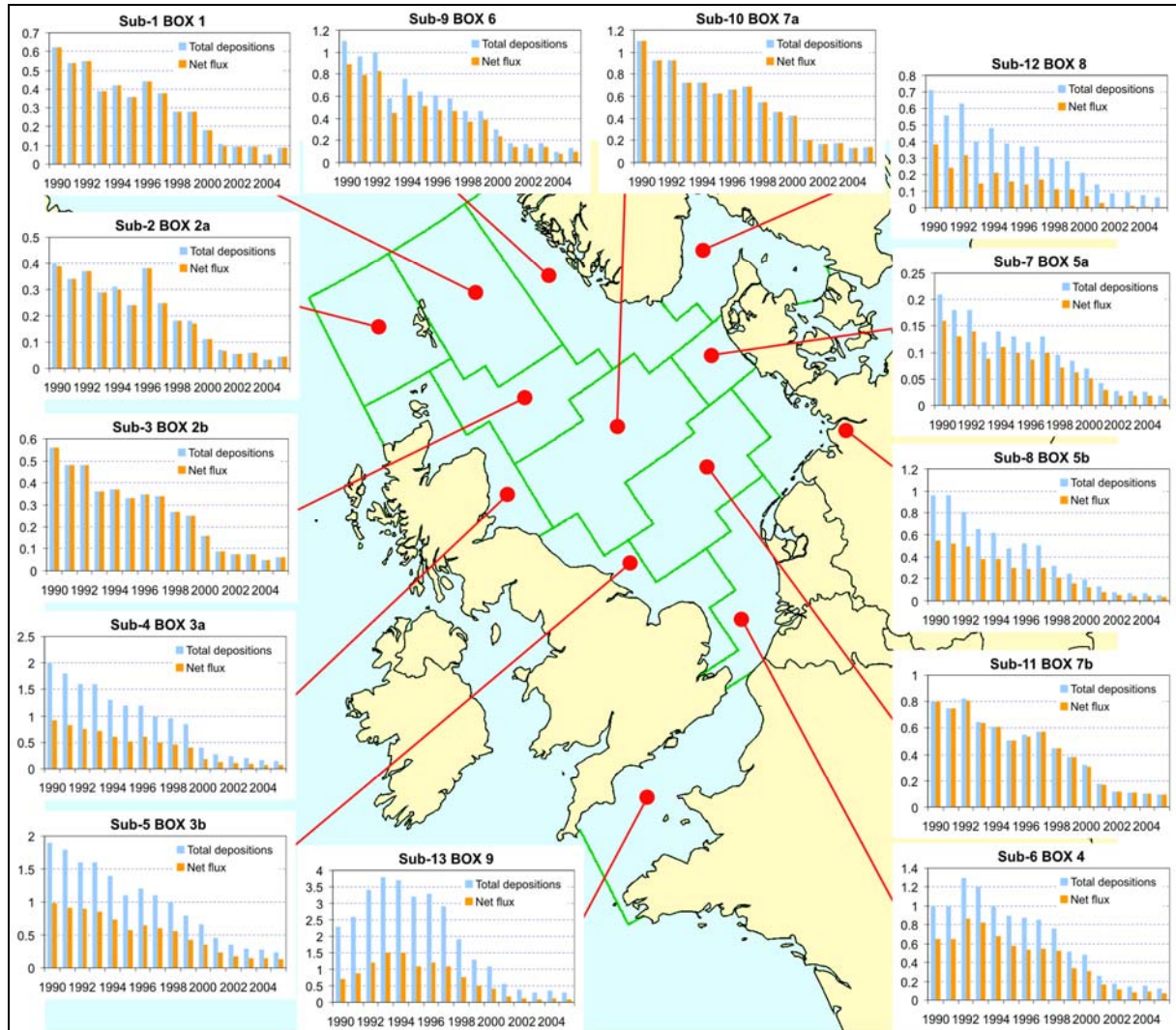


Figure B.8. Time series of modelled total annual deposition and net deposition flux of γ -HCH to 13 sub-regions of the OSPAR region 2 (Greater North Sea). Units: t/y.

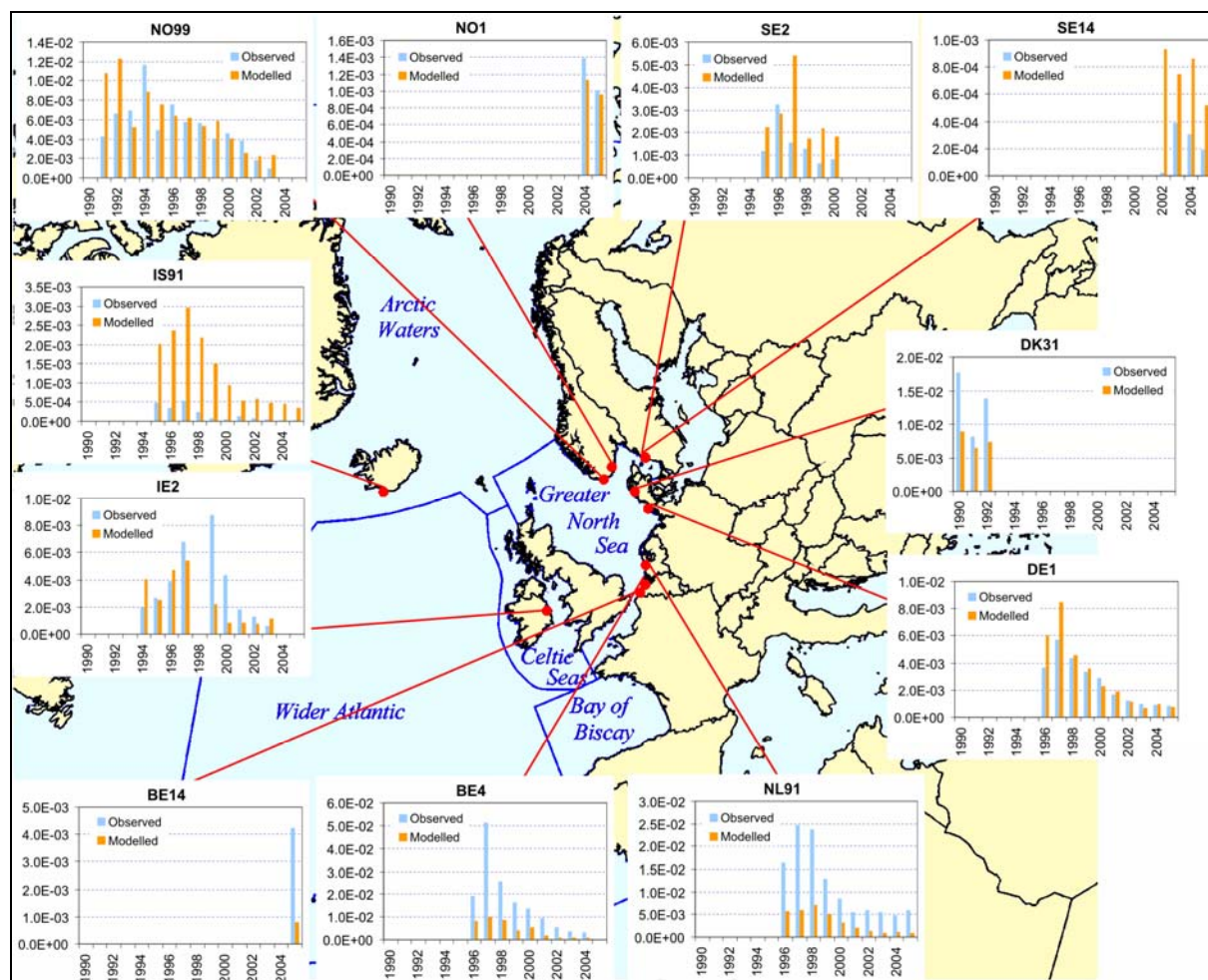


Figure B.9. Comparison of modelled and measured annual wet deposition flux of γ -HCH at the coastal monitoring stations in the five main OSPAR regions. Units: mg/m²/y

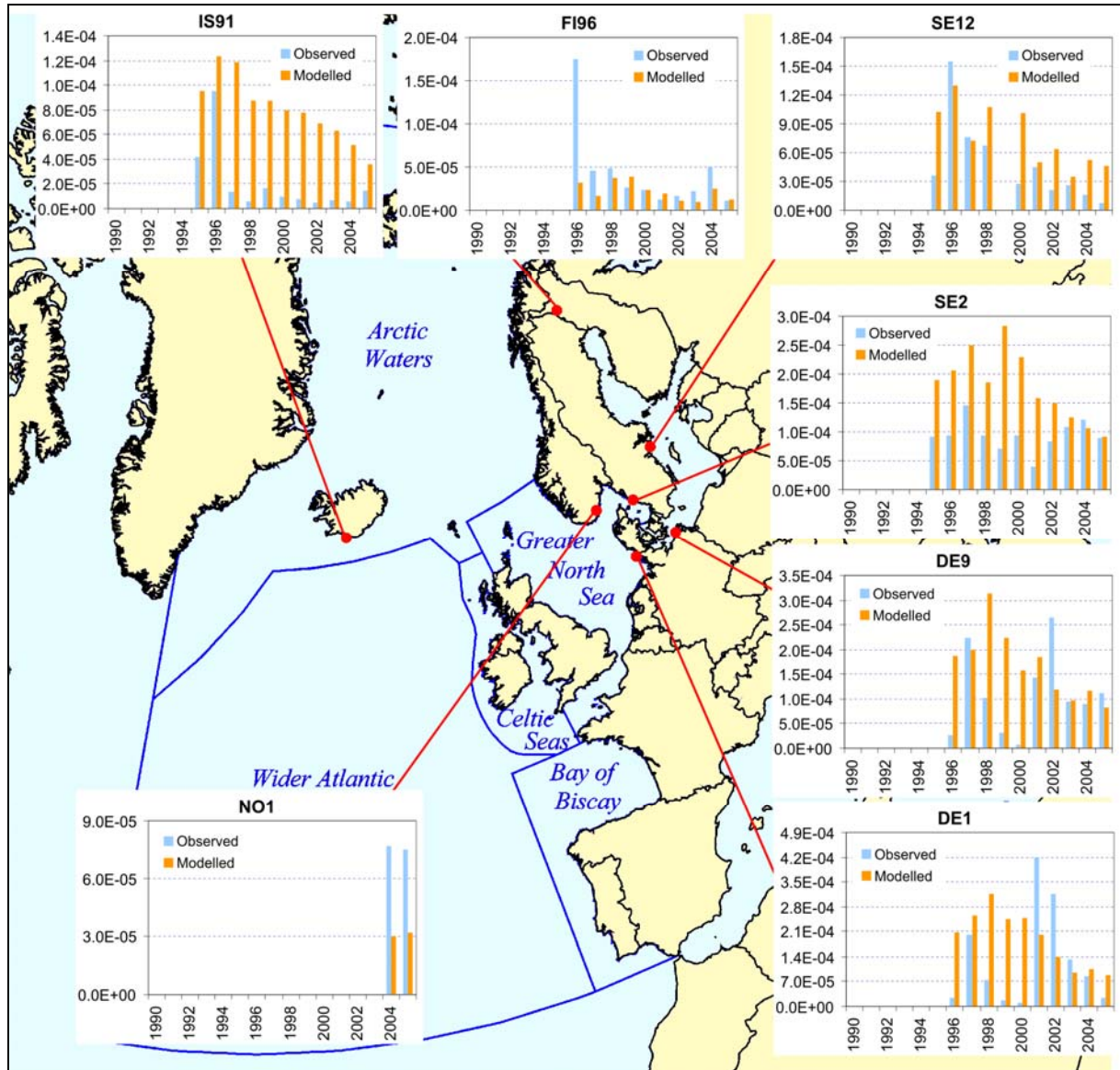


Figure B.10. Comparison of modelled and measured annual wet deposition flux of PCB-153 at the monitoring stations in the five main OSPAR regions. Units: mg/m²/y

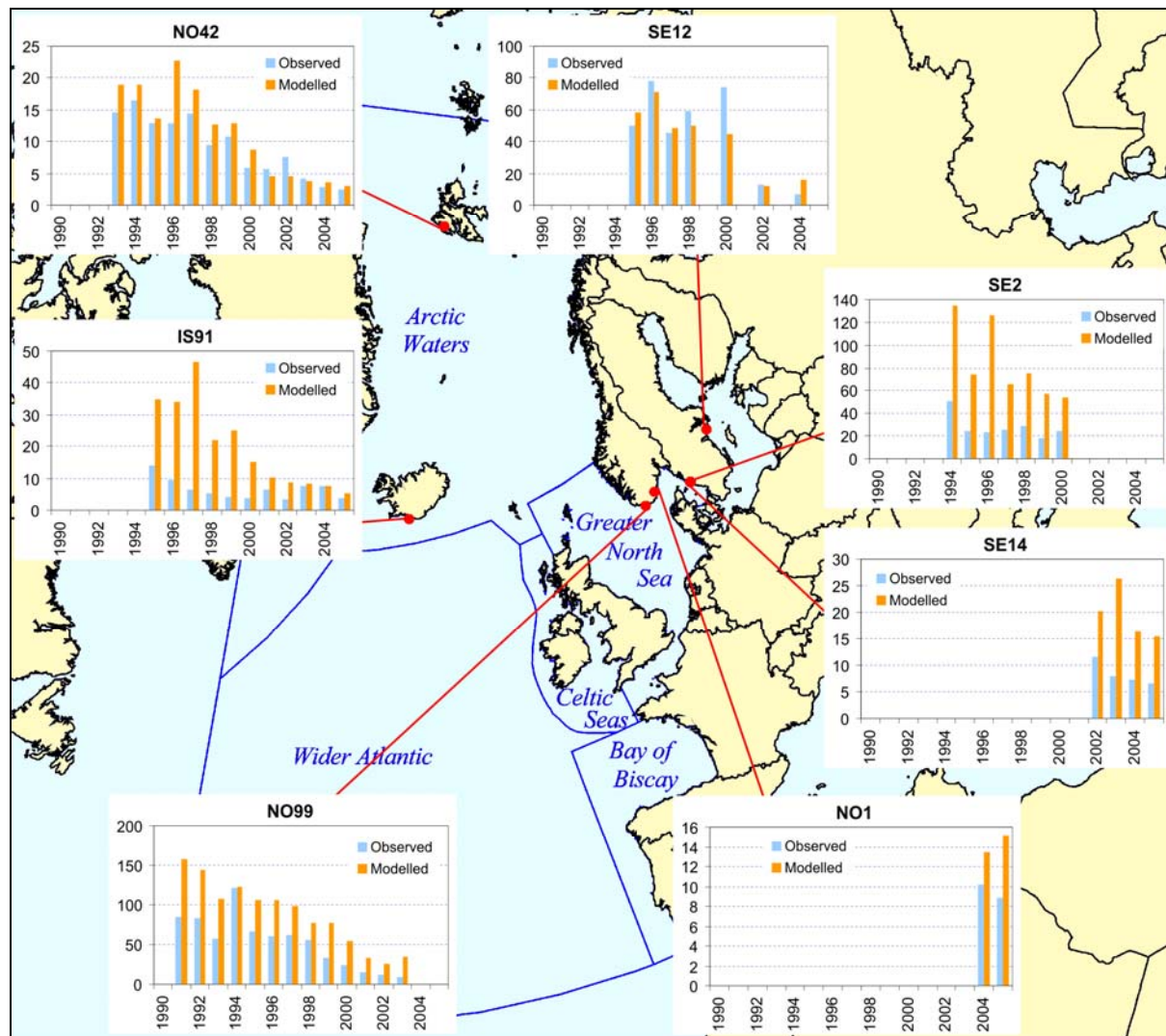


Figure B.11. Comparison of modelled and measured annual air concentrations of γ -HCH at the coastal monitoring stations in the five main OSPAR regions. Units: $\mu\text{g}/\text{m}^3$

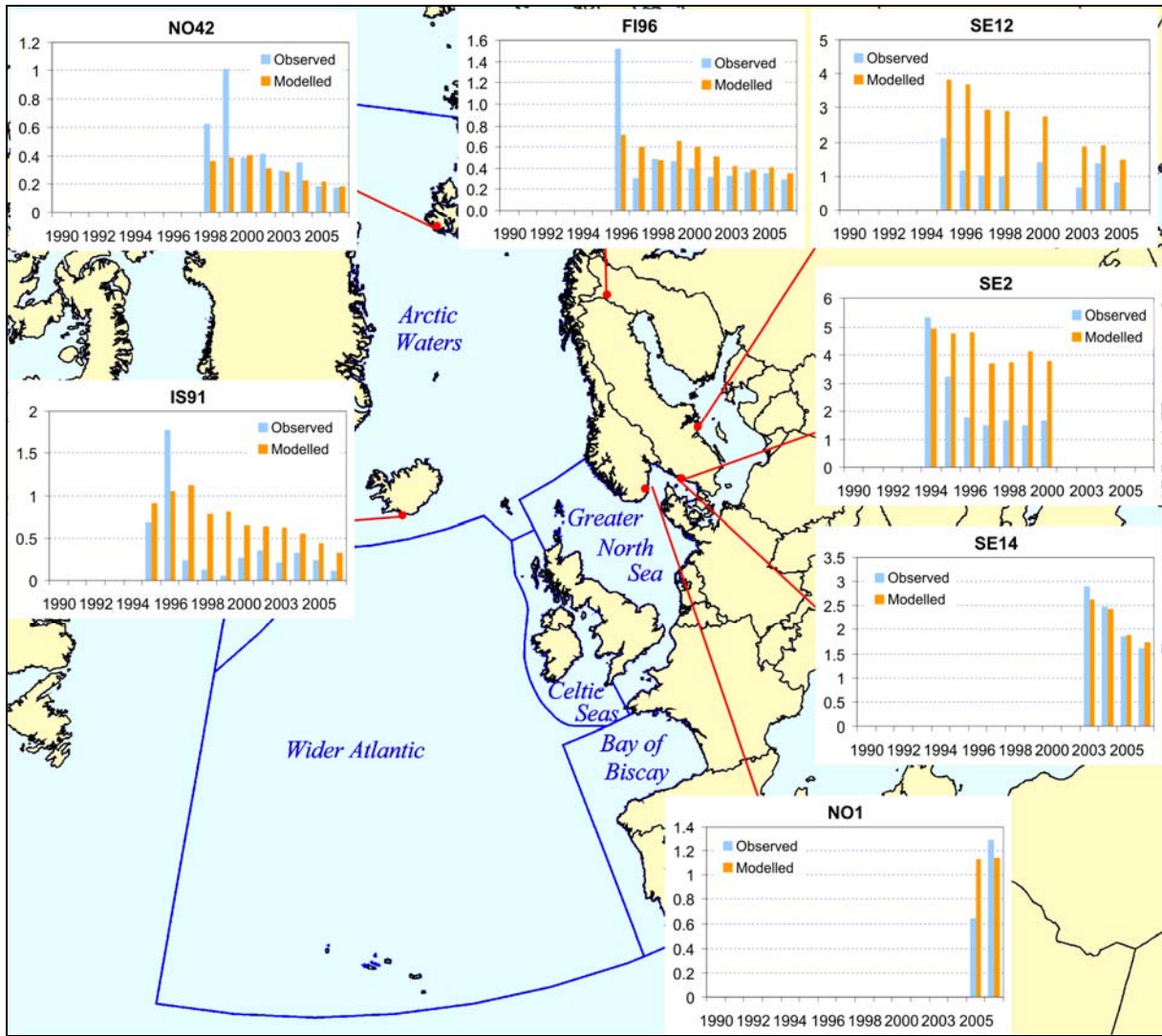


Figure B.12. Comparison of modelled and measured annual air concentrations of PCB-153 at the monitoring stations in the five main OSPAR regions. Units: pg/m³

Table B.1. Annual γ -HCH emissions from the OSPAR Contracting Parties used for model simulations. Unit: t/y.

Country	1990	1991	1992	1993	1994	1995	1996	1997	1998	1999	2000	2001	2002	2003	2004	2005
Belgium	0.16	0.16	0.16	0.16	0.16	0.16	0.17	0.17	0.17	0.17	0.17	0.17	0.17	0.17	0.17	0.17
Denmark	0	0	0	0	0	0	0	0	0	0	0	0	0	0	0	0
Finland	0	0	0	0	0	0	0	0	0	0	0	0	0	0	0	0
France	77.3	72.3	160.0	162.9	160.0	160.0	160.0	122.8	85.7	48.5	39.8	0	0	0	0	0
Germany	60.20	63.70	36.90	23.50	18.50	13.10	18.50	14.50	0	0	0	0	0	0	0	0
Iceland	0	0	0	0	0	0	0	0	0	0	0	0	0	0	0	0
Ireland	0.51	0.70	0.62	0.62	0.62	0.62	0.62	0.46	0.31	0.15	0	0	0	0	0	0
Luxembourg	0.04	0.04	0.04	0.04	0.04	0.04	0.04	0.03	0.02	0.01	0	0	0	0	0	0
Netherlands	0	0	0	0	0	0	0	0	0	0	0	0	0	0	0	0
Norway	0.04	0	0	0	0	0	0	0	0	0	0	0	0	0	0	0
Portugal	0.97	1.09	1.01	0.61	0.56	3.27	3.77	4.76	5.75	6.74	7.73	0	0	0	0	0
Spain	9.11	9.11	6.65	5.83	10.6	9.48	9.66	9.84	10.1	11.0	11.1	11.6	11.5	11.5	11.5	11.5
Sweden	0	0	0	0	0	0	0	0	0	0	0	0	0	0	0	0
Switzerland	0	0	0	0	0	0	0	0	0	0	0	0	0	0	0	0
United Kingdom	100.4	90.7	81.3	73.6	66.1	59.4	54.2	49.2	46.1	41.6	33.2	29.3	22.3	19.4	16.9	14.6
OSPAR	249	238	287	267	257	246	247	202	148	108	92	41	34	31	29	26
Other	213	180	163	79	75	58	47	15	17	21	26	4	4	1	1	1
EMEP	462	418	449	346	332	304	294	217	165	129	118	45	38	32	29	27

Table B.2. Annual PCB-153 emissions from the OSPAR Contracting Parties used for model simulations. Unit: t/y.

Country	1990	1991	1992	1993	1994	1995	1996	1997	1998	1999	2000	2001	2002	2003	2004	2005
Belgium	0.16	0.15	0.15	0.14	0.14	0.13	0.13	0.12	0.12	0.11	0.11	0.10	0.09	0.09	0.09	0.08
Denmark	0.03	0.03	0.03	0.03	0.03	0.03	0.02	0.02	0.02	0.02	0.01	0.01	0.01	0.01	0.005	0.004
Finland	0.04	0.04	0.04	0.04	0.03	0.03	0.03	0.03	0.02	0.02	0.02	0.02	0.01	0.01	0.01	0.01
France	1.74	1.66	1.58	1.51	1.45	1.36	1.28	1.20	1.12	1.06	0.93	0.79	0.62	0.50	0.47	0.45
Germany	1.81	1.72	1.63	1.55	1.49	1.37	1.26	1.15	1.04	0.93	0.77	0.58	0.35	0.34	0.32	0.30
Iceland	0.003	0.003	0.003	0.003	0.003	0.003	0.003	0.003	0.002	0.002	0.002	0.002	0.002	0.002	0.002	0.001
Ireland	0.02	0.02	0.02	0.02	0.02	0.02	0.02	0.02	0.02	0.02	0.02	0.02	0.02	0.02	0.01	0.01
Luxembourg	0.005	0.004	0.004	0.004	0.004	0.004	0.004	0.003	0.003	0.003	0.003	0.003	0.003	0.003	0.003	0.001
Netherlands	0.06	0.06	0.06	0.06	0.05	0.05	0.04	0.04	0.03	0.03	0.02	0.01	0.01	0.01	0.01	0.01
Norway	0.03	0.03	0.02	0.02	0.02	0.02	0.02	0.02	0.01	0.01	0.01	0.01	0.01	0.004	0.004	0.003
Portugal	0.02	0.02	0.02	0.02	0.02	0.02	0.02	0.01	0.01	0.01	0.01	0.01	0.01	0.01	0.01	0.005
Spain	1.35	1.31	1.28	1.26	1.25	1.19	1.14	1.10	1.07	1.05	0.95	0.84	0.73	0.62	0.53	0.41
Sweden	0.07	0.06	0.06	0.06	0.05	0.05	0.05	0.04	0.04	0.03	0.03	0.02	0.02	0.02	0.02	0.02
Switzerland	0.07	0.06	0.06	0.06	0.06	0.05	0.05	0.04	0.04	0.04	0.03	0.03	0.02	0.02	0.02	0.01
United Kingdom	1.13	1.08	1.04	1.02	1.00	0.93	0.85	0.78	0.71	0.63	0.55	0.47	0.38	0.32	0.26	0.22
OSPAR	6.5	6.2	6.0	5.8	5.6	5.3	4.9	4.6	4.3	4.0	3.5	2.9	2.3	2.0	1.7	1.5
Other	3.1	3.0	2.8	2.7	2.5	2.4	2.2	2.0	1.9	1.8	1.7	1.6	1.4	1.3	1.2	1.1
EMEP	9.7	9.2	8.8	8.5	8.2	7.6	7.1	6.6	6.2	5.8	5.1	4.5	3.7	3.3	2.9	2.6

Table B.3. Annual modelled PCB-153 total depositions to the main regions of the OSPAR maritime area. Units: t/y.

Year	OSPAR Region				
	I. Arctic Waters	II. Greater North Sea	III. Celtic Seas	IV. Bay of Biscay	V. Wider Atlantic
1990	0.35	0.33	0.10	0.16	0.52
1991	0.32	0.32	0.11	0.15	0.48
1992	0.32	0.29	0.08	0.15	0.40
1993	0.31	0.30	0.11	0.16	0.47
1994	0.32	0.31	0.10	0.13	0.45
1995	0.26	0.27	0.09	0.13	0.40
1996	0.32	0.27	0.10	0.14	0.47
1997	0.26	0.26	0.09	0.12	0.40
1998	0.21	0.23	0.07	0.11	0.31
1999	0.23	0.22	0.07	0.11	0.31
2000	0.20	0.21	0.06	0.09	0.27
2001	0.17	0.16	0.05	0.09	0.24
2002	0.15	0.14	0.05	0.07	0.21
2003	0.14	0.12	0.04	0.06	0.18
2004	0.12	0.10	0.03	0.05	0.15
2005	0.10	0.09	0.03	0.04	0.14

Table B.4. Annual modelled PCB-153 net atmospheric input to the main regions of the OSPAR maritime area. Units: t/y.

Year	OSPAR Region				
	I. Arctic Waters	II. Greater North Sea	III. Celtic Seas	IV. Bay of Biscay	V. Wider Atlantic
1990	0.32	0.18	0.02	0.08	0.45
1991	0.29	0.18	0.03	0.08	0.42
1992	0.28	0.17	0.03	0.07	0.33
1993	0.28	0.17	0.04	0.08	0.40
1994	0.29	0.18	0.03	0.06	0.39
1995	0.24	0.14	0.02	0.06	0.34
1996	0.29	0.15	0.03	0.07	0.41
1997	0.24	0.14	0.03	0.06	0.35
1998	0.18	0.13	0.02	0.06	0.25
1999	0.21	0.11	0.01	0.05	0.26
2000	0.18	0.11	0.01	0.04	0.22
2001	0.14	0.09	0.02	0.04	0.20
2002	0.13	0.07	0.00	0.03	0.18
2003	0.12	0.05	0.00	0.03	0.15
2004	0.10	0.05	-0.01	0.02	0.12
2005	0.08	0.04	-0.01	0.02	0.11

Table B.5. Annual modelled γ -HCH total depositions to the main regions of the OSPAR maritime area. Units: t/y.

Year	OSPAR Region				
	I. Arctic Waters	II. Greater North Sea	III. Celtic Seas	IV. Bay of Biscay	V. Wider Atlantic
1990	9.5	14.0	4.3	3.0	12.0
1991	7.9	13.0	4.5	2.6	12.0
1992	8.9	14.0	3.6	3.8	9.7
1993	7.8	13.0	4.5	5.1	14.0
1994	7.7	12.0	4.2	4.2	11.0
1995	6.8	10.0	3.6	4.7	11.0
1996	9.1	11.0	3.8	4.2	12.0
1997	7.0	9.8	3.7	3.6	12.0
1998	4.7	7.6	2.6	2.3	7.6
1999	5.0	6.2	2.2	1.8	7.4
2000	2.9	4.6	1.6	1.5	4.8
2001	1.6	2.7	1.1	0.5	2.7
2002	1.7	2.0	0.8	0.4	2.6
2003	1.7	1.8	0.8	0.4	2.4
2004	1.3	1.6	0.6	0.4	2.2
2005	1.2	1.5	0.6	0.3	2.2

Table B.6. Annual modelled γ -HCH net atmospheric input to the main regions of the OSPAR maritime area. Units: t/y.

Year	OSPAR Region				
	I. Arctic Waters	II. Greater North Sea	III. Celtic Seas	IV. Bay of Biscay	V. Wider Atlantic
1990	9.1	8.8	2.5	2.2	12.0
1991	7.6	8.0	2.6	1.9	12.0
1992	8.5	8.6	2.2	2.6	9.7
1993	7.5	7.4	2.8	3.7	14.0
1994	7.4	7.3	2.7	3.0	11.0
1995	6.5	6.0	2.2	3.3	11.0
1996	8.7	6.4	2.4	3.0	12.0
1997	6.7	6.1	2.4	2.5	12.0
1998	4.5	4.8	1.6	1.7	7.6
1999	4.8	4.0	1.4	1.4	7.4
2000	2.8	2.9	0.9	1.1	4.7
2001	1.6	1.6	0.6	0.4	2.7
2002	1.6	1.2	0.5	0.3	2.5
2003	1.6	1.1	0.4	0.3	2.4
2004	1.2	0.9	0.3	0.3	2.2
2005	1.2	0.9	0.3	0.3	2.2

Table B.7. Annual modelled PCB-153 total deposition to the sub-regions of the Region II (Greater North Sea) of the OSPAR maritime area. Units: t/y.

Year	Sub-regions of the OSPAR Region II												
	1	2	3	4	5	6	7	8	9	10	11	12	13
1990	0.014	0.008	0.011	0.018	0.032	0.036	0.007	0.023	0.040	0.025	0.022	0.034	0.058
1991	0.014	0.009	0.011	0.019	0.034	0.039	0.006	0.018	0.034	0.025	0.020	0.027	0.064
1992	0.012	0.008	0.010	0.015	0.028	0.039	0.006	0.021	0.034	0.023	0.021	0.027	0.052
1993	0.013	0.008	0.010	0.017	0.030	0.039	0.006	0.020	0.030	0.023	0.021	0.025	0.061
1994	0.014	0.009	0.011	0.017	0.030	0.038	0.006	0.021	0.033	0.025	0.021	0.028	0.057
1995	0.011	0.007	0.008	0.015	0.026	0.032	0.006	0.018	0.029	0.019	0.017	0.025	0.056
1996	0.013	0.010	0.010	0.017	0.027	0.030	0.005	0.016	0.025	0.020	0.017	0.021	0.055
1997	0.012	0.007	0.010	0.015	0.026	0.030	0.005	0.016	0.026	0.021	0.018	0.022	0.054
1998	0.011	0.006	0.009	0.012	0.023	0.029	0.005	0.016	0.025	0.021	0.018	0.021	0.039
1999	0.010	0.005	0.007	0.011	0.021	0.026	0.005	0.015	0.025	0.016	0.014	0.023	0.040
2000	0.009	0.005	0.007	0.011	0.020	0.025	0.005	0.015	0.022	0.018	0.016	0.023	0.035
2001	0.007	0.004	0.006	0.009	0.016	0.020	0.004	0.011	0.017	0.013	0.013	0.016	0.030
2002	0.006	0.004	0.005	0.009	0.014	0.017	0.003	0.009	0.015	0.012	0.010	0.014	0.025
2003	0.006	0.003	0.004	0.007	0.011	0.014	0.002	0.007	0.014	0.009	0.007	0.012	0.024
2004	0.004	0.003	0.004	0.006	0.011	0.013	0.002	0.007	0.010	0.008	0.007	0.010	0.019
2005	0.004	0.002	0.003	0.005	0.009	0.011	0.002	0.006	0.011	0.007	0.007	0.009	0.018

Table B.8. Annual modelled PCB-153 net atmospheric input to the sub-regions of the Region II (Greater North Sea) of the OSPAR maritime area. Units: t/y.

Year	Sub-regions of the OSPAR Region II												
	1	2	3	4	5	6	7	8	9	10	11	12	13
1990	0.014	0.008	0.010	0.008	0.012	0.019	0.003	0.014	0.020	0.024	0.021	0.003	0.024
1991	0.013	0.008	0.010	0.009	0.015	0.022	0.002	0.011	0.017	0.024	0.020	0.001	0.031
1992	0.011	0.007	0.009	0.007	0.011	0.021	0.003	0.012	0.017	0.021	0.020	0.008	0.024
1993	0.012	0.007	0.009	0.008	0.012	0.022	0.003	0.012	0.014	0.022	0.021	0.001	0.028
1994	0.014	0.009	0.011	0.008	0.012	0.020	0.003	0.013	0.017	0.024	0.021	0.003	0.026
1995	0.011	0.006	0.007	0.007	0.009	0.016	0.002	0.010	0.014	0.018	0.017	0.001	0.025
1996	0.012	0.009	0.010	0.008	0.010	0.016	0.002	0.010	0.011	0.020	0.017	0.001	0.027
1997	0.012	0.006	0.009	0.007	0.010	0.016	0.002	0.009	0.012	0.020	0.018	-0.001	0.025
1998	0.010	0.005	0.009	0.005	0.008	0.015	0.003	0.009	0.012	0.020	0.016	0.005	0.017
1999	0.009	0.005	0.006	0.004	0.006	0.012	0.002	0.008	0.012	0.015	0.013	0.001	0.016
2000	0.008	0.005	0.006	0.005	0.007	0.013	0.003	0.009	0.010	0.017	0.015	0.003	0.015
2001	0.006	0.004	0.005	0.004	0.005	0.010	0.002	0.006	0.007	0.012	0.012	0.003	0.014
2002	0.006	0.003	0.005	0.003	0.004	0.008	0.001	0.005	0.005	0.011	0.010	-0.003	0.010
2003	0.005	0.003	0.004	0.002	0.002	0.006	0.001	0.004	0.005	0.008	0.007	-0.002	0.009
2004	0.004	0.002	0.003	0.002	0.003	0.006	0.001	0.003	0.003	0.008	0.007	-0.002	0.007
2005	0.004	0.002	0.003	0.001	0.002	0.005	0.000	0.003	0.004	0.007	0.006	-0.002	0.007

Table B.9. Annual modelled γ -HCH total deposition to the sub-regions of the Region II (Greater North Sea) of the OSPAR maritime area. Units: t/y.

Year	Sub-regions of the OSPAR Region II												
	1	2	3	4	5	6	7	8	9	10	11	12	13
1990	0.62	0.40	0.56	2.00	1.90	1.00	0.21	0.96	1.10	1.10	0.80	0.71	2.30
1991	0.54	0.34	0.48	1.80	1.80	1.00	0.18	0.96	0.96	0.93	0.75	0.56	2.60
1992	0.55	0.37	0.48	1.60	1.60	1.30	0.18	0.81	1.00	0.93	0.82	0.63	3.40
1993	0.39	0.29	0.36	1.60	1.60	1.20	0.12	0.65	0.58	0.72	0.65	0.40	3.80
1994	0.42	0.31	0.37	1.30	1.40	1.00	0.14	0.62	0.76	0.72	0.61	0.48	3.70
1995	0.36	0.24	0.33	1.20	1.10	0.90	0.13	0.48	0.64	0.63	0.51	0.39	3.20
1996	0.44	0.38	0.35	1.20	1.20	0.88	0.12	0.52	0.61	0.66	0.55	0.37	3.30
1997	0.38	0.25	0.34	1.00	1.10	0.85	0.13	0.50	0.58	0.69	0.57	0.37	2.90
1998	0.28	0.18	0.27	0.96	1.00	0.76	0.10	0.32	0.47	0.55	0.45	0.30	1.90
1999	0.28	0.18	0.25	0.85	0.80	0.51	0.08	0.25	0.47	0.46	0.38	0.28	1.30
2000	0.18	0.11	0.16	0.40	0.66	0.48	0.07	0.19	0.30	0.42	0.32	0.21	1.10
2001	0.11	0.07	0.09	0.28	0.46	0.26	0.04	0.13	0.18	0.20	0.18	0.14	0.55
2002	0.09	0.06	0.07	0.23	0.35	0.18	0.03	0.08	0.17	0.17	0.12	0.09	0.37
2003	0.09	0.06	0.08	0.20	0.29	0.14	0.03	0.07	0.18	0.18	0.11	0.10	0.30
2004	0.05	0.03	0.05	0.16	0.28	0.15	0.03	0.07	0.10	0.13	0.10	0.07	0.34
2005	0.09	0.05	0.06	0.15	0.24	0.12	0.02	0.06	0.13	0.14	0.09	0.06	0.29

Table B.10. Annual modelled γ -HCH net atmospheric input to the sub-regions of the Region II (Greater North Sea) of the OSPAR maritime area. Units: t/y.

Year	Sub-regions of the OSPAR Region II												
	1	2	3	4	5	6	7	8	9	10	11	12	13
1990	0.62	0.39	0.56	0.92	0.99	0.65	0.16	0.55	0.89	1.10	0.80	0.38	0.71
1991	0.54	0.34	0.48	0.83	0.91	0.65	0.13	0.52	0.79	0.93	0.75	0.24	0.87
1992	0.55	0.37	0.48	0.76	0.89	0.86	0.14	0.49	0.83	0.93	0.81	0.32	1.20
1993	0.39	0.29	0.36	0.72	0.86	0.82	0.09	0.38	0.45	0.72	0.64	0.15	1.50
1994	0.42	0.30	0.37	0.61	0.74	0.68	0.11	0.38	0.61	0.72	0.61	0.21	1.50
1995	0.36	0.24	0.33	0.52	0.58	0.58	0.10	0.30	0.51	0.63	0.51	0.16	1.10
1996	0.44	0.38	0.35	0.60	0.64	0.54	0.09	0.29	0.48	0.66	0.54	0.14	1.20
1997	0.38	0.25	0.34	0.49	0.60	0.55	0.10	0.30	0.47	0.69	0.57	0.17	1.10
1998	0.28	0.18	0.27	0.46	0.56	0.52	0.07	0.21	0.37	0.55	0.45	0.11	0.76
1999	0.28	0.17	0.25	0.40	0.43	0.34	0.06	0.16	0.39	0.46	0.38	0.11	0.51
2000	0.18	0.11	0.16	0.19	0.36	0.31	0.05	0.12	0.24	0.42	0.31	0.07	0.41
2001	0.10	0.07	0.09	0.12	0.24	0.16	0.03	0.08	0.14	0.20	0.17	0.03	0.17
2002	0.09	0.06	0.07	0.11	0.18	0.11	0.02	0.05	0.13	0.17	0.12	0.00	0.12
2003	0.09	0.06	0.08	0.09	0.15	0.08	0.02	0.04	0.14	0.18	0.11	0.01	0.10
2004	0.05	0.03	0.05	0.07	0.14	0.09	0.02	0.05	0.08	0.13	0.10	0.01	0.11
2005	0.09	0.04	0.06	0.07	0.13	0.07	0.01	0.03	0.10	0.14	0.09	0.00	0.10



New Court
48 Carey Street
London WC2A 2JQ
United Kingdom

t: +44 (0)20 7430 5200
f: +44 (0)20 7430 5225
e: secretariat@ospar.org
www.ospar.org

**OSPAR's vision is of a clean, healthy and biologically diverse
North-East Atlantic used sustainably**

ISBN 978-1-906840-16-7
Publication Number: 375/2008

© OSPAR Commission, 2008. Permission may be granted by the publishers for the report to be wholly or partly reproduced in publications provided that the source of the extract is clearly indicated. Permission may be granted by EMEP/MSC-E for the use and publication of any data, measured under the EMEP Programme and modelled for the purpose of this report, and all related data products (tables and figures) presented in this report.

© Commission OSPAR, 2008. La reproduction de tout ou partie de ce rapport dans une publication peut être autorisée par l'Editeur, sous réserve que l'origine de l'extrait soit clairement mentionnée. L'utilisation et la publication des données, obtenues dans le cadre du programme EMEP et modélisées aux fins de ce rapport, et de tous les éléments relatifs aux données (tableaux et figures) présentés dans ce rapport, peut être autorisée par l'EMEP/MSC-E.